



Studies on central carbon metabolism and respiration of *Gluconobacter oxydans* 621H

Inaugural-Dissertation

zur Erlangung des Doktorgrades
der Mathematisch-Naturwissenschaftlichen Fakultät
der Heinrich-Heine-Universität Düsseldorf

vorgelegt von

Tanja Hanke
aus Solingen

Düsseldorf, Dezember 2009

Aus dem Institut für Biotechnologie 1
des Forschungszentrums Jülich GmbH

Gedruckt mit der Genehmigung der
Mathematisch-Naturwissenschaftlichen Fakultät der
Heinrich-Heine-Universität Düsseldorf

Referent: Prof. Dr. H. Sahm

Koreferent: Prof. Dr. M. Bott

Tag der mündlichen Prüfung: 22.01.2010

Publications

Hanke T, Noack S, Nöh K, Bringer S, Oldiges M, Sahm H, Bott M, Wiechert W (2010) Characterisation of glucose catabolism in *Gluconobacter oxydans* 621H by ¹³C-labeling and metabolic flux analysis. Submitted to FEMS Microbiology Letters

Hanke T, Bringer S, Polen T, Sahm H, Bott M (2010) Genome-wide microarray analyses of *Gluconobacter oxydans*: Response to oxygen depletion, growth phases and acidic growth conditions. Manuscript for submission to J Bacteriol

Hanke T, Bringer S, Sahm H Bott M (2010) The cytochrome *bc*₁ complex in *Gluconobacter oxydans* 621H: Functional analysis by fermentation studies and whole cell kinetics with a marker-free deletion mutant. Manuscript for submission to J Bacteriol

Abstract

Gluconobacter oxydans shows a number of exceptional characteristics, like the biphasic growth on glucose and the incomplete oxidation of glucose to gluconate (phase I, exponential growth,) and ketogluconates (phase II, linear growth), leading to an acidification of the medium down to pH values less than 4. Furthermore, growth and metabolism of *G. oxydans* is strongly dependent on the availability of oxygen. In the respiratory chain, two terminal end acceptors are present. The ubiquinol *bd* oxidase, preferably used under acidic pH, is less efficient in contribution to the proton motive force than the *bo*₃ oxidase.

An open question was the function of a cytochrome *bc*₁ complex as well as soluble cytochrome *c*₅₅₂, in the absence of a cytochrome *c* oxidase. For elucidation of the function of these respiratory chain components, a deletion mutant lacking the genes encoding the cytochrome *bc*₁ complex was constructed and characterised. When cultivated on mannitol at pH 4 the deletion mutant showed retarded growth and substrate consumption. Therefore, the cytochrome *bc*₁ complex is involved in energy supply of the cells under acidic pH when the more inefficient ubiquinol *bd* oxidase is upregulated. Interestingly, under oxygen limitation the deletion mutant released heme into the culture medium in the late stationary phase. Since hemes *b* and *c* are the prosthetic groups of the cytochrome *bc*₁ complex heme excretion of the mutant is a consequence of absence of the corresponding apoenzymes, which is formed under oxygen limitation. The membrane-bound and respiratory chain-linked alcohol dehydrogenase (ADH) was reported to be a component of the respiratory chain and not merely an oxidoreductase. A connection to the cytochrome *bc*₁ complex was investigated in this work. The oxidation velocity of the ADH of the mutant was significantly lower than that of the wild type was. Furthermore, the cytochrome *bc*₁ complex was shown to be involved in the energy-dependent activation of the ADH in cells grown at pH 4, but a direct interaction between the cytochrome *bc*₁ complex and the ADH was not demonstrated yet.

In order to throw light on the regulation of the respiratory chain in conjunction with the overall metabolism, genome-wide DNA microarray analyses were carried out with *G. oxydans* 621H. Three conditions were investigated: I) oxygen limitation vs. oxygen excess, II) cultivation at decreased pH of 4 vs. cultivation at standard pH of 6 and III) growth phase II vs. growth phase I during growth on glucose pH 6, since the cytochrome *bc*₁ complex deletion mutant showed growth retardation in growth phase II. Transcriptional analyses of oxygen-limited cells displayed an upregulation of genes encoding the cytochrome *bc*₁ complex and both terminal oxidases. In cells grown at

pH 4, an enhanced transcription of the genes encoding the more inefficient ubiquinol *bd* oxidase occurred. Since no direct connection between the glucose metabolism and the cytochrome *bc*₁ complex was evident, glucose metabolism was further characterised in the wild type. ¹³C-Metabolome analysis and metabolic flux analysis (MFA) were applied to solve the question of the quantity and oxidation state of the substrate entering the cell for catabolism. MFA of phase I glucose cultures showed that 97% of the initial glucose was oxidised in the periplasm by the highly active and respiratory chain-linked glucose dehydrogenase, whereas only 3% of glucose proceeded into the cytoplasm. According to the model, intracellular glucose was predominantly oxidised to gluconate, subsequently phosphorylated by gluconate kinase and further metabolised via the pentose phosphate pathway. In addition, genome-wide transcriptional analysis of *G. oxydans* approved the reported assumption of a highly active pentose phosphate pathway, which is enhanced in growth phase II. In contrast, the Entner-Doudoroff pathway was almost inactive in growth phase I.

Zusammenfassung

Zu den Besonderheiten von *G. oxydans* gehören das biphasische Wachstum mit Glukose und die unvollständige Oxidation von Glukose zu Glukonat (Phase I, exponentielles Wachstum) und Ketoglukonat (Phase II, lineares Wachstum), die zu einer Ansäuerung des Mediums mit pH Werten kleiner als 4 führt. Wachstum und Metabolismus von *G. oxydans* sind stark von der Sauerstoffverfügbarkeit abhängig. Die Atmungskette des Bakteriums enthält zwei terminale Oxidasen: die Ubichinon *bd* Oxidase wird bevorzugt bei sauren pH Werten genutzt und ist weniger effizient in ihrem Beitrag zur Generierung der protonenmotorischen Kraft als die Ubichinon *bo₃* Oxidase.

Da die Cytochrom *c* Oxidase fehlt, ist die Funktion des Cytochrom *bc₁* Komplexes und des löslichen Cytochrom *c₅₅₂* nicht geklärt. Zur Aufklärung der Funktion dieser Atmungskettenkomponenten wurde eine Deletionsmutante des Cytochrom *bc₁* Komplexes konstruiert und charakterisiert. Bei Kultivierung mit Mannitol bei pH 4 zeigte diese Mutante eine Verzögerung im Wachstum und im Substratverbrauch. Offensichtlich ist der Cytochrom *bc₁* Komplex an der Energieversorgung von pH 4 kultivierten Zellen beteiligt, in denen die ineffizientere Ubichinon *bd* Oxidase verstärkt genutzt wird. Unter Sauerstoffmangel gab die Mutante in der stationären Phase Häm in das Medium ab. Da Häm *b* und Häm *c* die prosthetischen Gruppen des Cytochrom *bc₁* Komplexes sind, ist die Exkretion des Häms die Konsequenz der Abwesenheit des Apoenzyms, das der Wildtyp unter Sauerstoffmangelbedingung produziert. Eine japanische Arbeitsgruppe beschrieb die membrangebundene Alkohol Dehydrogenase (ADH) als Bestandteil der Atmungskette. Daher wurde in der vorliegenden Arbeit eine Verbindung mit dem Cytochrom *bc₁* Komplex untersucht. Die Oxidationskapazität der ADH war in der Mutante gegenüber dem Wildtyp signifikant verringert und der Cytochrom *bc₁* Komplex war an der energieabhängigen Aktivierung der ADH in pH 4 kultivierten Zellen beteiligt.

Um die Regulation der Atmungskette und des Metabolismus gleichzeitig zu untersuchen, wurden genomweite Transkriptionsanalysen mit *G. oxydans* 621H durchgeführt. Drei Bedingungen wurden gewählt: I) Sauerstofflimitierung vs. Sauerstoffüberschuss, II) Kultivierung bei pH 4 vs. Kultivierung bei pH 6 und III) Wachstumsphase II vs. Wachstumsphase I bei Kultivierung mit Glukose pH 6, da die Cytochrom *bc₁* Deletionsmutante verzögertes Wachstum in Phase II zeigte. Die Gene, kodierend für den Cytochrom *bc₁* Komplex und die beiden Endoxidasen, wurden in sauerstofflimitierten Zellen verstärkt transkribiert. Bei pH 4 kultivierten Zellen zeigte sich eine verstärkte Transkription der Gene kodierend für die

ineffizientere Ubichinon *bd* Oxidase. Weil kein direkter Zusammenhang zwischen dem Glukosemetabolismus und dem Cytochrom *bc*₁ Komplex ersichtlich war, wurde der Glukosemetabolismus des Wildtyps näher untersucht. Um zu klären, wie viel und welche Oxidationsstufe des Substrates in die Zellen aufgenommen wird, wurden eine ¹³C-Metabolomanalyse und eine metabolische Flussanalyse (MFA) durchgeführt. Die MFA der ersten Wachstumsphase zeigte dass 97% der ursprünglichen Glukose im Periplasma oxidiert wurden und 3% der Glukose in das Cytoplasma aufgenommen wurden. Dem Modell entsprechend wurde die Glukose intrazellulär erst durch die cytoplasmatische Glukose Dehydrogenase zu Glukonat oxidiert, bevor dieses durch die Glukonat Kinase phosphoryliert und in den Pentosephosphatweg eingeschleust wurde. Die Transkriptomanalyse bestätigte die Verstärkung der Aktivität des Pentosephosphatweg in Phase II. Hingegen war der Entner-Doudoroff Weg in Phase I fast inaktiv.

Contents

I Abbreviations	1
II Introduction	3
III Materials and Methods	11
1. Bacterial strains	11
2. Plasmids and oligonucleotides	12
3. Chemicals and enzymes	14
4. Media	15
5. Culture conditions of <i>G. oxydans</i> and <i>E. coli</i>	15
6. Determination of cell dry weight	17
7. Stock cultures	17
8. Molecular biological methods	17
8.1 Isolation of DNA	17
8.2 Recombinant DNA-techniques	18
8.3 Polymerase chain reaction (PCR)	18
8.4 Agarose gel electrophoresis.....	19
8.5 Transformation of <i>E. coli</i> and <i>G. oxydans</i>	19
8.6 Overexpression of the <i>G. oxydans</i> <i>ccp</i> gene encoding cytochrome <i>c</i> peroxidase.....	20
8.7 Construction of marker-free deletion mutants	21
8.8 RNA preparation.....	21
8.9 cDNA labeling and RT PCR	22
8.10 <i>G. oxydans</i> DNA microarrays.....	22
9. Biochemical methods	23
9.1 Cell disruption, preparation of crude extracts and membrane fractions.....	23
9.2 Determination of protein concentration.....	24
9.3 Polyacrylamide gel electrophoresis of proteins (SDS-PAGE)	24
9.4 Protein purification by column chromatography	24
9.5 Determination of oxygen consumption rates with a Clark electrode	26
9.6 Determination of enzyme activities.....	26
9.7 Conversion of inactive alcohol dehydrogenase to active enzyme in resting cells.....	30
10. Bioanalytical methods	30
10.1 Sampling and sample processing for LC-MS analysis	30
10.2 Determination of metabolites by high performance liquid chromatography (HPLC)	31
10.3 ¹³ C Metabolic flux analysis	31
10.4 MALDI-TOF-Mass spectrometry.....	32
IV Results	33
1. Characterisation of the deletion mutant <i>G. oxydans</i> 621H-Δ<i>qcrABC</i>	33
2. Genome-wide transcription analyses	51
3. ¹³C-Metabolome analysis and flux analysis (MFA)	63
V Discussion	73
1. Analysis of physiological and metabolic functions of the cytochrome <i>bc</i>₁ complex in <i>G. oxydans</i>	73
2. Differential gene regulation at oxygen limitation and at low pH	80
3. Characterisation of growth of <i>G. oxydans</i> 621H on glucose with micro- array-, ¹³C-metabolome- and flux-analysis	84

VI References..... 89
VII Appendix..... 101

I Abbreviations

λ	Wavelength (nm)
$^{\circ}\text{C}$	Degree Celsius
ε	molar extinction coefficient
Ω	Ohm
2-KGA	2-Keto-gluconate
5-KGA	5-Keto-gluconate
A	Ampère
ADH	Alcohol dehydrogenase
ATP	Adenosine triphosphate
BCA	Bicinchonine acid
bp	Base pairs
C	Carbon
CCCP	Carbonylcyanide- <i>m</i> -chlorophenylhydrazone
CDW	Cell dry weight
Cef	Cefoxitin
CTR	Carbon dioxide transfer rate
Da	Dalton
DCPIP	2,6-Dichlor-indophenol
DDM	<i>n</i> -Dodecylmaltoside
DNA	Desoxyribonucleic acid
dNTP	Desoxyribonukleotidtriphosphate
DO	Dissolved oxygen
DTT	Dithiothreitol
EDP	Entner-Doudoroff Pathway
EDTA	Ethylendiamine tetraacetate
EMP	Embden-Meyerhof pathway
EP	Electroporation
FA	Formaldehyde
FAD	Flavin adenine dinucleotide
<i>g</i>	Gravitational acceleration (9,81 m/s ²)
G6P-DH	Glucose 6-phosphate dehydrogenase
GK	Glucose kinase
Gntk	Gluconate kinase
H ₂ O ₂	Hydrogen peroxide
H ₂ SO ₄	Sulfuric acid
HClO ₄	Perchloric acid
HEPES	2-(4-(2-Hydroxyethyl)-1-piperazinyl)-ethanesulfonic acid
HPLC	High Performance Liquid Chromatography
IPTG	Isopropyl- β -D-thiogalactoside
Kan	Kanamycine
kb	kilo base pairs
kDa	Kilo Dalton
KPi	Potassium phosphate buffer
LC	Liquid Chromatography
M	Molar; Mol per liter
MgCl ₂	Magnesium chloride
mGDH	Membrane-bound glucose dehydrogenase
MOPS	Morpholinopropane sulfonic acid

I Abbreviations

MS	Mass spectroscopy
NAD ⁺	Nicotinamide-adenine-dinucleotide
NADP ⁺	Nicotinamide-adenine-dinucleotide phosphate
OD _x nm	Optical density at a wavelength of x nm
ox	oxidised
PAGE	Polyacrylamide gel electrophoresis
PCR	Polymerase chain reaction
PMS	Phenazine methane sulfate
PPP	Pentose phosphate pathway
PQQ	Pyrroloquinoline quinone
RC	Respiratory chain
red	reduced
RNA	Ribonucleic acid
RNase	Ribonuclease
rpm	Rounds per minute
RT	Room temperature
RT-PCR	Reverse transcription PCR
SDS	Sodium dodecylsulfate
Stl/h	Standard liter per hour
TAE	Tris/Acetate/EDTA
TCA	Citric acid cycle
TNI	Tris sodiumchloride imidazole buffer
Tris	Tri-(hydroxymethyl)-aminomethane
U	Unit
UV	Ultraviolet
V	Volt
v/v	Volume per volume
w/v	Weight per volume

II Introduction

Acetic acid bacteria are Gram negative bacteria existing in natural sweet habitats like fruits, flowers and sweet or alcoholic drinks (Swings 1992, Gupta *et al.* 2001, Battey and Schaffner 2001). The family of *Acetobacteriaceae* splits into 10 genera, among those are *Acetobacter*, *Gluconobacter*, *Gluconacetobacter* and *Acidomonas* (Yamada and Yukphan 2008). *Gluconobacter* and *Acetobacter* are similar to each other, but a distinction is possible by 16S-rRNA analysis (Sievers *et al.* 1995). Furthermore, *Acetobacter* is capable of oxidising lactate and acetic acid completely to CO₂, in contrast to *Gluconobacter*. The genus *Gluconobacter* consists of four species named *G. asaii*, *G. cerinus*, *G. frateurii* and *G. oxydans* (Sievers *et al.* 1995, Tanaka *et al.* 1999). *G. oxydans* is strictly aerobic and forms flagella when cells are oxygen-limited (De Ley and Swings 1981, De Ley *et al.* 1984, Gupta *et al.* 2001). Cells of *G. oxydans* are oval or rod-shaped and sized 0.9 x 1.55 to 2.63 µm depending on the growth phase (Heefner and Claus 1976). They exist as singular cells or form pairs and short chains (**Fig. 1**).

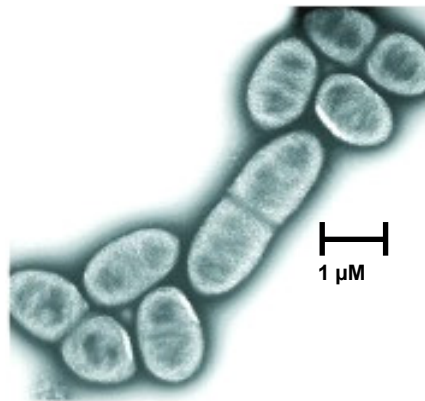


Fig. 1: Picture of *G. oxydans* in the electron microscope

Kindly approved by Dr. A. Ehrenreich, Department of Microbiology, Technische Universität München

Optimal growth conditions for *G. oxydans* range from 25-30°C (Gupta *et al.* 2001). The organism prefers growing at a pH 5.5 when grown on glucose but is able to grow at low pH values of 3.7 (Olijve and Kok 1979). Since *G. oxydans* exists in sugar-rich habitats, sugars or sugar-alcohols like mannitol, sorbitol, glucose, fructose and glycerol are the favoured carbon sources (Olijve and Kok 1979, Gosselé *et al.* 1980). Growth on defined medium is weak (Olijve and Kok 1979); complex media containing

yeast extract permit growth of the organism to higher cell densities (Raspor and Goranovič 2008).

In 2005 the genome sequence of *G. oxydans* 621H was published by Prust *et al.*, offering new insights into the metabolic pathways. The genome size is 2.9 Mbp including 5 plasmids and 2664 putative protein-coding ORFs of which 1877 ORFs were functionally characterised. The GC-content of the genomic DNA of 61% is relatively high in comparison to other bacteria (De Ley *et al.* 1984, Shimizu *et al.* 1999, Prust *et al.* 2005). The genome annotation affirmed that *G. oxydans* lacks genes of the citric acid cycle (TCA) and of the Embden-Meyerhof pathway (EMP) (Greenfield *et al.* 1972, Fritsche 1999, Prust *et al.* 2005). The genes encoding for succinate dehydrogenase, succinyl-CoA-synthetase and 6-phosphofructokinase are not present. Since both, Embden-Meyerhof-Parnas pathway and the citrate cycle are interrupted, these pathways serve for the formation of precursors only. The pentose phosphate pathway (PPP) and the Entner-Doudoroff pathway (EDP) are both completely present in *G. oxydans* (Deppenmeier *et al.* 2002, Kersters *et al.* 1968).

G. oxydans is used since 1930 industrially due to its many membrane-bound and respiratory chain linked dehydrogenases, which enable the organism to oxidise various substrates, like sugars or polyols, in one or more steps (Kulhanek 1989). These reactions take place in the periplasm and the oxidation intermediates accumulate in the culture medium. Only a small fraction of the substrate enters the cells and serves for growth and biomass production (Weenk *et al.* 1984). Concomitant with the high oxidation capacity are the low growth yields of *G. oxydans* allowing a conversion of more than 90% of the substrates into industrially relevant products. The organism is utilised for the production of acetic acid, miglitol (antidiabetic drug) and for dihydroxyacetone serving as a tanning agent (Campbell *et al.* 2000, Schedel 2000, Claret *et al.* 1994). *G. oxydans* has industrial relevance due to its capacity to oxidise glucose to gluconate that serves as a solvent of dirt in the textile industry (Meiberg *et al.* 1983, Pronk *et al.* 1989). The most prominent product manufactured with *G. oxydans* is vitamin C via a sequence of three oxidations starting from sorbitol (Bemus *et al.* 2006, Hancock 2009). Finally, genetically engineered strains of the organism produce up to 300 mM 5-ketogluconic acid from glucose. This prochiral ketoacid is a precursor of enantiopure L-(+)-tartaric acid (Klasen *et al.* 1992, Elfari *et al.* 2005, Merfort *et al.* 2006).

The respiratory chain of *G. oxydans*

The name *G. oxydans* stresses the fact, that this organism strictly depends on oxygen and has a high capacity to oxidise substrates. It possesses many membrane-bound oxidoreductases, which are part of the respiratory chain. The membrane-bound dehydrogenases (oxidoreductases) of *G. oxydans* pass electrons to the respiratory chain (Prust *et al.* 2005). PQQ, heme *c* or FAD serve as prosthetic groups (Shinagawa *et al.* 1990, Matsushita *et al.* 2003, Toyama *et al.* 2007, Toyama *et al.* 2004). The electrons derived from the enzyme catalysed oxidations are transferred to ubiquinone (Fig. 2).

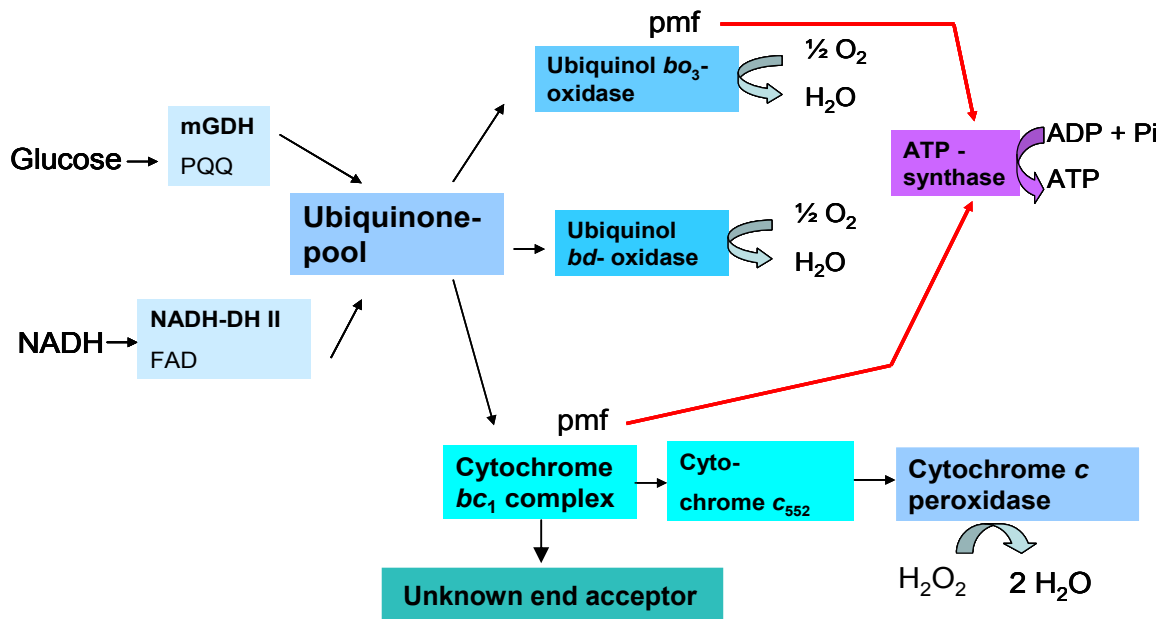


Fig. 2 Components of the respiratory chain in *G. oxydans*

Pmf: proton motive force; PQQ: Pyrroloquinoline quinone; FAD: Flavine adenine dinucleotide

G. oxydans possesses the monomeric, non-proton pumping NADH dehydrogenase II (NADH: ubiquinone oxidoreductase, *ndh*) (Prust *et al.* 2005) (Fig. 2). The respiratory chain of *G. oxydans* is branched; electrons can be transferred either to an ubiquinol *bo*₃ oxidase or to a copper containing ubiquinol *bd* oxidase (Matsushita *et al.* 1987, Matsushita *et al.* 1994). The ubiquinol *bo*₃ oxidase is more efficient in generating a proton motive force than the ubiquinol *bd* oxidase because it pumps two protons per electron pair into the periplasm (Verkhovskaya *et al.* 1997). In contrast, the ubiquinol *bd* oxidase is a non-proton pumping oxidase (Millers *et al.* 1985). The ubiquinol *bo*₃ oxidase is very similar to cytochrome *c* oxidases. Three of four subunits are nearly identical; the fourth is highly homologous to the analogous subunit of the cytochrome *c* oxidase (Abramson *et al.* 2000). These oxidases have distinct cytochrome *c* or ubiquinol binding sites, but the overall

mechanism is very similar (Abramson *et al.* 2000). The ubiquinol *bd* oxidase and the ubiquinol *bo*₃ oxidase are both present in *E. coli* (Anraku and Gennis 1987), and regulated by oxygen availability. If cells become oxygen-limited, the concentration of the ubiquinol *bd* oxidase rises (Tseng *et al.* 1995). In *G. oxydans*, the upregulation of the ubiquinol *bd* oxidase has been shown indirectly when the pH of the medium dropped from 6 to 4 (Matsushita *et al.* 1989).

Surprisingly, *G. oxydans* also possesses the genes encoding for a cytochrome *bc*₁ complex, as well as for cytochrome *c*₅₅₂, which was disclosed by genome sequencing in 2005 (Prust *et al.* 2005). The complex consists of three subunits: the cytochrome *c* subunit with one cytochrome *c* as prosthetic group, a cytochrome *b* subunit with two cytochrome *b* and an iron-sulfur subunit with one [Fe-S]-cluster. The genes for a cytochrome *c* oxidase are missing (Prust *et al.* 2005) and therefore the function of the cytochrome *bc*₁ complex is not clear. The fate of the electrons is in question as well as the conditions, under which electrons might be channelled through the cytochrome *bc*₁ complex. The complex might sustain the proton motive force when the concentration of the unproductive, non-proton translocating *bd* type oxidase is increased.

Genome annotation revealed the occurrence of a cytochrome *c* peroxidase localised in the periplasm (Prust *et al.* 2005). This enzyme is reduced via soluble cytochrome *c*₅₅₂ and transfers electrons to H₂O₂ (Atack and Kelly 2007). Another suggestion for the function of the cytochrome *bc*₁ complex in *G. oxydans* was therefore involvement in detoxification of the cells under conditions, where reactive oxygen species like H₂O₂ are formed. *G. oxydans* possesses the gene encoding for the periplasmatic cytochrome *c* peroxidase, which transfers electrons from cytochrome *c*₅₅₂ to H₂O₂ and reduces it to water. However, in other bacteria like *Pseudomonas denitrificans*, this enzyme is not the only end acceptor of electrons from the cytochrome *bc*₁ complex via reduced cytochrome *c* (Nicholls and Ferguson 2002); thus the nature of the end acceptor of electrons from the cytochrome *bc*₁ pathway is still in question. The anaerobic bacterium *Zymomonas mobilis* occurs in the same habitats like *G. oxydans* and its respiratory chain is very similar to that of *G. oxydans* (Kalnenieks 2006). In this organism, the occurrence of a cytochrome *bc*₁ complex is more peculiar (Sootsuwan *et al.* 2008, Kouvelis *et al.* 2009). It is hardly acceptable, that two organisms possess the cytochrome *bc*₁ complex pathway exclusive of an end acceptor and the search for the terminal acceptor became more crucial.

The membrane-bound alcohol dehydrogenase (ADH) is an enzyme of great interest in *Gluconobacter* research (Adachi *et al.* 1978, Jongejan *et al.* 2000) since it

functions not only as an oxidoreductase like the other membrane-bound dehydrogenase. It was reported to have integral functions in the respiratory chain (Adachi *et al.* 1978, Jongejan *et al.* 2000). It belongs to the ADH type III family and consists of three subunits (Matsushita *et al.* 2008). Three cytochrome *c* are located within the cytochrome *c* subunit, PQQ and one cytochrome *c* are bound within the large subunit. The function of the 15 kDa subunit is not clear yet. Matsushita *et al.* 2008 reported a bound ubiquinol in the enzyme. Besides its normal catalytic function, ADH plays a more general role in the respiratory chain. On the one hand, it can transfer electrons from ethanol to the ubiquinol pool; on the other hand, it can receive electrons from a soluble ubiquinol to an ubiquinone bound to the enzyme (Matsushita *et al.* 2008). These electrons can be received from the membrane-bound glucose dehydrogenase mGDH, which does not exhibit ferricyanide reductase activity when the ADH is not present or when the cytochrome *c* subunit of the ADH is missing (Shinagawa *et al.* 1990). Thus, the electron transfer from GDH to ferricyanide is mediated by ubiquinone and ADH (Shinagawa *et al.* 1990), but the authors did not mention a possible reason for such an electron transport. There are indications in the literature, that the ADH is interconnected with the ubiquinol *bd* oxidase, which is synonymously named “cyanide-insensitive” oxidase. This connection has only been shown indirectly and the mechanism is not known yet. It was reported that the cyanide-sensitivity of the cells increased, when the cytochrome *c* subunit of the ADH was missing (Matsushita *et al.* 1989). The authors concluded that the second subunit cytochrome *c* of the alcohol dehydrogenase might be involved in the cyanide-insensitive respiratory chain bypass (cytochrome *bd*) (Matsushita *et al.* 1991). Furthermore, it was reported that a decreased ADH activity in pH 4 grown cells was restored after incubation of the cells at pH 6 if the cells were actively generating a membrane potential (Matsushita *et al.* 1995). In the present work, we put forward a possible involvement of the cytochrome *bc*₁ complex in the activation of the ADH, since the cytochrome *bc*₁ complex actively generates a proton motive force. Further indications for presence of super-complex structures were provided by Soemphol *et al.* 2008 who investigated the interaction of the two membrane bound sorbitol dehydrogenases (GLDHs) of *Gluconobacter frateurii* with the two terminal oxidases. In a mutant strain defective in PQQ-GLDH, oxidase activity with sorbitol was more resistant to cyanide than in either the wild-type strain or the mutant strain defective in FAD-SLDH. These results suggested that PQQ-GLDH connects efficiently to the cytochrome *bo*₃ terminal oxidase whereas FAD-SLDH linked preferably to the cyanide-insensitive terminal oxidase (cytochrome *bd*).

Glucose metabolism in *G. oxydans*

Beside a branched, complex respiratory chain, the glucose metabolism of *G. oxydans* is not simple, either. *G. oxydans* possesses three pathways for the catabolism of glucose. The predominant one is the periplasmic oxidation by mGDH and membrane-bound gluconate dehydrogenases (Levering *et al.* 1988, Pronk *et al.* 1989) (**Fig. 3**).

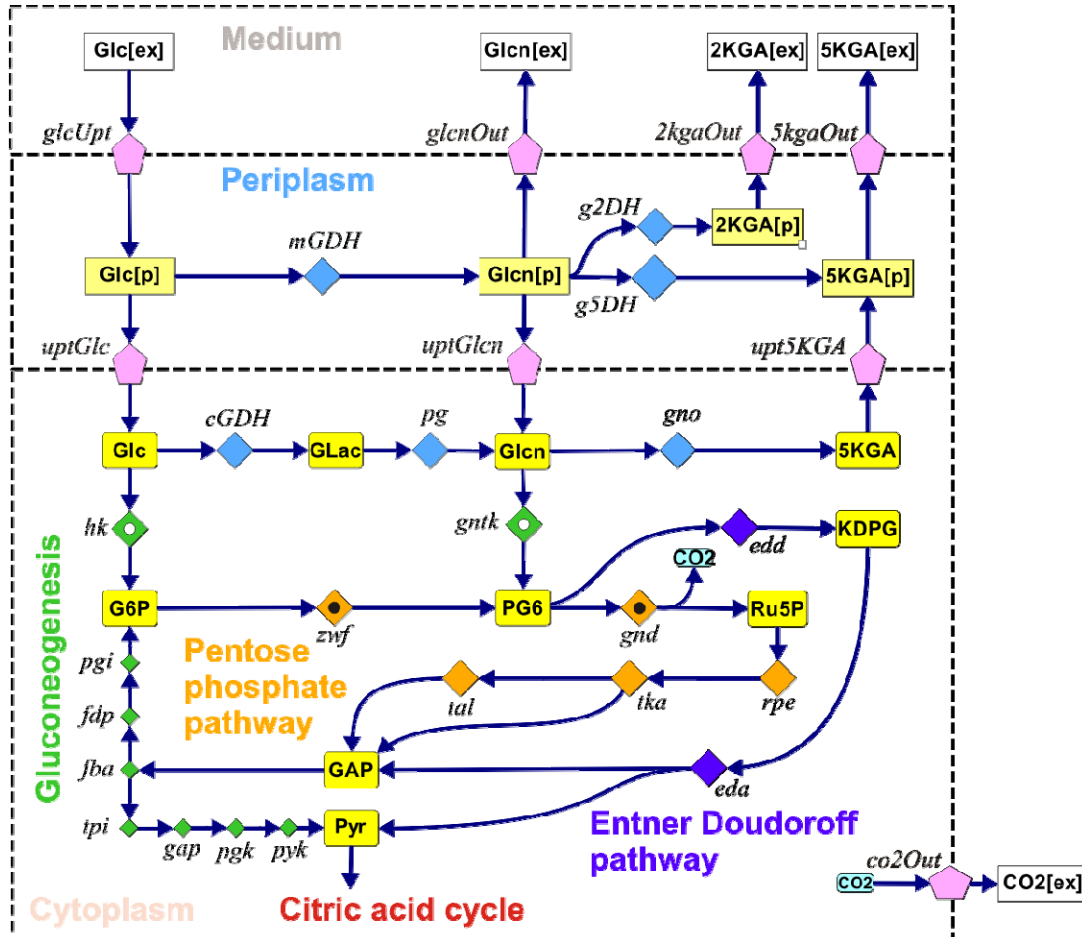


Fig. 3 Pathways of glucose and gluconate oxidation in *G. oxydans*

pentose phosphate pathway (orange); Entner-Doudoroff pathway (dark blue); reactions of gluconeogenesis in green; oxidative reactions of glucose or gluconate in light blue, intermediates in yellow; DH: dehydrogenase; p: periplasmic; ex: extern; Upt: uptake; Glc: Glucose; Glcn: Gluconate; KGA: ketogluconates; mGDH: membrane-bound glucose DH; cGDH: cytosolic glucose DH; g2DH: gluconate 2-DH; g5DH: gluconate 5-DH; KDPG: 2-keto-3-deoxy-6-phospho-gluconate; P: phosphate; GAP: glyceraldehyde 3-phosphate; GLac: gluconolacton; hk: hexokinase; gntk: gluconokinase; pg: gluconolactonase; gno: gluconate-5-dehydrogenase; edd: 6-phosphogluconate dehydratase; eda: 2-Keto-3-deoxygluconate 6-phosphate aldolase; zwf: glucose 6-phosphate dehydrogenase; gnd: 6-phosphogluconate dehydrogenase; rpe: ribulose 5-phosphate epimerase; tka: transketolase; tal: phosphate isomerase; pgi: glucose 6-phosphate isomerase; fdp: fructose bisphosphatase; fba: fructose-1,6-diphosphate aldolase; tpi: triosephosphate isomerase; gap: glyceraldehyde 3-phosphate dehydrogenase; pgk: phosphoglycerate kinase; pyk: pyruvate kinase

Intermediates and products of these reactions accumulate in the medium. In parallel, glucose is taken up into the cytoplasm by an unknown transport system (Pronk *et al.* 1989, Olijve 1979). Here, glucose can either be oxidised to gluconate by a soluble NAD(P)-linked glucose dehydrogenase or be phosphorylated to glucose 6-phosphate by glucose kinase. As *G. oxydans* lacks phosphofructokinase, glucose 6-phosphate cannot be metabolised via glycolysis, but only via the pentose phosphate pathway (PPP) or the Entner-Doudoroff pathway (EDP) (Deppenmeier and Ehrenreich 2008, Deppenmeier *et al.* 2002, Kersters and De Ley 1968). Intracellular gluconate can either be oxidised to 5-ketogluconate by an NAD(P)-linked gluconate 5-dehydrogenase (Merfort 2006) or phosphorylated by gluconate kinase to 6-phosphogluconate, which is then metabolised via PPP or EDP (**Fig. 3**) (Pronk *et al.* 1989). Pyruvate formed in EDP and in the late reactions of glycolysis can be oxidized to acetyl-CoA by the pyruvate dehydrogenase complex (Prust *et al.* 2005). Growth of *G. oxydans* on glucose divides into two metabolic phases (Olijve and Kok 1979a, Levering *et al.* 1988). In the first phase, cells oxidise glucose rapidly to gluconate by the membrane-bound glucose dehydrogenase (mGDH); gluconate mainly accumulates in the medium. In the second growth phase, gluconate present in the medium is further oxidized to 5-keto and 2-ketogluconates by the membrane-bound sorbitol dehydrogenase and gluconate 2-dehydrogenase, respectively (Weenk *et al.* 1984, Hölscher *et al.* 2009). Since this periplasmatic oxidation is the prevailing route of glucose catabolism, only a small fraction of the carbon source is utilised for cell growth. In growth phase I cells grow exponentially whereas growth in phase II is slow and linear (Olijve and Kok 1979).

Aims of the work

The presence of genes encoding the cytochrome *bc*₁ complex was one of the surprising results when the genome of *G. oxydans* was sequenced in 2005. The absence of an electron end acceptor, like the cytochrome *c* oxidase, initiated the search for the function of the complex. One aim of the present work was elucidation of the role of the cytochrome *bc*₁ complex in the respiratory chain of *G. oxydans*. One strategy to attain this goal was construction of a marker-free deletion mutant lacking the cytochrome *bc*₁ complex. Based on the literature on the respiratory chain of *G. oxydans*, clarification of the function of the complex with the help of a deletion mutant appeared most promising by variation of the parameters oxygen supply and pH-value of the growth medium. Furthermore, performance of short time oxidation kinetics with intact cell and different substrates were planned, in order to check an

influence of the cytochrome *bc*₁ complex on primary oxidative steps of the membrane. Since there were several indications in the literature of formation of super complexes among components of the respiratory chain, co-purification experiments were envisaged. Presence of a gene in the *G. oxydans* genome encoding a periplasmatic cytochrome *c* peroxidase was a perspective to identify an alternative terminal electron acceptor of the cytochrome *bc*₁ complex pathway. This enzyme was to be characterised, although in most other bacteria, it is not the sole acceptor of electrons from cytochrome *c*, but occurs in combination with a cytochrome *c* oxidase.

To evaluate the results obtained from phenotypical characterisation of the deletion mutant and to relate them to possible impacts on the central carbon metabolism, genome-wide microarray analyses under three conditions were scheduled: I) oxygen limitation vs. oxygen excess, II) pH 4 grown cells vs. pH 6 grown cells and III) cells of growth phase II vs. cells of growth phase I during cultivation on glucose. The concentration of the ubiquinol *bd* oxidase was reported to enhance under oxygen limitation and acidic pH, therefore these conditions were likely to provoke regulation of genes encoding the respiratory chain components.

The membrane-bound glucose dehydrogenase is a highly active enzyme feeding electrons into the respiratory chain and releasing gluconate into the culture medium. Upon glucose exhaustion, *G. oxydans* enters a second phase of growth on gluconate. An unexplained phenomenon is the strongly decreased cell growth in phase II, although most of the gluconate is oxidised by the membrane-bound gluconate-2-dehydrogenase. Thus, the energy supply of the cells should be similar to that of growth phase I. In order to obtain data on the changes in catabolism occurring in growth phase II, genome-wide transcription analysis, enzyme activity measurements and a first ¹³C-metabolome analysis with *G. oxydans* were planned. At the same time, metabolic flux analysis would allow an identification of the principal pathway of glucose catabolism. Genome sequencing and annotation in 2005 demonstrated the presence of all genes encoding the enzymes of the pentose phosphate pathway and the Entner-Doudoroff pathway in *G. oxydans*. In this work resolution of the relative contributions of the two pathways to overall catabolism by metabolic flux analysis was pursued.

III Materials and Methods

1. Bacterial strains

Strains of *Escherichia coli*, *Gluconobacter oxydans* and *Corynebacterium glutamicum* were used in this work (**Table 1**). Recombinant *E. coli* and *G. oxydans* were constructed by transformation with the plasmids shown in **Table 2**; relevant oligonucleotides are listed in **Table 3**.

Table 1: Bacterial strains used in this work

Strain	Genotype	Reference
<i>Escherichia coli</i>		
DH5 α	F ⁻ , Φ 80d/ <i>lacZ</i> M15, <i>recA1</i> , <i>endA1</i> , <i>gyrA96</i> , <i>thi-1</i> , <i>hsdR17</i> (r_k^- , m_k^+), <i>supE44</i> , <i>relA1</i> , <i>deoR</i> , (<i>lacZYAargF</i>) U169	(Hanahan 1983; Yanisch-Perron <i>et al.</i> 1985)
S17-1	<i>recA</i> pro <i>hsdR</i> RP4-2-Tc::Mu-Km::Tn7	(Simon <i>et al.</i> 1983)
BL21/DE3	F ⁻ <i>ompT gal dcm lon hsdS_B</i> (r_B^- m_B^-) λ (DE3 [<i>lacI lacUV5-T7</i> gene 1 <i>ind1 sam7 nin5</i>])	Novagen Inc., Madison, USA
BL21/DE3-pET24- <i>ccp</i>	BL21/DE3 carrying pET24- <i>ccp</i> for over expression of the cyt. c peroxidase of <i>G. oxydans</i>	This work
<i>Gluconobacter oxydans</i>		
621H	Wild type Cef ^R	(De Ley <i>et al.</i> 1984)
621H Δ <i>qcrC</i>	Derivate of 621H, in frame deletion of <i>qcrC</i>	This work
621H Δ <i>qcrABC</i>	Derivate of 621H, in frame deletion of the cyt. <i>bc₁</i> complex operon <i>qcrABC</i>	This work
621H Δ <i>hsdR adh-cyt c_{St}</i>	Derivate of 621H, N-terminal StrepTagII of GOX1067 (Cyt. c subunit of the ADH)	This work
621H-pEXGOX-K- <i>ccp</i> _{His}	Derivate of 621H, carrying the over expression vector for <i>ccp</i> of <i>G. oxydans</i> (Cyt. c peroxidase) and a HisTag sequence	This work
621H Δ <i>hsdR</i>	Derivate of 621H, in frame deletion of the restriction endonuclease HsdR of the restriction-modification system operon <i>hsdRSM</i> (GOX2569-2567)	Schweikert <i>et al.</i> unpublished
<i>Corynebacterium glutamicum</i>		
ATCC13032	Wild type isolate	(Abe <i>et al.</i> 1967)
WT- Δ <i>qcr</i>	Derivate of ATCC13032; deletion of <i>qcrABC</i>	(Niebisch and Bott 2001)

2. Plasmids and oligonucleotides

Table 2: Plasmids used in this work

Plasmid	Relevant characteristics	Reference
pEXGOX-K	Km ^R ; <i>PtufB</i> , Derivate of pEXGOX-G	(Schleyer <i>et al.</i> 2007)
pEXGOX-K _{His}	Km ^R ; Derivate of pEXGOX-K; contains a 175 bp-PCR-fragment including the HisTag and the terminator region of pET24 (Primer His-for and His-rev)	This work
pEXGOX-K- <i>ccp</i> _{His}	Km ^R ; Derivate of pEXGOX-K _{His} ; contains a 1.6 kb-PCR-fragment including the <i>ccp</i> of <i>G. oxydans</i> (Primer <i>ccp</i> -for and <i>ccp</i> -rev)	This work
pLO ₂	Km ^R , <i>sacB</i> , RP4 <i>oriT</i> , ColE1 <i>ori</i>	(Lenz <i>et al.</i> 1994)
pLO ₂ - Δ <i>ccp</i>	Km ^R ; Derivate of pLO ₂ ; contains a 1.5 kb-“crossover-PCR-fragment” of <i>G. oxydans</i> spanning the <i>ccp</i> -region	This work
pET24	Km ^R ; T7 promoter, HisTag coding sequence, T7 terminator, <i>lacI</i> ,	Novagen Inc., Madison, USA
pET24- <i>ccp</i>	Km ^R ; Derivate of pET24; contains a 1.6 kb-PCR-fragment including the <i>ccp</i> of <i>G. oxydans</i> (Primer <i>ccp</i> -for-2 and <i>ccp</i> -rev-2)	
pK19 <i>mobsacB</i>	Km ^R ; <i>E. coli</i> vector suitable for conjugation; <i>oriVEc oriT sacB</i>	(Schäfer <i>et al.</i> 1994)
pK19 <i>mobsacB</i> - Δ <i>ccp</i>	Km ^R , Derivate of pK19 <i>mobsacB</i> ; contains a 1.5 kb-“crossover PCR-fragment” of <i>G. oxydans</i> spanning the <i>ccp</i> -region	This work
pK19 <i>mobsacB</i> - Δ <i>qcrC</i>	Km ^R ; Derivate of pK19 <i>mobsacB</i> ; contains a 1.0 kb-“crossover PCR-fragment” of <i>G. oxydans</i> spanning the <i>qcrC</i> -region	This work
pK19 <i>mobsacB</i> - Δ <i>cydAB</i>	Km ^R ; Derivate of pK19 <i>mobsacB</i> ; contains a 1.1 kb-“crossover PCR-fragment” of <i>G. oxydans</i> spanning the <i>cydAB</i> -region	This work
pK19 <i>mobsacB</i> - Δ <i>qcrABC</i>	Km ^R ; Derivate of pK19 <i>mobsacB</i> ; contains a 1.4 kb-“crossover PCR-fragment” of <i>G. oxydans</i> spanning the <i>qcrABC</i> -region	This work
pK19 <i>mobsacB</i> - <i>adh</i> <i>cyt</i> _{St}	Km ^R ; Derivate of pK19 <i>mobsacB</i> ; contains a 0.7 kb-PCR-fragment of <i>G. oxydans</i> (Primers <i>adh</i> _{St} -for and <i>adh</i> _{St} -rev) with a StrepTagII coding sequence (WSHPQFEK) at the 3'-end of <i>adh</i>	This work
pK18 <i>GII</i> - Δ <i>qcrC</i>	Km ^R ; Derivate of pK18 <i>mobGII</i> ; contains a 1.0 kb-“crossover PCR-fragment” of <i>G. oxydans</i> spanning the <i>qcrC</i> -region	This work

Table 3: Oligonucleotides used in this work. Oligonucleotides were obtained by Eurofins MWG Operon (Ebersberg, Germany). The sequences are given in 5'→ 3'-direction. The relevant features of the oligonucleotides are underlined (Restriction sites), **bold** (Sequences for StrepTag-II) and *italic* (homologous sequences for crossover PCR; us: upstream, ds: downstream)

PCR primer	Sequence	Enzyme
His-for	TATATAG <u>TCGAC</u> CCGGATATAGTTCCTCCTTTCAG	<i>Sall</i>
His-rev	TATATAATTTAAATCACTCGAGCACCACC	<i>SwaI</i>
<i>ccp</i> -for	GTGGTGC GTTCCAGCA	
<i>ccp</i> -rev	GTTTCGAGGAACCAGAACC	
<i>ccp</i> -for-2	TATATACATATGGTGC GTTCCAGCACGATTAC	<i>NdeI</i>
<i>ccp</i> -rev-2	TATATAC <u>TCGAG</u> GTTTCGAGGAACCAGAACCCGACACA	<i>XhoI</i>
<i>adh_{St}</i> -for	TATATA TCTAGA CACCGAGCCTGCGCAG	<i>XbaI</i>
<i>adh_{St}</i> -rev	TATATAG <u>TCGAC</u> TCACTTCTCGAACTGTGGGTGGGAC CATTGTGCGTCGTCCACGCC	<i>Sall</i>
PCR primers used for deletion		
Δ <i>ccp</i> -us-for	TATATAG <u>TCGAC</u> CCATGAGCATGTGTTCCATCTGACCAA G	<i>Sall</i>
Δ <i>ccp</i> -us-rev	CCCATCCACTAAACTTAAACACGTGCTGGAACGCACC ACTTTT	
Δ <i>ccp</i> -ds-for	TGTTTAAGTTTAGTGGATGGGCAGGCTCCTGTGTCTGG GTTCTG	
Δ <i>ccp</i> -ds-rev	TATATATCTAGACAATACACCCCCCATACACGACAGG C	<i>XbaI</i>
Δ <i>qcrC</i> -us-for	TATATAGCATGCCAGACCCTGCCGTTCCACC	<i>SphI</i>
Δ <i>qcrC</i> -us-rev	CCCATCCACTAAACTTAAACACCGGGTCCAGCGCGTC AT	
Δ <i>qcrC</i> -ds-for	TGTTTAAGTTTAGTGGATGGGCTGCTGCAACGCCGCA TC	
Δ <i>qcrC</i> -ds-rev	TATATAGGATCCCGTGTGGTTCGCTGCTTCTTTGC	<i>BamHI</i>
Δ <i>qcrC</i> -us-for-2	TATATAG <u>TCGAC</u> CCAGACCCTGCCGTTCCACC	<i>Sall</i>
Δ <i>qcrC</i> -ds-rev-2	TATATATCTAGACGTGTGGTTCGCTGCTTCTTTGC	<i>XbaI</i>
Δ <i>qcrABC</i> -us-for	TATATAG <u>TCGAC</u> GATCACATGAGCCGTCTGAAGGGCG G	<i>Sall</i>
Δ <i>qcrABC</i> -us-rev	CCCATCCACTAAACTTAAACACTGGGTCATGCGGAAC CTCTGCCG	
Δ <i>qcrABC</i> -ds-for	AGTTTAGTGGATGGGCGCCGCTGACCGAGCTGAACT ACATC	
Δ <i>qcrABC</i> -ds-rev	TATATATCTAGAGACAGCCGTGAGCCGCATCGTTTC	<i>XbaI</i>
Δ <i>cydAB</i> -us-for	TATATAG <u>TCGAC</u> GCAGGGCGCCCTCG	<i>Sall</i>
Δ <i>cydAB</i> -us-rev	CCCATCCACTAAACTTAAACACATGTCGATTGCCTTCT GGG	
Δ <i>cydAB</i> -ds-for	TGTTTAAGTTTAGTGGATGGGTGAGAACAGGGAGGCC	
Δ <i>cydAB</i> -ds-rev	TATATATCTAGAGCACATCCCCGCAGAAC	<i>XbaI</i>
Deletion control primer and sequencing primer		
<i>c</i> Δ <i>qcrC</i> -for	CCCTGCATGTCGCGGGC	
<i>c</i> Δ <i>qcrC</i> -rev	CCCGCGTTCAAAAGAACGGG	
<i>c</i> Δ <i>qcrABC</i> -for	GAATGAACGCAGCTAGTCAG	
<i>c</i> Δ <i>qcrABC</i> -rev	CTGCACGGCCAGGTG	
<i>c</i> Δ <i>cydAB</i> -for	GTGGTTTCAGCACTTCTC	
<i>c</i> Δ <i>cydAB</i> -rev	CGACGTTTGCGCGG	

III Materials and Methods

cΔ <i>ccp</i> -for	GCTGAACTCGGCGCGTTTC	
cΔ <i>ccp</i> -rev	CAGACATTCCGTGATGAAATGGC	
Univ (fragments in pK18 <i>mob</i> and derivatives)	CGCCAGGGTTTTCCCAGTCACGACG	
rspl (fragments in pK18 <i>mob</i> and derivatives)	GGAAACAGCTATGACCATG	
cDNA synthesis primer for RT-PCR		
cDNA0278	CTCCGCCATGCCAGCGTC	
cDNA1914	GCGGGACATCATGTTGATGG	
cDNA1675	CCAGATCAGGTTTGACCGGCG	
cDNA0564	CATGAGCCGTCTGAAGGG	
Primer for Light cycler		
LC0278-for	CCCCGCTGCTGTTCTTCTCCTTCC	
LC0278-rev	GAAGCCCGCAGGCGACATGAAC	
LC1914-for	ACCCAGGCTCCTACCACCACG	
LC1914-rev	CGATGATGACGATCACCGATGCC	
LC1675-for	GACCGGTTTCAGCCTCAAATCCGG	
LC1675-rev	CCTGCGTGGTCTGAAGCGTGGTG	
LC0564-for	GGGGACTTTTCCTCCGCTTG	
LC0564-rev	GCGGAATGAGGGCATGAATC	
Primer for amplification of “standard” genes, used for quantification in the light cycler		
Q0278-for	GTGGCTGGCGTTGCCGG	
Q0278-rev	GCACATGGGCCTCGC	
Q1914-for	AGTAAGAGGGGCGCATAAGACTT	
Q1914-rev	CTTTCGAAACCTGAGGGTAGG	
Q1675-for	CGTTTCGCACTTGATATGAGGAAAAATC	
Q1675-rev	CCTCTTTGACGGGCTTCTGAAAAG	
Q0564-for	GTACCGGGGAAAATGC	
Q0564-rev	CAAAATATGTCCGTTTTTC	

3. Chemicals and enzymes

Chemicals were obtained from Sigma-Aldrich Chemie GmbH (Taufkirchen, Germany), Merck KGaA (Darmstadt, Germany), Fluka (Neu-Ulm, Germany) or Roth GmbH + Co.KG (Karlsruhe, Germany). Biochemicals and enzymes (including related buffers) were from Roche Diagnostics GmbH (Mannheim, Germany), New England Biolabs (Frankfurt, Germany) and Invitrogen (Karlsruhe, Germany). 1-¹³C-D-glucose and U-¹³C-glucose were obtained from Deutero GmbH (Kastellaun, Germany). Auxiliary enzymes for activity assays (glucose 6-phosphate dehydrogenase and 6-phosphogluconate dehydrogenase from yeast) were purchased from Sigma-Aldrich (Taufkirchen, Germany) and Merck (Darmstadt, Germany). Media components

"Bacto-Peptone", "Bacto Yeast extract" and "Bacto-Agar" were obtained from Becton Dickinson GmbH (Heidelberg, Germany).

4. Media

E. coli was cultivated in Luria-Bertani (LB) medium (Sambrook and Russel 2000).

For anaerobic cultures, the following medium was used (Pope and Cole 1982):

<u>Medium for anaerobic growth</u>		<u>Trace element solution</u>	
50 ml	LB medium	0.4 g	FeCl ₂
1 ml	trace element solution	8.2 g	MgCl ₂
5.5 g	KH ₂ PO ₄	1.0 g	MnCl ₂
10.5 g	K ₂ HPO ₄	0.1 g	CaCl ₂
1.0 g	(NH ₄)SO ₄	2 ml conc. HCl	
0.5 g	Sodiumcitrate	Ad 100 ml aqua bidest	
0.1 g	MgSO ₄		
200 mg	Ammonium molybdate		
7.0 g	Fumaric acid		
2.0 g	Glucose		
4.0 g	Glycerol		
350 mg	Nitrate		
350 mg	Nitrite		

G. oxydans was cultivated in a medium which contained 5 g l⁻¹ yeast extract, 2.5 g l⁻¹ MgSO₄ x 7 H₂O, 0.5 g l⁻¹ glycerol and 80 g l⁻¹ glucose or mannitol as a carbon source (Bremus 2006). For growth of *G. oxydans* before electroporation, EP medium was used (Bremus 2006) (15 g l⁻¹ yeast extract, 2.5 g l⁻¹ MgSO₄ x 7 H₂O, 0.5 g l⁻¹ glycerol and 80 g l⁻¹ mannitol).

Media for bacterial growth were sterilised for 20 min at 121°C. Antibiotics were added after cooling down to 50°C. Cultures of *G. oxydans* and *E. coli* were supplemented with 50 ng µl⁻¹ cefoxitin or kanamycin as antibiotica. 15 g l⁻¹ agar was added for preparation of solid plates.

5. Culture conditions of *G. oxydans* and *E. coli*

For cultivation of *E. coli*, LB-medium was inoculated with single colonies and cells were cultivated at 37°C over night. The main cultures of 50-500 ml LB-medium were inoculated at an OD₆₀₀ of 0.1-0.3 in 0.3-2.0 l flasks and cultured at 120 rpm and 37°C. For anaerobically growth of *E. coli*, the over night culture was inoculated at a ratio of 1:100 in a 500 ml flask containing 500 ml of the medium for anaerobic growth and cultivated for 8 h at 90 rpm and 37°C. 50 ml of the culture were inoculated in 2 l flasks containing 2 l of the medium for anaerobic growth and cultured at 30 rpm and 37°C for 12 h. Induction with IPTG (0.5 mM final concentration) occurred after 9 h.

G. oxydans was grown in 0.3-5.0 l flasks filled with 0.05-1.0 l medium. Precultures were inoculated with single colonies and grown over night at 180 rpm and 30°C. Main cultures were inoculated at an OD₆₀₀ of 0.1-0.3 and grown as described. Growth of bacteria in liquid cultures was determined by measuring the optical density at 600 nm in an “Ultrospec 300 pro photometer” (Amersham Bioscience, Freiburg, Germany). Cell densities above absorption of 0.3 were diluted to assure linearity.

G. oxydans was cultivated in the “FedBatch-Pro” fermentation system (DASGIP AG, Jülich, Germany) for controlled growth conditions (control of pH and oxygen availability) in four parallel 250 ml bioreactors (**Fig. 4**). Each reactor was equipped with electrodes for measuring the pH value and the concentration of dissolved oxygen (DO) in the medium. Automatic titration with 2 M NaOH maintained the pH. The oxygen electrodes were calibrated by gassing with air (100% DO) and N₂ (0% DO). The cultures were gassed with a fixed concentration of O₂ (2% O₂) to obtain oxygen limitation if desired. At the beginning of growth, the concentration of oxygen was not limiting. When the cell density increased, oxygen consumption of the culture increased. The gassing with 2% O₂ did not allow an increase in oxygen concentration in the medium resulting in oxygen depletion during cell growth. Another approach was to keep the DO of the medium statically at e.g. 15% during growth. The software of the fermentation system was able to calculate the right gas mixture of O₂, N₂ and air in different ratios in order to maintain the 15% DO at any time of cell growth. Higher oxygen consumption caused by higher cell densities were balanced with higher percentage of air or O₂ in the mixture. Consequently, the cells were never oxygen-limited, independent of cell growth. Gassing rates as well as concentrations of gases, which were gassed into the cultures, were recorded as well as leaving gas concentrations. Thus, the O₂ consumption and CO₂ production of growing cells were calculated. The software of the DasGip fermentation system performed calculation of oxygen transfer rates and carbon dioxide transfer rates. Gassing rate was constant with 12 standard l min⁻¹ and the magnetic stirrer was set at 900 rpm. The pH was kept at 4 or 6 and the cells were cultured at 30°C.

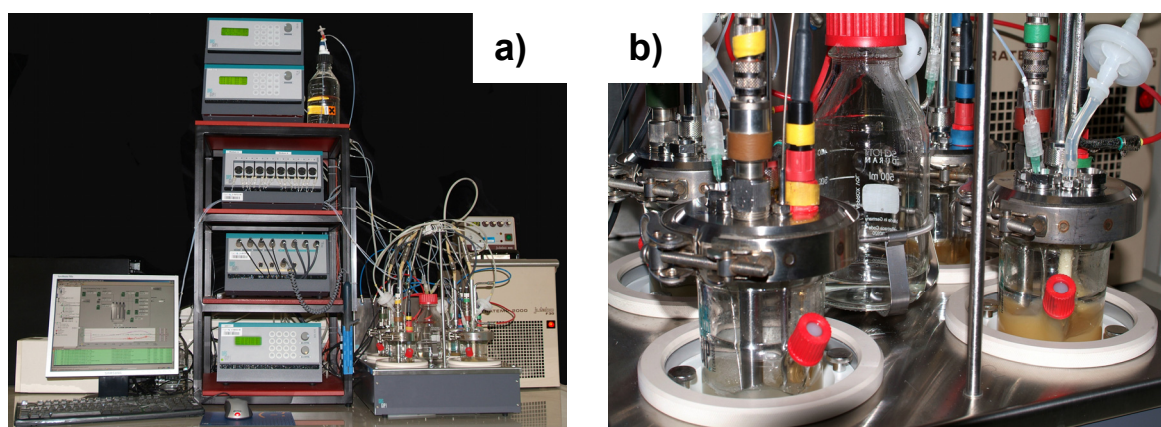


Fig. 4 “Fedbatch-Pro“-fermentation system a) Complete system of the „Fedbatch-Pro“-fermentation system; b) detailed picture of the four reaction bioreactors

6. Determination of cell dry weight

The cell dry weight of *G. oxydans* 621H was determined by applying membrane filtration (Bratbak and Dundas 1984). A cellulose filter with a pore diameter of 0.45 μm (Millipore, Schwalbach, Germany) was dried for 24 h at 110°C, cooled down in an exsiccator and weighted. 10 ml samples of growing *G. oxydans* was harvested at different time points, filtrated and washed with 100 ml of distilled water. Samples were weighted again after drying for 24 h at 110°C and cooling down in an exsiccator. From the net weight the following correlation was calculated for *G. oxydans*: Biomass cell dry weight (CDW) [g l^{-1}] = 0.23 x OD_{600 nm}.

7. Stock cultures

Strains of *G. oxydans* and *E. coli* were stored as glycerol stocks. Strains were grown until exponential growth phase and 1 ml of the culture was mixed with 1 ml stock solution (67% glycerol (w/v), 13 mM MgCl₂) and stored at -70°C (Sambrook and Russel 2000).

8. Molecular biological methods

8.1 Isolation of DNA

DNA fragments from agarose gels were isolated with the QIAquick Gel Extraction Kit (Qiagen, Hilden, Germany) following the manufacturer’s instructions. PCR products and fragments of restriction reactions were purified with the PCR Purification Kit (Qiagen, Hilden, Germany). Genomic DNA of *E. coli* or *G. oxydans* was isolated with the DNeasy Tissue Kit “DNA purification from bacteria” (Qiagen, Hilden, Germany) according to the manufacturer’s instructions. Genomic DNA was stored at 4°C. Plasmid DNA of *E. coli* for cloning, sequencing and transformation was isolated after alkaline lysis of the cells following the protocol of the QIAprep Spin

Miniprep Kit (Qiagen, Hilden, Germany). Plasmid DNA was isolated from *G. oxydans* in the same way by adapting the protocol to higher culture volumes (20 ml instead of 2 ml) and addition of 15 mg ml⁻¹ lysozyme to buffer P2. Plasmids were eluted from the column with 20 µl H₂O or elution buffer (Tris pH 8) and stored at -20°C. Concentration of nucleic acids was determined at 260 nm (Sambrook *et al.* 1989) (NanoDrop ND-1000 UV-Vis Spektralphotometers, Peqlab, Erlangen, Germany). The quality of the DNA was controlled using the OD₂₆₀/OD₂₈₀ ratio. Protein-free samples show a ratio between 1.8 and 2.2 (Gallagher and Desjardins 2007). Samples were sent to Agowa (Berlin, Germany) for sequencing.

8.2 Recombinant DNA-techniques

For DNA restriction, 2-10 µg DNA was digested in 50 µl total volume with 5 U enzyme and 5 µl of the required buffer (recommendations of manufacturer). If two or more restriction enzymes were used, it was necessary to use the same restriction buffer. Restriction was finished after 1-2 h. The restricted DNA-fragments were used for analytical applications or in order to ligate them into a desired vector. Before ligation, the restricted plasmid was dephosphorylated in order to keep down vector self-ligation. An alkaline dephosphatase was used following the manufacturer's instructions (Roche, Mannheim, Germany). The DNA-fragment was mixed with the dephosphorylated vector for ligation (Rapid DNA ligation kit, Roche, Mannheim, Germany). For blunt end ligations, 10-fold excess of the insert was used. For sticky end ligation, a 3-fold excess was sufficient. 50 ng of vector was applied and the required concentration of DNA-insert was calculated using the following formula (Instructions of ROCHE):

$$\frac{50 \text{ ng vector} \times \text{size of the fragment}}{\text{size of the vector}} \times \text{factor of excess} = \text{ng DNA-fragment}$$

8.3 Polymerase chain reaction (PCR)

The polymerase chain reaction was performed to amplify genomic DNA for cloning or for controlling deletion mutants (Mullis and Faloona 1987, Rabinow *et al.* 1996). Isolated genomic DNA and plasmids served as PCR templates. Colony PCR was used for screening for correct deletion clones. Amplification of DNA in colony PCR occurred with DNA of broken cells without an isolation of the genomic DNA as described previously. Therefore, a small amount of cells was heated in 100 µl water at 95°C for 5 min for cell disruption before adding 3 µl of this cells suspension in the PCR reaction. PCR was performed using the T3 thermocycler (Biometra, Göttingen).

Germany). For preparative applications, a high fidelity polymerase (Phusion, Finnzymes, MA, USA) was used according to the manufacturer's instructions. Denaturation of the DNA was achieved at 98°C. For non-preparative applications, the "Taq" polymerase was used (Qiagen, Hilden, Germany) which has its denaturation temperature at 95°C. The annealing temperature was dependent on the length and the GC-content of the primers used. In most cases, the primers had an annealing temperature of 60°C. The melting temperature was calculated according to the following formula:

T_M (Melting temperature) = 4 x (G+C) + 2 x (A+T) (Ashen *et al.* 2001).

Elongation occurred at 72°C and reactions were performed for 35 cycles.

8.4 Agarose gel electrophoresis

For analytical and preparative gel electrophoresis of DNA, horizontal electrophoresis chambers were used with 1% (w/v) agarose gels (GibcoBRL Ultra Pure Agarose, Invitrogen, Karlsruhe, Germany) in 1x TAE buffer. Separation of DNA fragments occurred at 80 V and gels were stained with ethidium-bromide solution (1 µg ml⁻¹) for at least 10 min. Washing was performed in water for 10 min. DNA-fragments were analysed using UV-light (Image Master VDS System, Amersham Biosciences). The size of the fragments was determined by comparison to an appropriate DNA-standard.

The quality of RNA was inspected with formaldehyde-containing agarose gels (Sambrook and Russell 2001). 10x FA buffer (200 mM MOPS, 50 mM sodium acetate, 10 mM EDTA ad 1 l with aqua bidest, pH 7.0) was used in the FA-running buffer (100 ml 10x FA buffer, 20 ml 37% formaldehyde 880 ml RNase-free water). The gel for separation of RNA contained 1.2 g agarose, 10 ml 10x FA buffer, 1.8 ml 37% formaldehyde, ad 100 ml RNase-free H₂O. RNA samples (0.5 µg) were mixed with RNA-loading dye (60 µl of saturated bromphenolblue, 80 µl 0.5 M EDTA pH 8.0, 720 µl 37% formaldehyde, 2 ml 100% glycerol, 4 ml 10x FA buffer, 3 ml formamide). After heating for 10 min at 65°C and incubation for 5 min on ice the RNA was loaded onto the gel. Electrophoresis was performed at 80 V. The quality of the RNA was analysed on the basis of the 16s and 23 s RNA, which should migrate as clear defined bands in the gel.

8.5 Transformation of *E. coli* and *G. oxydans*

Heat-shock competent cells of *E. coli* were generated following the RbCl-method (Cohen *et al.* 1972) and 60 ng plasmid DNA were added to the cells (Hanahan *et al.* 1983). Afterwards, cells were incubated on ice for 30 min. Then, cells were heated to

42°C for 2 min, cooled down on ice for 2 min and 1 ml LB-medium was added. Finally, cells were incubated at 37°C for at least 1 h before they were plated on selective solid plates.

For the electroporation of the wild type strain *G. oxydans* 621H competent cells were prepared by the method of Mostafa *et al.* 2002. Only replicative plasmids were transformed by electroporation (Trevors and Stradoub 1990, Choi *et al.* 2006). Cells were grown in 100 ml EP medium to an OD₆₀₀ of about 0.8, washed twice with 1 mM HEPES-buffer and resuspended in 400 µl 1 mM HEPES. 50 ng of plasmid DNA was added to 100 µl of cells. Electroporation of the cells was carried out with the Gene Pulser Xcell (BioRad, Munich, Germany) in electroporation cuvettes with 1 mm electrode distance. After the pulse (2.0 kV, 25 µF, 200 Ω), cells were directly resuspended in 1 ml electroporation medium and transferred to 15 ml falcon tubes. After 16 h incubation at 30°C at 100 rpm, cells were cultivated on selective solid plates and incubated at 30°C for 2-3 days.

Non-replicative plasmids had to be transferred into *G. oxydans* by biparental mating using *E. coli* S17-1 (Simon *et al.* 1983) containing the target vector as the donor since with electroporation no colonies were obtained. 50 ml cultures of *E. coli* and *G. oxydans* were grown to OD₆₀₀ of about 0.6 (*E. coli* in LB-medium with 50 µg ml⁻¹ kanamycin; *G. oxydans* in mannitol medium with 50 µg ml⁻¹ cefoxitin) and washed twice in non-selective medium. Cells were resuspended in mannitol medium without kanamycin or cefoxitin and mixed in a 1:1 ratio. The cells were plated on non-selective solid agar and incubated over night at 30°C. The cells were scraped from the plates and cultivated on selective mannitol medium agar containing cefoxitin and kanamycin (50 µg ml⁻¹ each). Only plasmid-containing cells of *G. oxydans* were able to survive since *E. coli* is cefoxitine sensitive. Plates were incubated at 30°C for 2-3 days until recombinant cells formed colonies.

8.6 Overexpression of the *G. oxydans* *ccp* gene encoding cytochrome *c* peroxidase

Cells of *E. coli* BL21 (DE3) carrying the recombinant vector pET24-*ccp* were inoculated in 50 ml LB medium with 50 µl ml⁻¹ kanamycin and grown over night at 37°C. Up to 500 ml culture volumes were inoculated at an OD₆₀₀ of 0.1 in LB medium, containing 50 µl ml⁻¹ kanamycin. Cells were grown to an OD₆₀₀ of 0.8 at 37°C and then expression of the target gene was induced by adding IPTG (0.5 mM final concentration). Cultures were incubated at room temperature for 4 h at 120 rpm. Cells were harvested by centrifugation at 5,300 *g* for 10 min at 4°C. To control the

overexpression of the cytochrome *c* peroxidase, 50 µl samples were taken before induction and every hour until cell harvest and analysed with SDS-PAGE.

8.7 Construction of marker-free deletion mutants

The non-replicative vector pK19mobsacB (Schäfer *et al.* 1994) was used to generate a vector for marker-free deletion. For in-frame deletions, around 600 bp flanking regions of the target gene or operon were amplified. The fragments were fused together by “crossover PCR” and this insert was cloned into pK19mobsacB. The *E. coli* strains bearing the deletion vector pK19mobsacB grew very weakly, so that the suicide vectors pLO₂ (bearing *sacB* for counter selection) and pK18mobGII (Katzen *et al.* 1999) (bearing the *gusA* gene for counter selection) were used as possible improvements of the method. However, the respective transformed S17-1 cells did not grow better than pK19mobsacB bearing cells and were not used further. The deletion vectors were transformed into *G. oxydans* 621H by biparental mating resulting in kanamycin-resistant, sucrose-sensitive colonies. Five colonies were selected and cultivated in 100 ml non-selective medium at 30°C over night. 100 µl of non diluted cells were directly cultivated on selective and non selective mannitol medium agar plates containing 10% sucrose and grown for 2-3 days at 30°C. Kanamycin-sensitive, sucrose-resistant colonies were picked and analyzed via colony PCR. *G. oxydans* DSM2343-Δ*qcrABC*, for example, was identified using 5′ GAATGAACGCAGCTAGTCAG and 5′ CTGCACGGCCAGGTG, resulting in a 3976 bp PCR fragment in wild type cells, but 1456 bp PCR fragment in the desired deletion strain, where the sequence encoding the cytochrome *bc*₁ complex was missing.

8.8 RNA preparation

For total RNA preparation the RNeasy kit (QIAGEN, Hilden, Germany) was used according to the manufacturer’s instructions. Cells were disrupted with a Mini-BeadBeater (Silamat S5, ivoclar, Ellwangen, Germany) by four intervals of 15 s each. DNA digestion was performed directly on the column where the DNA was bound for its isolation by adding 30 U DNase, RNase-free (QIAGEN, Hilden, Germany) for 20 min (manufacturer’s instructions). RNA concentration and quality was checked photometrically and on formaldehyde-containing gels according to standard procedures (Sambrook *et al.* 1989).

8.9 cDNA labeling and RT PCR

cDNA synthesis for microarray analysis was performed according to Polen *et al.* 2007. 25 µg RNA were used for random hexamer-primed synthesis of fluorescence-labeled cDNA with the fluorescent nucleotide analogues Cy3-dUTP and Cy5-dUTP (GE Healthcare, Freiburg, Germany). The mixture contained 3 µl 1 mM Cy3-dUTP or Cy5-dUTP, 3 µl 0.1 M DTT, 6 µl 5x first strand buffer (Invitrogen, Karlsruhe, Germany), 0.6 µl dNTP-mix (dATP: 25 mM, dCTP: 25 mM, dGTP: 25 mM and dTTP: 10 mM) and 2 µl Superscript II polymerase (Invitrogen, Karlsruhe, Germany).

For quantitative real time PCR experiments, 500 ng RNA were transcribed into cDNA using specific primers for the genes under investigation according to manufacturer's instructions (Omniscript RT, Qiagen, Hilden, Germany). The products were quantified via real-time PCR using a LightCycler instrument 1.0 (Roche, Basel, Switzerland) with SYBR Green I as the fluorescence dye following the instructions of the supplier (QuantiTect SYBR Green PCR, Qiagen, Hilden, Germany). To quantify the amount of cDNA, a calibration curve was generated from eight known concentrations of the genes of interest processed in parallel via real-time PCR. For each concentration of cDNA, the "no amplification control" (NAC) was subtracted; these controls contained water instead of RTase.

8.10 *G. oxydans* DNA microarrays

For genome-wide transcription analyses *G. oxydans* DNA microarrays were obtained from Eurofins MWG Operon, Ebersberg, Germany. The array design comprises 3864 sequence-specific oligonucleotide probes (70mer). 2731 oligonucleotides represent all annotated protein coding genes from *G. oxydans* 621H genome (NC_006677) and plasmids (NC_006672, NC_006673, NC_006674, NC_006675, NC_006676), as well as 67 genes for structural RNAs. 939 selected oligonucleotides represent intergenic regions >100 bp (2 probes for IGRs >500 bp). 127 further oligonucleotide probes (from *B. subtilis* 168, Alien spike controls, *lacI*, *lacZ*, *tetA*, *cat*, *aph*) were included as negative and positive controls to check for quality and specificity. Oligo probes for genes GOX0265, GOX0854, GOX1675, GOX2188 and GOX2290 with 100%, 90%, 80%, 70%, 60% and 50% sequence specificity served as specificity controls of hybridisation. The oligonucleotide set was spotted in duplicate on glass slides resulting in two identical sub-arrays of 2 x 2 cm, each having spot sizes of 80 to 100 µm and about 225 µm spot distance (MI Microarrays Inc., Huntsville, AL, USA).

Preparation of the oligonucleotide-slides for hybridization was performed in 50 ml Falcon tubes. All reagents were obtained from the OpArray system from Eurofins

MWG Operon. Slides were incubated at 42°C in Pre-Hybridisation solution for 1 h for blocking of potential unspecific binding sites, then transferred into Wash 1 (1.25 ml Wash B and 48.75 ml H₂O) and incubated for 5 min at 37°C. The slides were washed with H₂O and dried in a centrifuge at 1600 rpm for 5 min. Hybridization of the mRNA to the oligos on the slides was carried out for 16-18 h at 42°C using a “MAUI” hybridization system (BioMicro Systems, Salt Lake City, USA). For the post-hybridization, slides were washed with decreasing salt concentrations at 37°C in Wash 2 (5 ml Wash A, 2.5 ml Wash B and 42.5 ml H₂O) and Wash 3 (5 ml Wash A and 45 ml H₂O) for 10 minutes each. This procedure removed unspecifically-bound mRNA from the slides. The slides were rotated in Wash 4 solution (1 ml Wash A and 49 ml H₂O) for 5 min at room temperature and then dried by centrifugation.

The fluorescence of the hybridized DNA arrays was determined at 532 nm (Cy3-dUTP) and 635 nm (Cy5-dUTP) at a 10- μ m resolution with a GenePix 4000B laser scanner (Axon Instruments, USA). Quantitative image analysis was carried out using GenePix image analysis software and results were saved as GPR-file (GenePix Pro 6.0, Axon Instruments, CA, USA). For data normalization, GPR-files were processed using the BioConductor/R-packages *limma* (Dudoit and Yang 2003) and *marray* (Smyth 2005) (<http://www.bioconductor.org>). For further analysis, the processed and loess-normalized data, as well as detailed experimental information according to MIAME (Brazma *et al.* 2001) were stored in the in-house microarray database (Polen and Wendisch 2004).

Each microarray experiment was repeated at least three times in biological independent experiments. To search for differentially expressed genes, following criteria had to be fulfilled (i) Signal over background ratios exceeding a factor of 5 for the red or green signal for reliable signal detection, (ii) Reliable detection was confirmed in at least two out of three hybridizations, (iii) Average relative mRNA level changes were at least 1.8 fold, (iv) Significance was assured by a statistical test, the calculated *p*-value had to be < 0.05 to assure that the results were significant.

9. Biochemical methods

9.1 Cell disruption, preparation of crude extracts and membrane fractions

For disruption of cells in a French press, cells of *G. oxydans* or *E. coli* were resuspended in 20 ml disruption buffer, which was the reaction buffer for enzyme assays including one tablet of protease inhibitor (Complete, EDTA-free, Roche, Mannheim, Germany) and disrupted by passing three times through the French Press (1,600 Psi, sim aminco, Spectronic instruments, Rochester). For small cell volumes

(3 ml), cells were broken by 3 min of ultrasonification (UP 200s sonifier, Dr. Hielscher, Stuttgart, Germany, cycle 0.5, amplitude 70) in an ice bath.

In order to obtain cell crude extracts, cell debris of disrupted cells was removed by centrifugation at 5,500 *g* for 20 min at 4°C. This supernatant was used as crude extract. For preparation of membranes, the supernatant was centrifuged for 60 min at 180,000 *g* at 4°C. The membrane-bound enzymes in the resulting pellet were solubilised with 10% DDM (*n*-dodecylmaltoside) so that 2 g DDM per 1 g protein was added. To enhance solubilisation, the suspension was stirred for 1 h at 4°C. After that, the solution was centrifuged again for 60 min at 180,000 *g* at 4°C in order to separate the membranes in solution and the non-solubilised membranes from each other. That supernatant was used as membrane fraction.

9.2 Determination of protein concentration

Concentrations of proteins were determined with the BCA (bicinchoninic acid) assay (Smith *et al.* 1985). It is based on the Biuret-reaction, where Cu²⁺-ions react with proteins to Cu⁺. Cu⁺ forms violet complexes with the BCA. 25 µl protein-sample were added to 200 µl BCA solution and incubated at 37°C for 30 min. Protein concentrations were determined at 562 nm since the violet complex has its absorption maximum at this wave length. (Molecular device spectramax plus, GMI, Minnesota, USA) using bovine serum albumine as a standard.

9.3 Polyacrylamide gel electrophoresis of proteins (SDS-PAGE)

The SDS-PAGE (Laemmli *et al.* 1970) was used for separation of soluble or solubilised membrane proteins according to their molecular mass and performed in vertical chambers (BioRad laboratories, Munich). The proteins were separated in a collection gel containing 4% acryl amide and a separation gel (containing 12% acryl amide) after they were mixed with 2-fold loading dye (350 mM Tris, 10% (w/v) SDS, 6% β-mercaptoethanol, 30% (v/v) glycerol, 0.001% bromphenol blue, pH 6.8) and denatured for 5 min at 95°C. Separation occurred at a maximum voltage of 200 V. Protein staining was performed with Coomassie Blue. Gels were washed with aqua bidest, stained for 20 min (0.6 g Serva blue G250, 0.6 g Serva blue R250, 454 ml methanol and 92 ml 96% acetic acid ad 1 l aqua bidest) and washed again with aqua bidest. For destaining, the gel was incubated for 2 h in destaining solution (454 ml methanol and 92 ml 96% acetic acid ad 1 l aqua bidest).

9.4 Protein purification by column chromatography

Gel filtration was used to separate proteins from a reddish colored pigment, both present in the supernatant of *G. oxydans* 621H-Δ*qcrABC* after about 40 h of

cultivation under oxygen limitation. 70 ml of the supernatant was passed through a HiPrep 26/10 desalting column (GE Healthcare, Freiburg, Germany) connected to an Äkta explorer system (Amersham Bioscience, Freiburg, Germany). Proteins were eluted with 50 mM KPi buffer pH 8.0 at 4°C and a flow rate of 5 ml min⁻¹. Detecting wavelength were set at 280 nm and protein elution could be followed. The reddish pigment accumulated in the first fourth of the column and had to be eluted with 20% ethanol. Since it was assumed that the red pigment was heme, 410 nm and 552 nm were used as detecting wavelength. In a second approach, the reddish pigment was eluted with 20% methanol.

Affinity chromatography with StrepTactin-Sepharose (Skerra and Schmidt 2000) was used to purify the cytochrome *c* subunit of the alcohol dehydrogenase with a chromosomally introduced StrepTag II (Sequence: WSHPQFEK). The solubilised membrane fraction of a 3 l *G. oxydans adh-cyt c_{St}* culture was used for the purification. 60 µl of avidine solution (5 mg ml⁻¹ of hen protein, Sigma, Taufkirchen, Germany) was added for avoiding unspecific binding of natural biotinylated proteins to the column material. The solubilised membrane-suspension was loaded into a column with 2 ml volume (1 ml bed-volume) StrepTactin-Sepharose (IBA, Göttingen, Germany), which was equilibrated with 20 ml buffer (100 mM Tris/HCl pH 7.5 and 0.1% DDM). The tagged cytochrome *c* subunit of the ADH bound to the column material due to specific interaction between the StrepTagII and the StrepTactin Sepharose. After washing with 15 ml buffer (100 mM Tris/HCl pH 7.5, 100 mM NaCl, 2 mM MgSO₄ and 0.1% DDM) for removing unspecific proteins from the column material, the three subunits of the alcohol dehydrogenase were eluted by adding 1 ml elution buffer (washing buffer + 15 mM desthiobiotine, Sigma, Taufkirchen, Germany) for eight times.

Protein purification of polyhistidin tagged cytochrome *c* peroxidase of *G. oxydans* was performed with 2 ml Ni²⁺-NTA-agarose (1 ml bed-volume) in 15 ml polypropylene columns (Qiagen, Taufkirchen, Germany), after equilibration with 20 ml TNI5 buffer (Tris sodiumchloride with 5 mM imidazole). Unspecifically bound proteins were eluted by washing with 20 ml TNI20 (Tris sodiumchloride with 20 mM imidazole). Specific protein was eluted by increasing the concentration of imidazole. Therefore, 6 ml of TNI50, TNI70, TNI100, TNI200 and TNI400 were loaded to the column after each other. Specific-bound proteins eluted at TNI 100. The column was regenerated by washing with 20 ml "Strip" buffer (EDTA for removal of Ni²⁺ ions) and equilibrating with 5 ml 100 mM NiSO₄ for new chromatographies.

9.5 Determination of oxygen consumption rates with a Clark electrode

Oxygen consumption rates of exponential grown, intact cells of *G. oxydans* were measured in a 2 ml chamber with an oxygen electrode of the Clark type (Hansatech Instruments Ltd., Norfolk, GB). The chamber was used according to the manufacturer's instructions and the temperature of the measuring cell was set to 30°C. For quantification of oxygen concentrations in the reaction chamber, the chamber was filled with 50 mM KPi pH 6 or 4 and electrode was calibrated by gassing the buffer with air until a constant rate was measured. The baseline at zero was set by adding DTT, which consumed oxygen rapidly. Then, oxygen consumption measurements were performed in 50 mM KPi-buffer pH 6 or 4, cell density was set to OD₆₀₀ 0.5. The reaction started after addition of the substrate (end concentration of 25.5 mM glucose, 21.25 mM ethanol or 25.5 mM sorbitol). The linearity of the oxygen consumption was tested by doubling or reducing the cell density. The measurements were repeated in three biological independent approaches. 10 µl of 10 mM CCCP was added as uncoupler, which decreased the membrane potential. With this uncoupler addition, an energy dependency of the specific dehydrogenase activity was tested.

9.6 Determination of enzyme activities

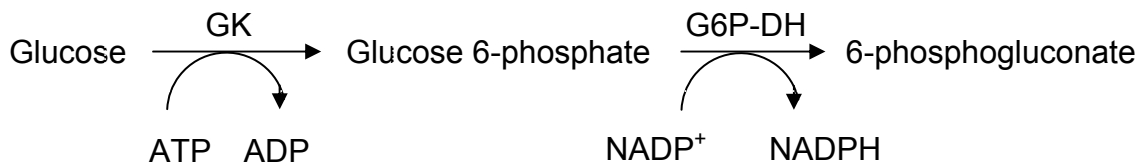
Enzyme activities were determined using an "Ultrospec 4300 pro" photometer (Amersham Bioscience, Freiburg, Germany). Substrate-dependent changes of redox states of cofactors and artificial electron acceptors were determined at 30°C at the specific wavelength. Measurements were performed in 1.5 ml cuvettes (see below for concentrations of substrates) after pre-warming for 2 min at 30°C and starting with the enzyme. Extinction changes were followed for 2 min. For calculation of the specific enzyme activities [U/mg protein], following formula was used:

$$A \text{ [U mg}^{-1} \text{ Protein]} = [(E \text{ t}^{-1} \times V) / (v \times d \times \epsilon)] / (\text{mg protein ml}^{-1})$$

(E, Change of extinction; t, time [min]; V, total volume [µl]; v, volume of the probe [µl]; d, thickness of the cell [cm]; ε, molar extinction coefficient).

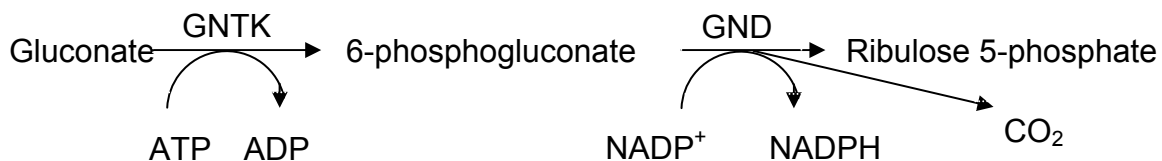
One unit of enzyme activity (U) was defined as the amount of enzyme catalysing the conversion of 1 µmol substrate per min at 30°C. Enzyme activities were determined for at least three biological independent replicates of 50 ml cultures and different dilutions of the samples were used to ensure linearity.

Glucose kinase (GK) (Fraenkel and Levison 1967)



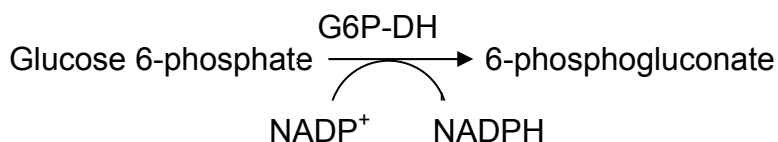
Glucose kinase (GK) catalyses the ATP-dependent phosphorylation of glucose to glucose 6-phosphate, which is then determined by using glucose 6-phosphate dehydrogenase (G6P-DH) as auxiliary enzyme. NADPH formation was followed at 340 nm ($\epsilon_{\text{NAD(P)H}} = 6.22 \text{ mM}^{-1} \text{ cm}^{-1}$). The reaction mixture contained 50 mM Tris/HCl pH 7.5, 10 mM MgCl_2 , 0.5 mM glucose, 0.2 mM NADP^+ , 2 mM ATP, 1.5 U glucose 6-phosphate dehydrogenase and 50 μl crude extract.

Gluconate kinase (GNTK) (Fraenkel and Levison 1967)



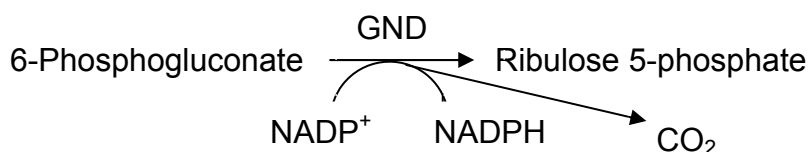
Gluconate kinase (GNTK) catalyses the ATP-dependent phosphorylation of gluconate to 6-phosphogluconate, which is then determined by using 6-phosphogluconate DH (GND) as auxiliary enzyme. NADPH formation was followed at 340 nm ($\epsilon_{\text{NAD(P)H}} = 6.22 \text{ mM}^{-1} \text{ cm}^{-1}$). The reaction mixture contained 50 mM Tris/HCl pH 7.5, 10 mM MgCl_2 , 0.5 mM gluconate, 0.2 mM NADP^+ , 2 mM ATP, 1.5 U 6-phosphogluconate dehydrogenase and 50 μl crude extract.

Glucose 6-phosphate dehydrogenase (G6P-DH) (Moritz *et al.* 2000)



Glucose 6-phosphate dehydrogenase (G6P-DH) catalyses the NADP^+ -dependent oxidation of glucose 6-phosphate to 6-phosphogluconate. NADPH formation was followed at 340 nm ($\epsilon_{\text{NAD(P)H}} = 6.22 \text{ mM}^{-1} \text{ cm}^{-1}$). The reaction mixture contained 50 mM Tris/HCl pH 7.5, 10 mM MgCl_2 , 2 mM NADP^+ , 4 mM glucose 6-phosphate and 100 μl crude extract.

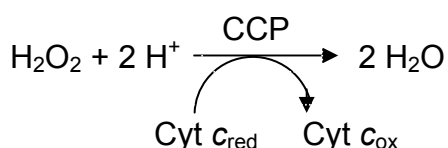
6-Phosphogluconate dehydrogenase (GND) (Moritz *et al.* 2000)



6-Phosphogluconate dehydrogenase (GND) catalyses the NADP⁺-dependent oxidation of 6-phosphogluconate to ribulose 5-phosphate. NADPH formation was followed at 340 nm ($\epsilon_{\text{NAD(P)H}} = 6.22 \text{ mM}^{-1} \text{ cm}^{-1}$). The reaction mixture contained 50 mM Tris/HCl pH 7.5, 10 mM MgCl₂, 2 mM NADP⁺, 1 mM 6-phosphogluconate and 100 μl crude extract.

Cytochrome c peroxidase (CCP) (Zahn *et al.* 1997, Gilmour *et al.* 1994)

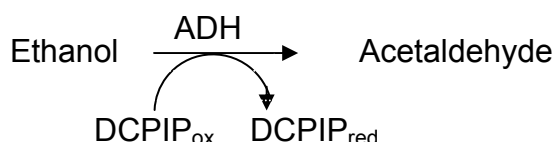
Cytochrome *c* peroxidase (CCP) catalyses the reduction of H₂O₂ to water, electron donor is reduced cytochrome *c*. The reaction was followed by the reduction of reduced cytochrome *c* at 549 nm ($\epsilon_{\text{Cyt } c \text{ (red)}} = 24.42 \text{ mM}^{-1} \text{ cm}^{-1}$). Cytochrome *c* was reduced by adding DTT. The assay was performed with crude extracts, to which a catalase specific inhibitor (20 μM 3-Amino-1H-1, 2, 4-triazol) was added or with protein extracts after purification by Ni-NTA chromatography. After solubilisation of the membranes, proteins were assayed, too. The enzyme was activated by adding 1 μM ascorbate and 5 μM PMS 45 min and 1 μM CaCl₂ for 15 min before activity measurement.



The reaction mixture contained 5 mM MES/HEPES pH 6, 10 mM NaCl₂, 30 mM cytochrome *c*_{red}, 250 μM H₂O₂ and 100 μl crude extract (additionally 0.1% DDM when membrane-fractions were used to keep the proteins in solution).

Membrane-bound alcohol dehydrogenase (ADH) (Matsushita *et al.* 1995)

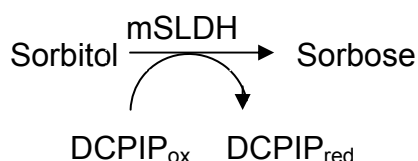
Membrane-bound alcohol dehydrogenase (ADH) catalyses the reduction of ubiquinone. ADH in membranes of *G. oxydans* was assayed with DCPIP ($\epsilon_{\text{DCPIP (pH 6)}} = 11 \text{ mM}^{-1} \text{ cm}^{-1}$) at 600 nm as direct electron acceptor.



The reaction mixture contained 50 mM KPi pH 6, 0.2 mM PMS, 0.15 mM DCPIP, 170 mM ethanol, 0.1% DDM and 100 μ l membrane-fractions. It was reported that the ADH loses its PQQ during purification (Matsushita *et al.* 1995). Therefore, the activity of the ADH was measured after holoenzyme formation with 4 μ M PQQ and 2 mM CaCl₂ for 1 h.

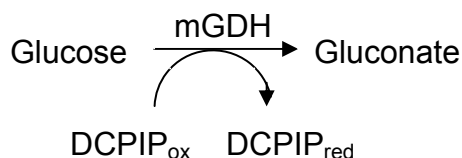
Membrane-bound sorbitol dehydrogenase (SLDH) (Sugisawa *et al.* 2002)

The membrane-bound sorbitol dehydrogenase (mSLDH) catalyses the oxidation of sorbitol, DCPIP can serve as a direct electron acceptor ($\epsilon_{\text{DCPIP (pH 6)}} = 11 \text{ mM}^{-1} \text{ cm}^{-1}$). The reaction was measured at 600 nm and the reaction mixture contained 50 mM KPi pH 6, 0.1% DDM, 0.2 mM PMS, 0.15 mM DCPIP, 20 μ l of a 1.7 M sorbitol solution and 100 μ l of cell membrane suspension.



Membrane-bound glucose dehydrogenase (mGDH) (Matsushita *et al.* 1980)

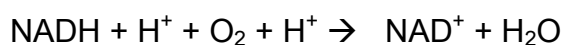
The membrane-bound glucose dehydrogenase (mGDH) catalyses the oxidation of glucose to gluconate. The reaction was measured at 600 nm and DCPIP served as a direct electron acceptor ($\epsilon_{\text{DCPIP (pH 6)}} = 11 \text{ mM}^{-1} \text{ cm}^{-1}$). The reaction mixture contained 50 mM KPi pH 6, 0.1% DDM, 0.2 mM PMS, 0.15 mM DCPIP, 20 μ l of a 1.7 M glucose solution and 100 μ l of cell membrane suspension.



NADH dehydrogenase (NADH-DH) (Mogi *et al.* 2009)

NADH dehydrogenase reduces the ubiquinone pool of the cells. As electrons are transferred in the respiratory chain to the terminal acceptor O₂, no direct electron acceptor has to be added in O₂-saturated cells. The NADH dehydrogenase activity was measured using solubilised membranes (100 mM Tris/HCl, 2 mM NADH, 0.1%

DDM, 100 μ l cell membrane suspension, pH 7.4) by following the decrease of NADH extinction ($\epsilon_{\text{NAD(P)H}} = 6,22 \text{ mM}^{-1} \text{ cm}^{-1}$) at 340 nm.



9.7 Conversion of inactive alcohol dehydrogenase to active enzyme in resting cells

The conversion of inactive alcohol dehydrogenase (ADH) into an active enzyme was performed as described previously (Matsushita *et al.* 1995). The ADH activity is decreased in pH 4 grown cells as was reported by Matsushita *et al.* 1995, but can be activated by incubation of resting cells in buffer at pH 6. For this, cells were cultivated over night in mannitol medium. Main cultures were cultivated at pH 6 (control) or at pH 4 with a start OD_{600} of 0.3, grown for 3-4 h at 30°C. Cells were harvested and washed three times in 50 mM KPi. One culture (pH 4) and the control culture (pH 6) were immediately disrupted using a French press and centrifuged at 18,000 g for 1 h. After solubilisation of the ADH and holoenzyme formation by addition of 4 μ M PQQ and 2 mM CaCl_2 for 0.5 h, ADH activity was measured photometrically. Two other cultures were grown at pH 4 and washed as described. Then they were incubated with 1% sorbitol in 50 mM KPi pH 6 for 4.5 h, to one of which 50 μ M CCCP was added. After that the activity of the ADH was measured as described.

10. Bioanalytical methods

10.1 Sampling and sample processing for LC-MS analysis

For LC-MS analysis, cells corresponding to at least 25 mg CDW were harvested and mixed immediately with a 3-fold volume 60% methanol at -80°C in order to stop metabolism (Bartek *et al.* 2008). For removal of the 60% methanol, the mixtures were centrifuged at 10,000 g and -20°C for 5 min and each cell pellet was resuspended in 1 ml pure methanol (-70°C). After mixing thoroughly, 2 ml chloroform (-20°C) for cell disruption were added. The suspension was shaken at -20°C for two hours and then centrifuged at 10,000 g at -20°C for 10 min. The upper methanol phase contained the metabolites and was filtrated through a 0.2 μ m filter (Millipore, MA, USA). It was frozen at -80°C for subsequent LC-MS analysis. Cell extraction samples were analyzed with an Agilent 1100 HPLC system (Agilent Technologies, Waldbronn, Germany) coupled to an API 4000 mass spectrometer (Applied Biosystems, Concord, Canada) equipped with a Turbolon spray source.

10.2 Determination of metabolites by high performance liquid chromatography (HPLC)

For the determination of metabolites via high performance liquid chromatography (HPLC), 1 ml cell culture was centrifuged at 13,000 g for 2 min and the supernatant was filtrated through a 0.22 μm filter (Millipore, MA, USA) prior to HPLC analysis. Gluconate, 5-keto-gluconate (5-KGA) and 2-keto-gluconate (2-KGA) were analysed by HPLC as described previously (Herrmann *et al.* 2004). The substances were separated using a Shodex DE 613 150 x 0.6 column (Phenomenex, Aschaffenburg, Germany) using 2 mM HClO_4 as eluant at a flow rate of 0.5 ml min^{-1} . Glucose, fructose and mannitol were analysed by an Aminex HPX-87C, 300 mm column (Bio-rad Laboratories, Munich, Germany) using water as eluant at a flow rate of 0.6 ml min^{-1} . Determination of amino acids was performed after derivatisation with *o*-phthaldialdehyd (OPA) (Lindroth and Mopper 1979) in reversed phase HPLC using a ODS Hypersil 120 x 4 mm column (CS Chromatographie Service GmbH, Langerwehe, Germany). 1 μl of the sample was mixed with 20 μl OPA/2-mercaptoethanol reagent (Pierce Europe BV, Oud-Beijerland, Netherlands) and incubated for 1 min at room temperature. Substances were eluted according to their hydrophathy using a flow rate of 0.35 ml min^{-1} within the first minute and of 0.6 ml min^{-1} in the following 15 min at 40°C with a gradient of 0.1 M sodium acetate (pH 7.2) as polar phase and methanol as unpolar phase. Fluorescence of amino acid-isoindol-derivates was detected at 450 nm after excitation at 230 nm. Amino acids were identified due to their specific retention times.

10.3 ^{13}C Metabolic flux analysis

Metabolic flux analysis with ^{13}C -tracer experiments serve for the quantification of *in vivo* not directly observable metabolic flux rates (Nöh *et al.* 2006). This objective is addressed by a model-based evaluation with the aid of computational routines. In a ^{13}C -labeling experiment specifically labeled substrate (4.0% naturally labeled glucose, 7.7% 1- ^{13}C -glucose, and 88.3% U- ^{13}C) was fed to the cells while metabolic stationarity (intra- and extra cellular rates must be in equilibrium, and have to correlate to the growth phase of the cells) within the cells was maintained. The metabolites' emerging specific mass isotope isomer (isotopomer) patterns are measured using mass spectrometry (LC-MS, Luo *et al.* 2007; GC-MS, Fischer *et al.* 2004). For more details about ^{13}C -MFA it is referred to recent review papers (Wiechert 2001, Zamboni *et al.* 2009). Based on the genome information of *G. oxydans* a metabolic network model of central metabolism was formulated. The

software toolbox 13CFLUX (<http://www.13cflux.net>) was used for all modeling and evaluation steps (Wiechert *et al.* 2001).

10.4 MALDI-TOF-Mass spectrometry

MALDI-TOF-Mass spectroscopy was used for identification of proteins (over production of the cytochrome *c* peroxidase and co-purification experiments with the StrepII-tagged cytochrome *c* subunit of the alcohol dehydrogenase). For peptide mass fingerprinting, protein spots of interest were excised from destained colloidal Coomassie-stained gels and subjected to in-gel digestion with trypsin essentially as described previously (Schaffer *et al.* 2001). Briefly, gel pieces were washed three times with 350 μ l 0.1 M ammoniumbicarbonate in 30% (v/v) acetonitril for 10 min at RT to remove the SDS and the Coomassie-blue. 4 μ l 3 mM Tris/Cl-buffer (pH 8.8) with 10 ng μ l⁻¹ trypsin (Promega, Mannheim, Germany) for in-gel digesting of the proteins were added to the completely dried probes. After 30 min at RT, additional 6 μ l 3 mM Tris/HCl (pH 8.8) was added for increasing the reaction volume in order to avoid dehydration over night at RT. The next day, 10 μ l H₂O were added to solve water-soluble peptides from the gel. 15 min later, 10 μ l 0.2% (v/v) trifluoroacetic acid in 30% (v/v) acetonitril were added to solve the remaining peptides from the gel piece. After incubation at RT for 10 minutes, all proteins were eluted from the gel. 0.5 μ l sample was mixed with 0.5 μ l 0.1% (v/v) trifluoroacetic acid (for better integration of the peptides into the matrix) on a PAC (Prespotted-Anchor-Chip)-target-plate (Bruker Daltonics, Eppendorf, Hamburg, Germany). This plate contained already spots with matrix material (saturated α -cyano-4-hydroxy-trans-cinnamic acid) and a standard (Mass spectrum from 1046-3657 Da). Probes were analysed with an Ultraflex MALDI-TOF/TOF37 Mass spectrometer III (Bruker Daltonics, Bremen, Germany) with a positive reflector modus and an acceleration potential of 26.3 kV. Probes were significant if the MOWSE-score (molecular weight search, Pappin *et al.* 1993) was \geq 50.

IV Results

1. Characterisation of the deletion mutant *G. oxydans* 621H- $\Delta qcrABC$

Several deletions of genes encoding for components of the respiratory chain of *G. oxydans* were planned in order to obtain information on the relative contributions of single components to the total flux of electrons through the respiratory chain. The deletion vectors pK19mobsacB- $\Delta qrcC$ (deletion of the cytochrome *c* subunit of the cytochrome *bc*₁ complex), pK19mobsacB- $\Delta qrcABC$ (deletion of the operon of the cytochrome *bc*₁ complex), pK19mobsacB- Δccp (deletion of the cytochrome *c* peroxidase) and pK19mobsacB- $\Delta cydAB$ (deletion of the ubiquinol *bd* oxidase) were constructed. Screens of about 300 clones each after the second recombination in order to find correct deletion mutants missing the *ccp* gene or the *cydAB* operon were unsuccessful. Surprisingly, only about 20 clones had to be analysed by colony-PCR after the second selection round to find the deletion strains *G. oxydans* 621H- $\Delta qrcC$ and *G. oxydans* 621H- $\Delta qcrABC$ with shortened amplicates compared to those of the wild type. The positive clones were sequenced. The strain missing the entire operon of the cytochrome *bc*₁ complex showed no significant differences to the strain missing only the cytochrome *c* subunit during the following investigations. Therefore, only results obtained with the deletion mutant *G. oxydans* 621H- $\Delta qcrABC$ are shown.

First of all, the deletion mutant 621H- $\Delta qcrABC$ and the wild type were analysed under standard conditions (80 g l⁻¹ mannitol, 15% DO, gas flow rate 12 l h⁻¹ and pH 6) Both strains showed no significant differences concerning growth, substrate consumption and product formation (Fig. 5).

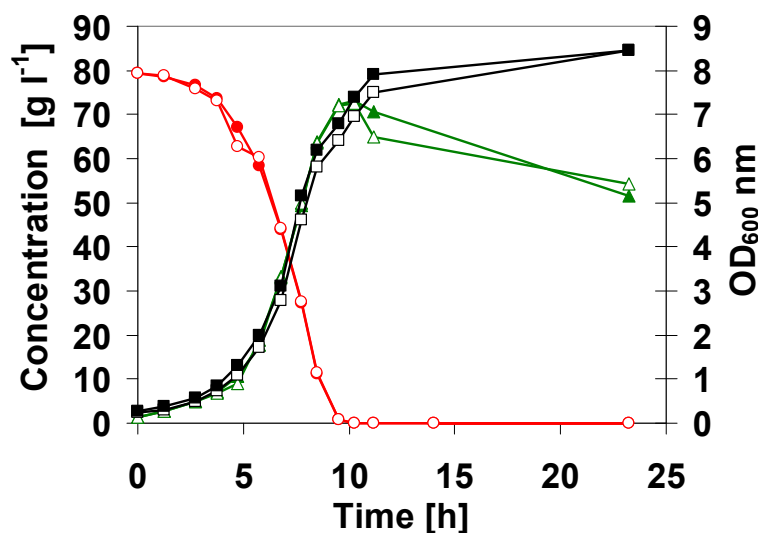


Fig. 5 Growth of *G. oxydans* wild type cells and deletion mutant 621H- $\Delta qcrABC$ on 80 g l⁻¹ mannitol at pH 6, optimal oxygen supply DO = 15%. (-●-): mannitol; (-▲-): fructose; (-■-): growth; open symbols: wild type; closed symbols: *G. oxydans* 621H- $\Delta qcrABC$; average of four independent experiments each

Mannitol was consumed in the first 10 h, about 75 g l^{-1} fructose accumulated in the medium and cells reached an OD_{600} of about 8. Cells did not grow during the next hours, but consumed fructose at low but measurable quantities ($5\text{-}10 \text{ g l}^{-1} 10 \text{ h}^{-1}$). Increasing the DO from 15% to 45% did not result in increased growth or faster oxidation rates. Significant differences between both strains appeared during cultivation at pH 4 (**Fig. 6**).

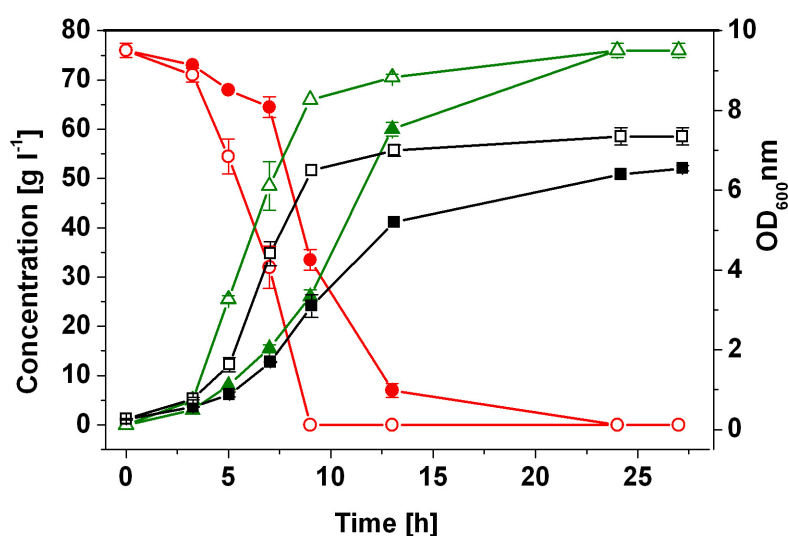


Fig. 6 Growth of *G. oxydans* wild type cells and deletion mutant 621H- Δ qcrABC on 80 g l^{-1} mannitol at pH 4, optimal oxygen supply DO = 15%. (-●-): mannitol; (-▲-): fructose; (-■-): growth; open symbols: *G. oxydans* 621H wild type; closed symbols: *G. oxydans* 621H- Δ qcrABC; average of four independent experiments each

The wild type showed similar growth, substrate consumption and product formation like at pH 6, whereas the deletion mutant showed a delay in substrate consumption and product formation. Growth was slower than that of the wild type ($\mu = 0.27$ compared to $\mu = 0.41$) and resulted in slightly fewer biomass formation. Likewise, the oxygen consumption rates and the carbon dioxide production rates of the deletion mutant were retarded compared to the wild type (**Fig. 7**). These results indicate that at pH 4 the cytochrome bc_1 complex is used and contributes to the cell's energy generation.

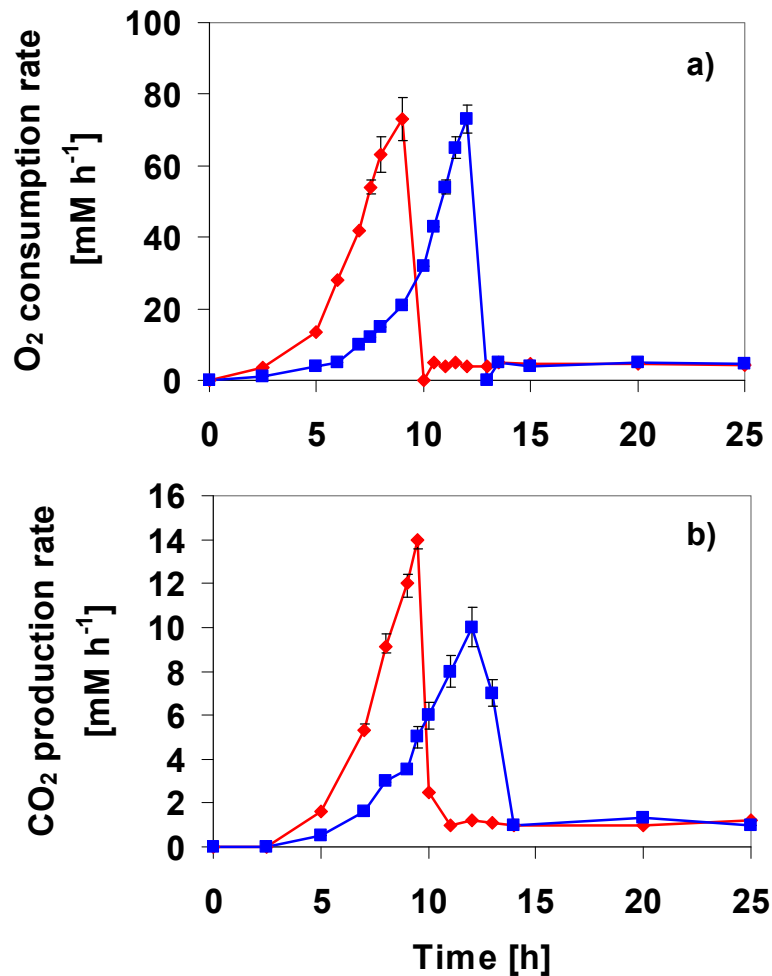


Fig. 7 Oxidation parameters during growth of *G. oxydans* wild type cells and deletion mutant 621H- $\Delta qcrABC$ on 80 g l⁻¹ mannitol pH 4, DO = 15%. a) O₂ consumption rates, b) CO₂ production rates; (- \blacklozenge -): *G. oxydans* 621H wild type; (- \blacksquare -): *G. oxydans* 621H- $\Delta qcrABC$. Two biological experiments each

Cultivation of wild type cells and deletion mutant at oxygen limitation at pH 6 resulted in no growth defect of the deletion strain. The gassing with 2% pure O₂ was sufficient to supply the cells with oxygen in the first 3 h, but during growth, oxygen consumption of the culture increased. The setting of the parameter of the fermentation system did not allow for gassing with higher O₂ concentrations, so that the dissolved oxygen in the medium (DO) dropped to zero within the 3 h and cells were oxygen-limited. Both strains grew linearly when the gassing of the culture was set 2% pure O₂ (Fig. 8). Growth stopped after 35 h at a final OD of about 6 when the mannitol was completely oxidised to fructose (mannitol oxidation and fructose formation not shown in Fig. 8). In the end of growth, oxygen consumption stopped and the DO increased again. The assumed function of the cytochrome *bc*₁ complex

as additional energy generating electron pathway under oxygen limitation was not verifiable with this experimental setup.

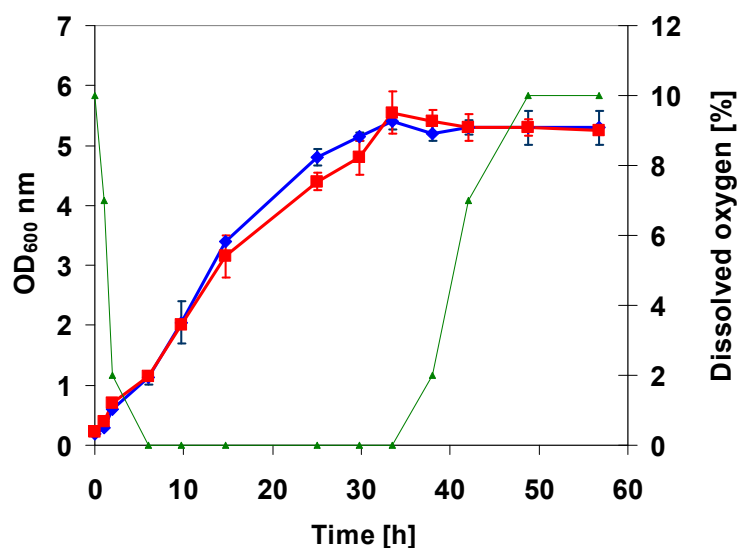


Fig. 8 Growth of *G. oxydans* wild type cells and deletion mutant 621H- Δ qcrABC on 80 g l⁻¹ mannitol at pH 6, oxygen limitation O₂ = 2%. (-■-): *G. oxydans* 621H wild type; (-◆-): *G. oxydans* 621H- Δ qcrABC, (-▲-): dissolved oxygen DO; average of four independent experiments each

Under oxygen limitation, the colour of the culture supernatant of the *G. oxydans* 621H- Δ qcrABC strain began to turn reddish in the last 2-3 h of cell growth. After 40 h of cultivation, the colour difference was clearly visible (**Fig. 9**).

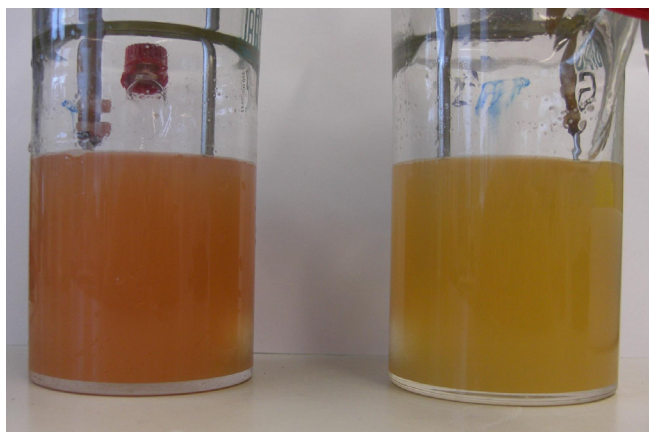


Fig. 9 Cultures of *G. oxydans* deletion mutant 621H- Δ qcrABC and wild type cells after 40 h growth on 80 g l⁻¹ mannitol at pH 6, oxygen limitation O₂ = 2%. Left: 621H- Δ qcrAB; right: *G. oxydans* 621H wild type

The red pigment was present in the supernatant, not in the cells after centrifugation. In order to identify the red pigment, proteins were separated from the supernatant of the deletion mutant by gel size exclusion chromatography (Sephadex G25, GE Healthcare). The reddish substance accumulated in the upper quarter of the

column and did not elute with the protein fraction, therefore it was concluded that the pigment was not a protein. The red substance was elutable when 20% ethanol was applied as eluant. Finally, 20% methanol delivered the sharpest elution peaks. The elution did not contain any proteins as was shown by protein-fast test with Bradford's reagent. The pigment was reduced by addition of dithiothreitol and oxidised with potassium hexacyano-ferrate (III). Then difference spectroscopy (reduced-oxidised) was performed by measuring the absorption spectra of the reduced and the oxidised probes using an "Ultrospec 4300 pro" photometer (Amersham Bioscience, Freiburg, Germany). Wavelength scan was from 450 to 650 nm. Reduced-oxidised spectra of the probe showed two distinct peaks at 535 nm and 575 nm (**Fig. 10**) which is in the same range as spectra of cytochromes or hemes without the protein. This spectrum as well as the reddish colour of the pigment was a strong indication that the pigment present in the supernatant of the deletion mutant was heme.

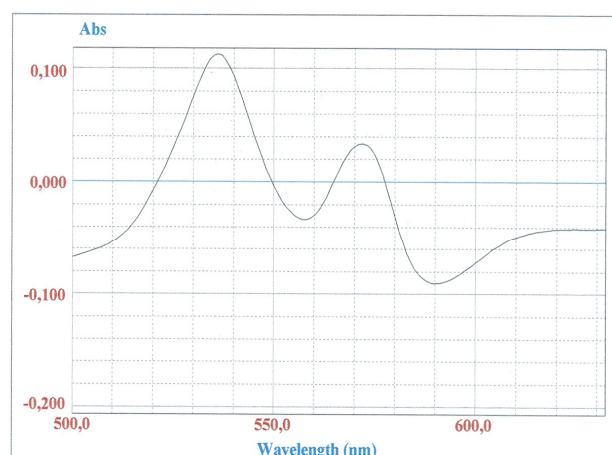


Fig. 10 Reduced-oxidised spectra of the reddish coloured pigment emerging in oxygen-limited cultures of *G. oxydans* 621H- Δ *qcrABC* after 40 h cultivation

In order to determine if there were differences in the protein fraction of the supernatants of the wild type and the deletion mutant, these proteins were analysed. The protein fractions, which were eluted in the gel size exclusion chromatography, were concentrated 40-fold and analysed via SDS-PAGE (**Fig. 11**). In the wild type's protein fraction, three proteins were identified via MALDI-analysis. The upper band was a mixture of the large subunit of the alcohol dehydrogenase (GOX1068, 82 kDa) and a metalloprotease (GOX2034, 77 kDa). The lower band was identified as an outer-membrane protein (GOX1787, 40 kDa). The single protein band in the supernatant of the deletion mutant was identified as flagellin B (GOX0787, 49 kDa). These results suggest that the cytochrome *bc*₁ complex is involved in flagellum

assembly, since this protein was only present in the supernatant of the mutant. The assembly of flagella might be disturbed in the deletion mutant, so that the flagellin B cannot be integrated into the flagellum and therefore accumulates in the medium.

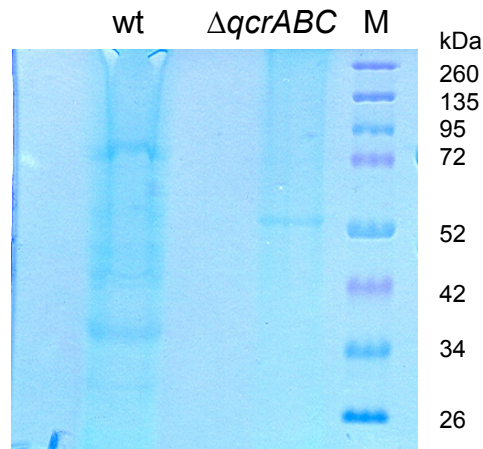


Fig. 11 SDS-PAGE analysis of culture supernatants' protein fraction of oxygen-limited cultures of *G. oxydans* wt: wild type *G. oxydans* 621H; $\Delta qcrABC$: *G. oxydans* 621H- $\Delta qcrABC$; M: Marker; proteins were analysed in a 12% polyamide gel and stained with Coomassie-blue

During cultivation on glucose at pH 6 and 15% DO (oxygen excess), *G. oxydans* showed a biphasic growth (**Fig. 12**). In the first growth phase (until 10 h), wild type and mutant grew exponentially to an OD_{600} nm of 6. Glucose consumption was very fast and gluconate accumulated in the medium. The wild type culture formed less gluconate than the mutant culture, which is explainable by a faster oxidation of gluconate to ketogluconate. During the second growth phase, gluconate was used as substrate and growth was strongly decreased to linear growth behaviour. Gluconate was mainly oxidised to 2-ketogluconate. In the second growth phase, the deletion mutant grew slower than the wild type did and formation of 2-ketogluconate was retarded. Parallel to biphasic growth, oxygen consumption rates also formed two maxima in phase I and phase II (**Fig. 13**).

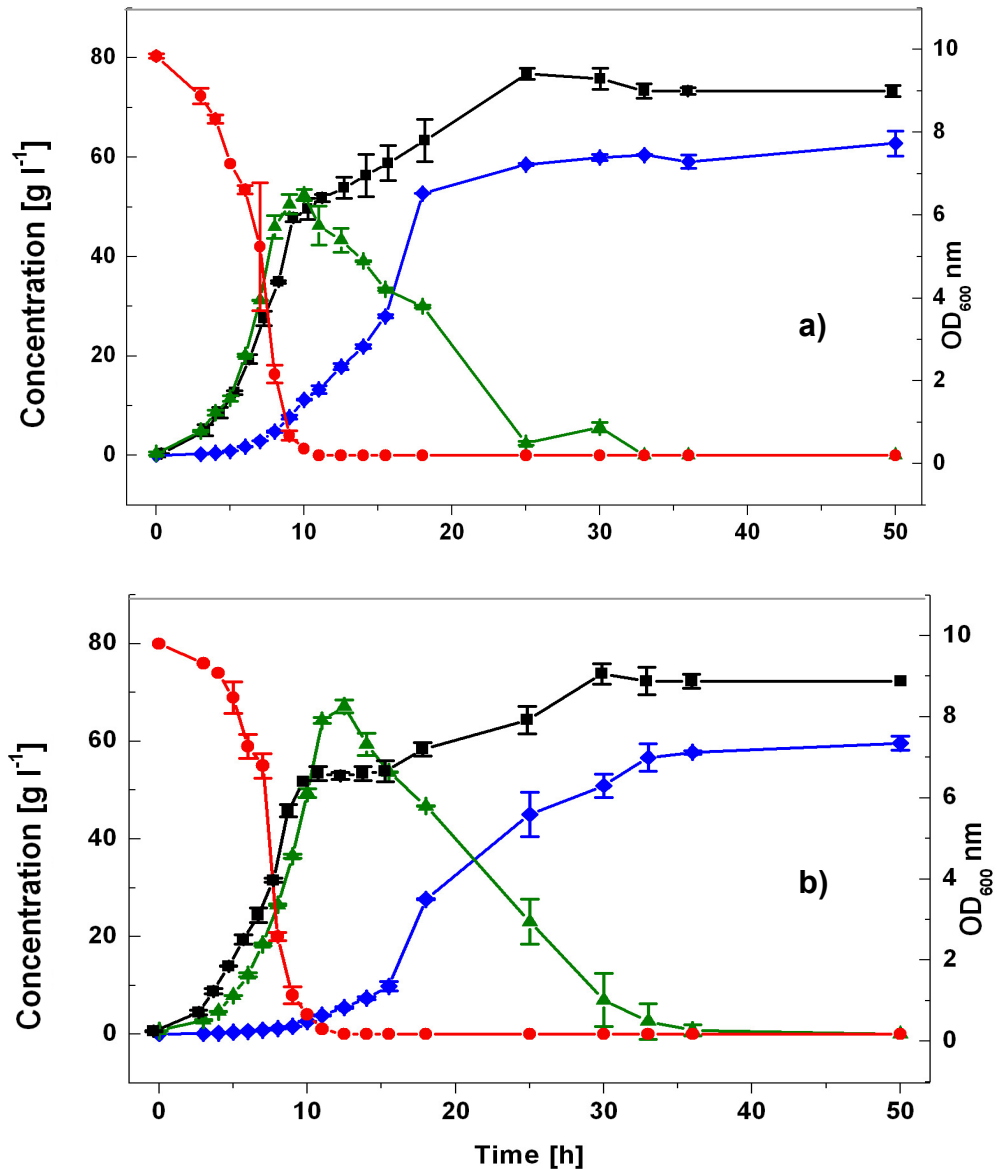


Fig. 12 Growth of *G. oxydans* wild type cells and deletion mutant 621H- $\Delta qcrABC$ on 80 g l⁻¹ glucose pH 6, oxygen supply DO = 15%. a): *G. oxydans* wild type; b): *G. oxydans* 621H- $\Delta qcrABC$; (-●-): glucose; (-▲-): gluconate; (-◆-): 2-ketogluconate; (-■-): growth; average of four independent experiments each

During the first oxidation phase of the wild type, when glucose was oxidised to gluconate, the cells rapidly consumed oxygen at a maximum oxidation rate of about 70 mM h⁻¹ (46.7 mmol h⁻¹ g⁻¹ CDW). When cells entered the second growth phase, oxygen consumption rates decreased (11.4 mmol h⁻¹ g⁻¹ CDW) and O₂ was consumed over a longer period compared to the first oxidation phase. This indicated that oxidation of gluconate to ketogluconate occurred more slowly than the oxidation of glucose to gluconate, partially due to a lower activity of membrane-bound gluconate-2-dehydrogenase compared to membrane-bound glucose dehydrogenase. In both, the first and second oxidation phases 220 mM (146.7 mmol g⁻¹ CDW and

122.22 mmol g⁻¹ CDW, respectively) O₂ were consumed, as expected for the oxidation of 440 mM glucose via gluconate to ketogluconate. The differences observed in cell growth and substrate consumption between the wild type and the deletion mutant were also apparent in the O₂ consumption rates and the CO₂ production rates (**Fig. 13**). The deletion mutant showed retarded oxygen consumption rates and there was a break in the CO₂ production rates during transition from the first to the second oxidation phase. Hence, the cytochrome *bc*₁ complex is used during the transition from growth phase I to growth phase II.

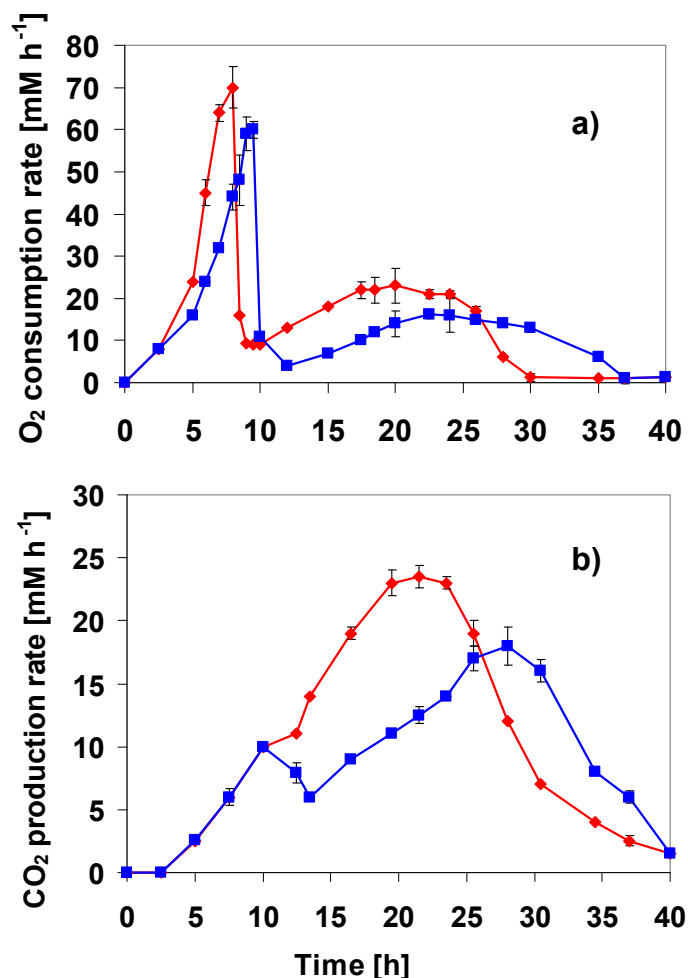


Fig. 13 Oxidation parameters during growth of *G. oxydans* wild type cells and deletion mutant 621H- Δ *qcrABC* on 80 g l⁻¹ glucose pH 6. a) O₂-consumption rates; b) CO₂- production rates; (-♦-): *G. oxydans* 621H wild type; (-■-): *G. oxydans* 621H- Δ *qcrABC*; two biological experiments each

As a combination of the two conditions provoking a growth defect of the deletion mutant (growth on mannitol pH 4 and growth phase II during growth on glucose pH 6, both oxygen excess DO = 15%), the two strains were cultivated with glucose at pH 4 (**Fig. 14**). However, cells of both strains only showed the first growth and oxidation phase and did not differ from each other (**Fig. 14, 15**). Cell growth stopped after 10 h

at a final OD of 6. It may be concluded that beside the pH-value of the medium the nature of the substrate and the corresponding membrane-bound dehydrogenase oxidising the substrate are decisive for a functional cytochrome bc_1 complex.

Glucose consumption at pH 4 was as fast as at higher pH values indicating that the membrane-bound glucose dehydrogenase was active, leading to a total consumption of glucose. 440 mM glucose were oxidised at the membranes, corresponding to the measured total 220 mM O_2 consumption (according to the stoichiometry that oxidation of one mol glucose leads to reduction of $\frac{1}{2}$ mol O_2).

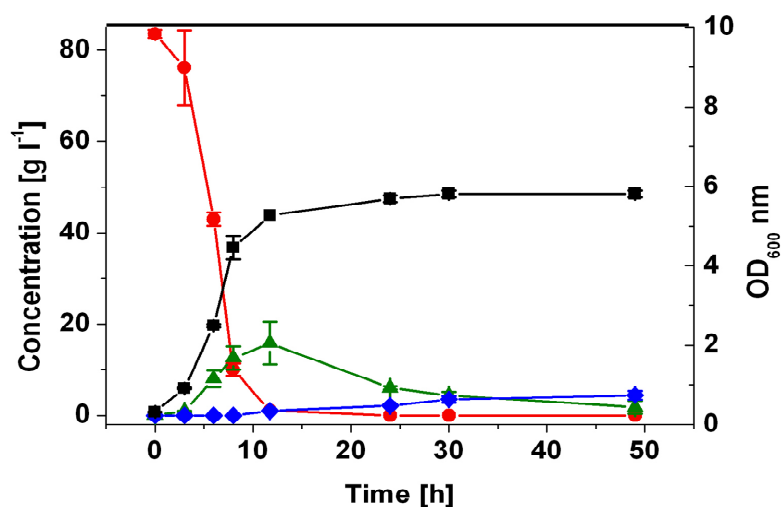


Fig. 14 Growth of *G. oxydans* wild type cells on 80 g l⁻¹ glucose pH 4, DO: 15%. Only wild type shown, deletion mutant showed no significant differences; (-●-): glucose; (-▲-): gluconate; (-◆-): 2-ketogluconate; (-■-): growth; average of four independent experiments each

Thus, glucose was fully oxidised to gluconate. However, only 23 % of the initial substrate glucose accumulated as gluconate in the medium. Nearly no ketogluconates were produced. In order to determine, if gluconate or ketogluconate are instable at pH 4, cell-free medium containing 80 g l⁻¹ gluconate, 5-ketogluconate and 2-ketogluconate was incubated for 24 h at 30°C. The concentrations of the sugar did not change and the fate of the gluconate was still questioned. No membrane oxidation occurred after the first 10 h (**Fig. 15**) since the membrane-bound 2-ketogluconate dehydrogenase has its pH optimum at pH 6 (Shinagawa *et al.* 1984). Therefore, gluconate must have been taken up into the cells. The stop of growth after depletion of glucose in the culture medium is explainable because the cells lacked the energy delivered by periplasmatic gluconate oxidation. However, it cannot be excluded, that a byproduct like acetate was formed. The main question, if there are

differences between the wild type and the deletion mutant when grown at pH 4 on glucose was answered.

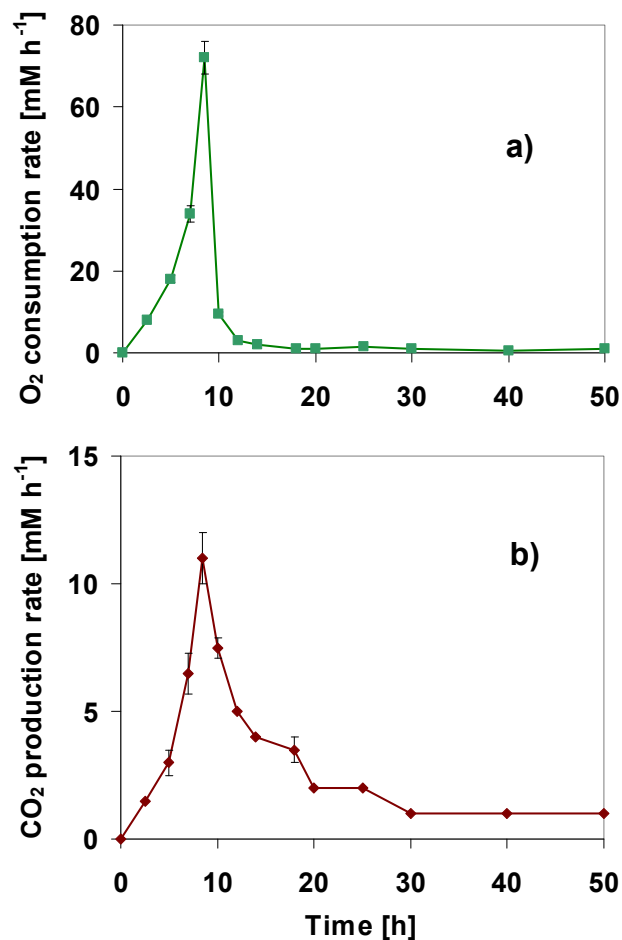


Fig. 15 Oxidation parameters during growth of *G. oxydans* wild type on 80 g l⁻¹ glucose pH 4, DO = 15%. Only wild type shown, deletion mutant showed no significant differences; a) O₂-consumption rates; b) CO₂-production rates; two biological experiments each

The growth experiments had shown that use of the substrate mannitol at pH 4 led to significant retardation of growth of the deletion mutant compared to the wild type. In contrast, if glucose was used as initial substrate at an acidic pH of 4, growth of the deletion mutant was not affected. Therefore, the acidic pH of the medium was not the only reason for the growth defect of the deletion mutant. The primary dehydrogenases of the respiratory chain of *G. oxydans* had an influence on growth and oxidation activities of the mutant *G. oxydans* 621H- Δ *qcrABC*, too. Nevertheless, growth of the cells is not only supported by the respiratory oxidation of different substrates, but also by cytoplasmatic metabolism. The use of the Clark oxygen electrode allowed for the investigation of only the oxidation step connected to the

respiratory chain. Respiration rates with different substrates at pH 6 and at pH 4 were determined in short time kinetics in a Clark oxygen electrode in order to investigate the effect of the cytochrome *bc*₁ deletion on the primary substrate oxidation rate and the corresponding primary dehydrogenase (**Table 4**). Glucose and ethanol as substrates led to significantly lower specific oxidation rates (62%, 38%) of the mutant strain compared to those of the the wild type. At pH 4, rates were lower, but the overall picture was the same.

Table 4 Oxidation kinetics of the *G. oxydans* 621H wild type (WT) and the deletion mutant *G. oxydans* 621H- Δ *qcrABC* (Mutant) at pH 4 and pH 6.

Strain	Substrate	Specific oxidation rate [nmol ml ⁻¹ min ⁻¹ OD ⁻¹]	
		pH 6	pH 4
Wt	Glucose	235 (± 7)	82 (± 8)
Mutant		146 (± 9)	57 (± 8)
WT	Gluconate	45 (± 6)	25 (± 4)
Mutant		30 (± 4)	11 (± 3)
WT	Ethanol	262 (± 7)	50 (± 6)
Mutant		100 (± 9)	20 (± 3)
WT	Sorbitol or Mannitol	104 (± 7)	16 (± 2)
Mutant		81 (± 9)	9 (± 3)

Interestingly, this experiment showed that there is hardly a correlation between the oxidation activity of the dehydrogenases and cell growth. For example, at pH 6, glucose oxidation activity of the wild type mGDH in the Clark electrode was much higher compared to the mannitol oxidation activity of the wild type major polyol dehydrogenase. In contrast, during growth of the wild type at pH 6, no differences in growth rates were observed when glucose or mannitol served as substrate. On the other hand, the deletion mutant grew as fast as the wild type during growth in phase I on glucose at pH 6, although the glucose oxidation rate measured in the Clark electrode was significantly lower than that of the wild type. Likewise, the decreased growth of the deletion mutant compared to the wild type during growth phase II with glucose is not solely explainable by the oxidation activity of the gluconate-2-dehydrogenase because oxidation rates in the short time kinetics of both strains were similar when gluconate was used.

The specific oxidation rates of glucose or ethanol measured in the Clark electrode correlated best with the absence/presence of the cytochrome *bc*₁ complex.

Therefore, a connection between the responsible dehydrogenases, alcohol dehydrogenase and glucose dehydrogenase, with the cytochrome *bc*₁ complex was assumed. This connection might be physical and manifests itself in a supercomplex between the cytochrome *bc*₁ complex and the primary dehydrogenase. There are a number of indications in the literature, that components of the respiratory chain form complexes in *G. oxydans* (Matsushita *et al.* 1991, Shinagawa *et al.* 1990, Soemphol *et al.* 2008). In addition, Matsushita *et al.* 1995 showed a proton motive force-dependent activation of the alcohol dehydrogenase in resting cells. The authors reported that i) inactive alcohol dehydrogenase (ADH) was generated abundantly under acidic growth conditions, ii) the inactive ADH could be activated by incubating pH 4 grown cells in a buffer pH 6 and iii) the activation of alcohol dehydrogenase was repressed by the addition of a proton uncoupler and did not occur in spheroplasts. Taking into account that the cytochrome *bc*₁ complex contributes to the proton motive force and that there seems to be a connection between the cytochrome *bc*₁ complex and the ADH as shown by oxidation activities measured in the Clark electrode, an involvement of the cytochrome *bc*₁ complex in the activation of the alcohol dehydrogenase was investigated. The ADH activity was determined photometrically in pH 4 and pH 6 grown cells. The latter served as control (see Materials and Methods) and activity was assumed to be less in pH 4 grown cells as reported by Matsushita *et al.* 1995 (see above). Indeed, the activity of the ADH in pH 4 grown cells of the wild type and of the deletion mutant was weaker than that of the control cells grown at pH 6 (**Table 5**).

Table 5 Activity of alcohol dehydrogenase of *G. oxydans* wild type and *G. oxydans* 621H- Δ *qcrABC* in cell grown at pH 4 or 6 (control) measured photometrically. 4.5 h after activation: cells were incubated in KPi pH 6 for 4.5 h before measurement of activity; 50 μ M CCCP: CCCP was added during the incubation time; determined with two independent biological experiments

	Activity [U/mg]	
	Wild type	<i>G. oxydans</i> 621H- Δ <i>qcrABC</i>
pH 6 control	5.68 \pm 0.01	2.29 \pm 0.11
pH 4 before activation (control)	1.84 \pm 0.20	0.80 \pm 0.02
4.5 h after activation	5.84 \pm 0.21 (320%)	1.99 \pm 0.05 (250%)
4.5 h after activation + 50 μM CCCP	1.83 \pm 0.11	0.11 \pm 0.03

The ADH activity in both strains was restored after incubating the cells for 4.5 h in KPi buffer, pH 6. In the deletion mutant, the activity was restored to 250% instead of 320% in the wild type referred to the activity at pH 4. Therefore, the cytochrome *bc*₁ complex presumably plays a role in the activation.

The probability of supercomplex formation between components of the respiratory chain was described previously (Matsushita *et al.* 1991, Shinagawa *et al.* 1990, Soemphol *et al.* 2008). The experimental data of Clark electrode experiments together with the activation test of the ADH supported this view, at least between the cytochrome *bc*₁ complex and the ADH. Therefore, co-purification experiments were performed. A strain was constructed with genomically integrated StrepTagII at the C-terminus of the cytochrome *c* subunit of the ADH (*G. oxydans* 621H Δ *hsdR adh-cyt c*_{St}). The vector pK19*mobsacB-adhcytc*_{St} was integrated into the genome by homologous recombination. *G. oxydans* 621H Δ *hsdR* (Schweikert *et al.* in preparation) was used as parental strain, because this strain was transformable by electroporation, due to a deleted endonuclease HsdR.

The tagged cytochrome *c* subunit of the ADH interacts with the column material during the purification (see Materials and Methods), and is eluted specifically with elution buffer after washing the column for removal of unspecifically bound proteins. Proteins interacting with the tagged cytochrome *c* subunit of the ADH, like the two other subunits of the ADH or other components of the respiratory chain, which might form supercomplexes with the ADH, should bind on the column, too. Therefore, interaction partners in supercomplexes can be “fished” by binding one partner to the column with a StrepTagII. Each protein interacting with the ADH should be eluted with the tagged ADH subunit. The large subunit of the alcohol dehydrogenase was purified in addition with the tagged cytochrome *c* subunit of the ADH, as well as the 15 kDa subunit (**Fig. 16**, left). Eluates containing the ADH were reddishly coloured (**Fig. 16**, right) indicating a high content of the red pigment cytochrome *c* (Matsushita *et al.* 2008). Bands of the SDS-PAGE were cut out and analysed with MALDI-TOF to assure the correct identification of the protein. The band at 72 kDa was a mixture of the large subunit of the ADH and the tagged cytochrome *c* subunit of the ADH. This indicated, that the interaction between these subunits was so strong, that they could not fully be separated in a denaturing SDS-gel. The band at 48 kDa consisted of only the tagged subunit. No other components of the respiratory chain were co-purified with the three subunits of the alcohol dehydrogenase. Hence, the co-

purification experiments for verification of a super complex formation of the cytochrome bc_1 complex and the alcohol dehydrogenase were not yet successful. However, the interactions in such a proposed supercomplex might be disturbed by the StrepTagII if it was positioned in the interaction region. Even without disturbing effects of the StrepTagII, the interaction itself might not have been strong enough so that the interacting proteins did not bind to the column-bound ADH during purification and instead were eluted during the washing steps.

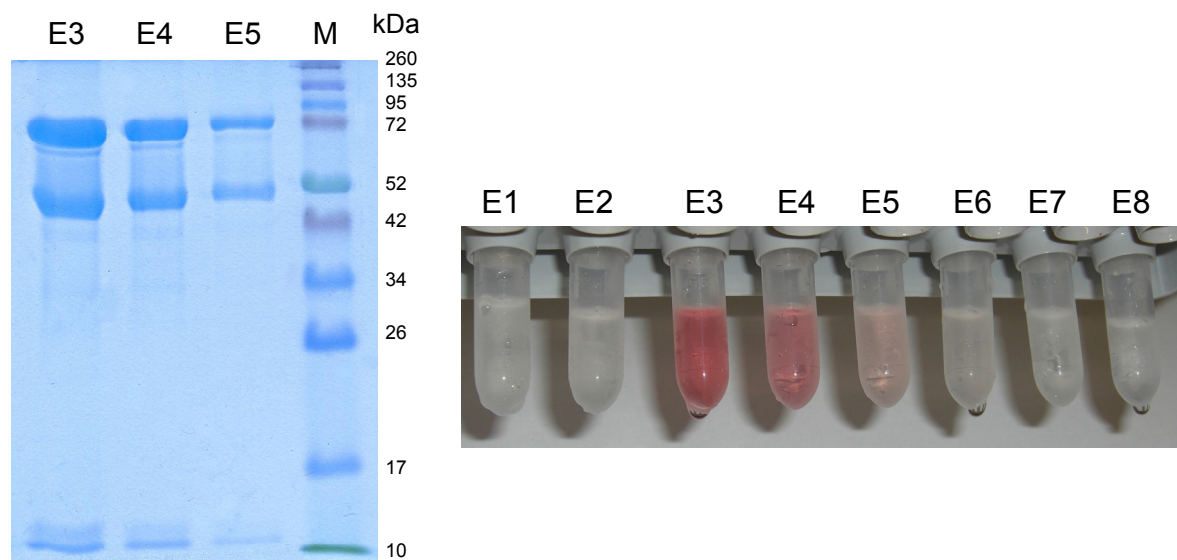


Fig. 16 SDS-PAGE analysis of the eluate (fraction E3-E5) of a Strep-tactin chromatography of DDM-solubilised membrane proteins of *G. oxydans* 621H $\Delta hsdR adh-cyt c_{St}$. left picture: eluted subunits of the alcohol dehydrogenase from elution fractions E3-E5 in a 15% SDS-gel, M: Marker; right picture: alcohol dehydrogenase was eluted from the Strep-tactin column in eight elution fractions (E1-E8)

Matsushita *et al.* 1987 reported the transfer of electrons via the ubiquinol pool to ubiquinol bo_3 as one of the two possible terminal oxidases. The ubiquinol bo_3 oxidase was able to oxidise ubiquinol, but activity of the cytochrome c oxidase was not tested. A simple test displays qualitatively the activity of the cytochrome c oxidase (Kovacs 1956) and was used to follow an electron flow from the cytochrome bc_1 complex via the soluble cytochrome c to a terminal acceptor in *G. oxydans*. TMPD in its reduced form is colourless. When it is oxidised by soluble cytochrome c , it turns blue. For this reaction, the cytochrome c itself has to be oxidised, e.g. by a cytochrome c oxidase. The TMPD turns blue within a few seconds, if there is an electron flow via the soluble cytochrome c . *E. coli* served as a negative control since this organism lacks cytochrome c when grown aerobically (Anraku and Gennis 1987). *B. subtilis* served as positive control (**Fig. 17**).

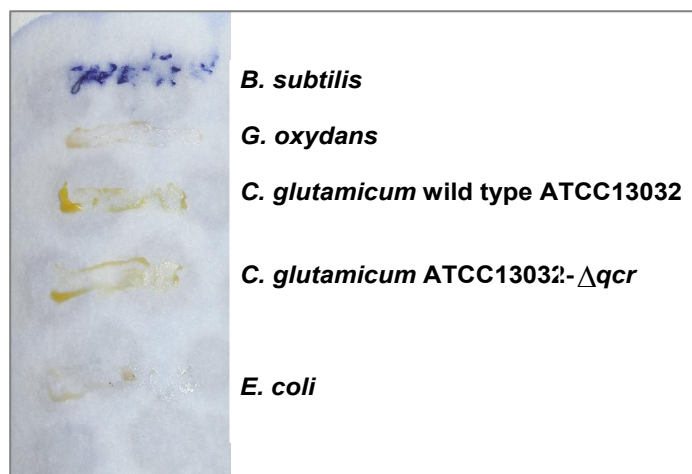


Fig. 17 Activity test of the cytochrome c oxidase in *G. oxydans*, *E. coli*, *Corynebacterium glutamicum* and *Bacillus subtilis*. Intact cells were streaked on Watmann's filter paper with 1% TMPD

Only the *B. subtilis* cells turned blue after three seconds. In 2001 Niebisch and Bott characterised the cytochrome bc_1 - aa_3 supercomplex in *C. glutamicum* (cytochrome *c* oxidase is named aa_3 in *C. glutamicum*). Nevertheless, cells of *C. glutamicum* did not turn blue, although a terminal acceptor for the oxidation of the cytochrome *c* was present. This was explainable since *C. glutamicum* forms a complex between the cytochrome bc_1 complex and the cytochrome *c* oxidase without a soluble cytochrome *c* bound. Instead of a soluble cytochrome *c*, the complex contains a second heme *c* binding site in the cytochrome bc_1 part (Niebisch and Bott 2001). The TMPD oxidase test showed that no electrons flowed through the soluble cytochrome *c* in *G. oxydans*. However, it can not be excluded that the soluble cytochrome *c* is bound in a complex since the test is only positive if the cytochrome *c* is free for the reaction with TMPD and not embedded in a complex. Beside the probability of a supercomplex formation of the cytochrome bc_1 complex and the ADH in *G. oxydans*, a periplasmatically localised cytochrome *c* peroxidase (CCP) possibly represents one terminal acceptor of electrons of the cytochrome bc_1 complex pathway (Nicholls and Ferguson 2002). The enzyme catalyses the following reaction:



The activity of the cytochrome *c* peroxidase was measured photometrically (Materials and Methods) by following the decrease of extinction of the reduced soluble cytochrome *c* at 549 nm. In its oxidised form, soluble cytochrome *c* does not

absorb light at 549 nm. However, activity of the cytochrome *c* peroxidase was not detectable in cell-free extracts. Catalase was assumed to exhaust the hydrogen peroxide immediately, so that no reaction of the cytochrome *c* peroxidase was measurable. Addition of 20 μ M of a catalase-specific inhibitor (3-Amino-1H-1, 2, 4-triazol) (Manilov *et al.* 1996) to the reaction mixture did not result in a measurable activity of the cytochrome *c* peroxidase so that the inhibitor was not active. In order to measure the activity of the cytochrome *c* peroxidase without disturbing influences of the catalase, the gene encoding the cytochrome *c* peroxidase was overexpressed in *E. coli* for purification. The gene was cloned into an overexpression vector providing a C-terminal His-tag (pET24). The cytochrome *c* peroxidase contains cytochrome *c*, which is not synthesised in aerobically grown *E. coli* (Atack and Kelly 2007, Anraku and Gennis 1987). To obtain an active enzyme by heterologous expression, the *E. coli* strain bearing the plasmid was cultivated anaerobically. However, anaerobic overproduction of the enzyme in *E. coli* was not detected after induction with IPTG, although sequencing verified the correctness of the vector. Therefore, overproduction of cytochrome *c* peroxidase was also tested in aerobically grown *E. coli* cells. These cells overproduced the apoenzyme of the cytochrome *c* peroxidase as proven by SDS-PAGE (Fig. 18) and MALDI-analysis; the enzyme was purified from the membrane fraction of the cells.

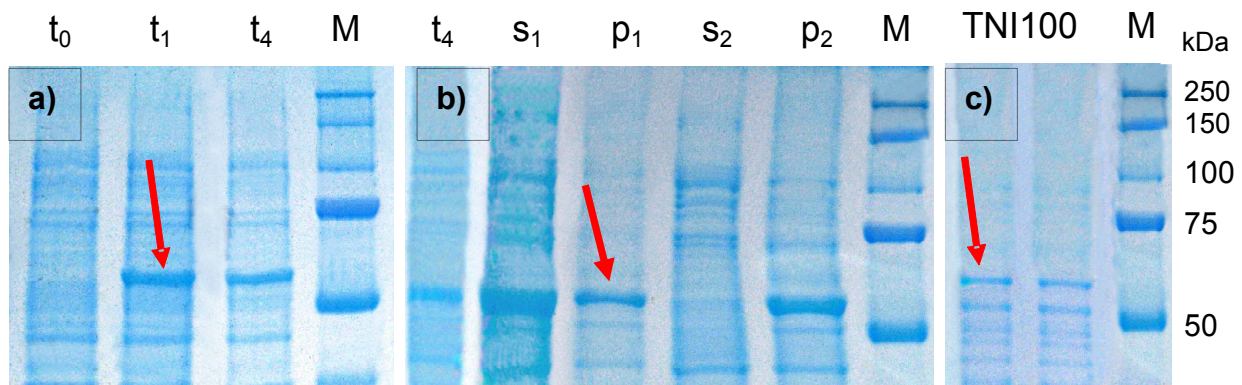


Fig. 18 SDS-PAGE analysis of cells of *E. coli* pET24-ccp and eluates of a Ni-NTA-chromatography of *E. coli* pET24-ccp. Proteins were analysed in a 12% polyamide gel and stained with Coomassie-blue, **a)** Proof for an overproduction of the cytochrome *c* peroxidase; t₀: cells before induction with 0.5 mM IPTG; t₁ and t₄: 1 h or 4 h after induction with IPTG resulting in overproduced cytochrome *c* peroxidase; **b)** steps for purification of the cytochrome *c* peroxidase; t₄: overproduced cytochrome *c* peroxidase after induction with IPTG; s₁: supernatant after cell disruption; p₁: pellet after cell disruption; s₂: supernatant after ultracentrifugation; p₂: pellet after ultracentrifugation; **c)** TN100: proteins eluted from the Ni-NTA-column with TN100; M: Marker (Precision plus, Bio-Rad, Munich, Germany)

As expected, the apo-CCP was not active because no cytochrome *c* was available in aerobically grown *E. coli* cells (Thöny-Meyer *et al.* 1995). In addition, functional expression of the CCP has a number of premises, concerning transport into the periplasm and protein assembly (apo-CCP and the cytochrome *c* as prosthetic group) in the periplasm (Ferguson *et al.* 2008). It can not be excluded that those cellular processes exerted adverse effects on functional expression in anaerobically cultivated *E. coli*.

In an alternative approach homologous overproduction of the enzyme in *G. oxydans* was performed. For the homologous overproduction of the cytochrome *c* peroxidase in *G. oxydans*, the HisTag-terminator sequence of the pET24 vector and the gene encoding for the cytochrome *c* peroxidase were cloned into the vector pEXGOX-K. A 3 l culture of *G. oxydans* containing the overproduction vector pEXGOX-K-*ccp*_{His} was used for the homologous overproduction of the cytochrome *c* peroxidase. SDS-gel analysis demonstrated no significant overproduction of the enzyme although the vector was sequenced and found to be correct.

The cytochrome *c* peroxidase still represented a possible *in vivo* terminal acceptor of the cytochrome *bc*₁ complex pathway. To test the condition, when the cytochrome *c* peroxidase is preferably used, transcription of the *ccp*-gene was investigated under different conditions of oxygen availability. H₂O₂ is formed when electrons are transferred to molecular oxygen; especially in highly active respiratory chains superoxide ions are formed which then are converted by superoxide dismutase into a molecule of hydrogen peroxide and one of oxygen (Fridovich 1978, 1995, Imlay and Fridovich 1991). Parallel to H₂O₂ formation, the transcription of the *ccp* gene was supposed to increase, when electrons entered the respiratory chain rapidly, which is the case when oxygen availability is high (Costa and Morradas-Ferreira 2001). Different conditions of oxygen availability were tested. Cells were cultivated under oxygen-limited conditions from the beginning of growth, or oxygen limitation was set in the middle of the exponential growth phase. The different oxygen availability conditions resulted in different growth behaviour of the cells (**Fig. 19**). Keeping the DO at 45% or 30% resulted in exponential cell growth; limiting the oxygen availability due to constant gassing with 2% O₂ resulted in decreased linear growth. This was true for a limitation from the beginning of growth and for a limitation set in the middle of the exponential growth phase. Oxygen excess conditions were established by provision of DO 30% and cells were harvested in the middle of the exponential

growth phase or in the late exponential growth phase. In late exponential cells under oxygen excess, the lowest concentration of *ccp*-mRNA was measured (**Table 6**). An increased concentration of *ccp*-mRNA was measured in cells harvested during exponential growth under oxygen excess, as well as in oxygen-limited cells. Concentration of *ccp*-mRNA was measured at a greater extent when the cells were oxygen-depleted for a longer time. The phenomenon, that the gene encoding the CCP is upregulated under oxygen limitation was reported before (Atack and Kelly 2008) for e.g. *Pseudomonas denitrificans*. The authors did not have an explanation for that “contradictory” regulation.

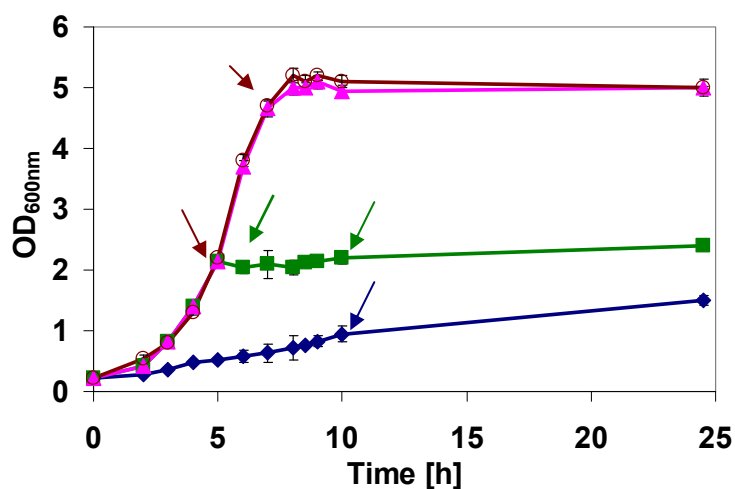


Fig. 19 Growth of *G. oxydans* 621H on 80 g l⁻¹ mannitol at pH 6 under different conditions of oxygen availability. (-○-): 45% DO; (-▲-): 30% DO; (-■-): 15% DO until OD_{600 nm} of 2, then 2% O₂; (-◆-): 2% O₂; arrows: cell harvest for RNA isolation; average of three independent experiments each

Table 6: mRNA concentration of the gene encoding cytochrome c peroxidase per 50 ng total-mRNA of cells of *G. oxydans* 621H grown oxygen-limited or with oxygen excess, 30% DO and 45% DO: oxygen excess, lim: limitation

Condition and time point of cell harvest	mRNA concentration of <i>ccp</i> per 50 ng total-mRNA in [fg/50ng total mRNA]
O ₂ -limitation (2.5% O ₂)	15.8
O ₂ -lim at OD ₆₀₀ = 2, cell harvest 1 h after lim.	6.5
O ₂ -lim at OD ₆₀₀ = 2, cell harvest 3.5 h after lim.	8.9
30% DO, exponential growth	17.1
30% DO, late exponential growth	4.0
45% DO, exponential growth	17.6
45% DO, late exponential growth	4.0

2. Genome-wide transcription analyses

So far, little knowledge exists on regulatory mechanisms in *G. oxydans*. Utilisation of oligonucleotide-based microarrays should provide an insight into transcriptional regulation. Three conditions for genome-wide transcription analyses were chosen: I) oxygen depletion vs. oxygen excess, II) acidic pH of 4 vs. standard pH of 6 and III) growth phase II vs. growth phase I of glucose grown cells pH 6. These conditions were analysed intending to enlighten the regulation in situations where the deletion mutant *G. oxydans* 621H- $\Delta qcrABC$ showed the differences to the wild type as previously described, in order to obtain further information on the function of the cytochrome bc_1 complex. The cut-off for the mRNA-level up- or downregulation was set at 1.8-fold (for all genes differently expressed see **Table 18**, appendix). The mRNA-levels of several genes were also tested by real time PCR since the method of genome-wide transcription analysis was newly developed for *G. oxydans* (**Table 7**). The measurement of ratios of mRNA-levels by RT-PCR was a quality control for the new oligonucleotide-based transcription analyses. For that control, genes encoding for enzymes of the respiratory chain, which showed up- or downregulation in the transcription analyses performed during this work, were randomly chosen.

Table 7 Ratio of mRNA-levels of selected genes under different conditions determined by qRT-PCR. Based on three independent biological experiments

Gene and condition	Gene product	Ratio qRT-PCR	Ratio Chip
pH 4/pH 6			
GOX0278	Cytochrome <i>d</i> ubiquinol oxidase subunit I	1.7 ± 0.32	2.2 ± 0.44
O₂ limitation/O₂ saturation			
GOX1914	Cytochrome <i>o</i> ubiquinol oxidase subunit IV	3.5 ± 0.91	3.8 ± 1.21
GOX1675	NADH dehydrogenase II	0.5 ± 0.05	0.4 ± 0.02
GOX0564	Cytochrome <i>c</i> precursor	1.8 ± 0.35	2.0 ± 0.42

The determined ratios of mRNA-levels were concordant with the mRNA-levels determined with microarray-analysis, so that the data obtained by microarray-analyses were verified.

The ubiquinol *bd* oxidase is known to be regulated in *E. coli* by oxygen availability (Tseng *et al.* 1995). As described in the results above, the cytochrome bc_1 complex was used under oxygen depletion and was involved in flagellum assembly. A general

regulation of respiratory chain components like the ubiquinol *bd* oxidase and the cytochrome *bc*₁ complex as well as membrane-associated components like flagella was therefore supposed in *G. oxydans* under oxygen limitation.

Cells for mRNA-isolation were grown under O₂-excess (DO = 15%) until an OD₆₀₀ of 3.5, then the oxygen limitation was set. Establishment of oxygen limitation was achieved by gassing the bioreactor with 2% O₂. Cells were harvested a few minutes before and 4 h after the start of oxygen limitation for extraction of mRNA (**Fig. 20**). Microarray analysis showed downregulation of the mRNA-levels of 351 genes and upregulation of the mRNA-levels of 291 genes. A selection of the regulated genes was summarised in functional groups as defined by Prust *et al.* 2005 (**Table 8**). Some of these genes exhibited regulation due to the different growth phases of the two time points of harvesting (e.g., 52 genes involved in protein biosynthesis were downregulated). To ascertain condition-specific regulations, a comparison of the two data sets obtained by the conditions oxygen limitation vs. oxygen excess and gluconate-grown cells vs. glucose-grown cells (see next chapter, cell harvest in different growth phases, as well) was made.

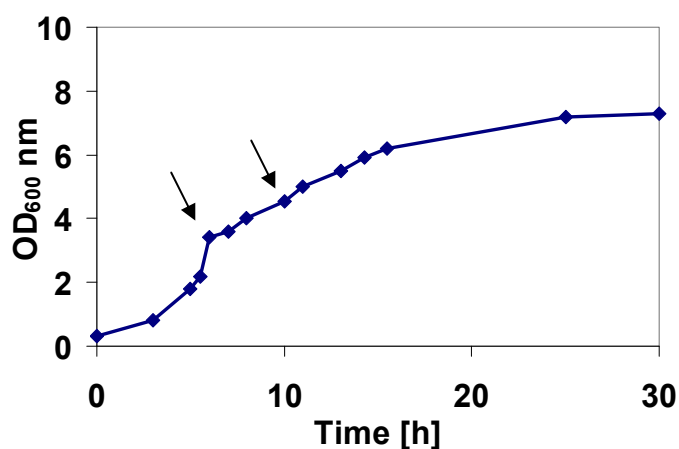


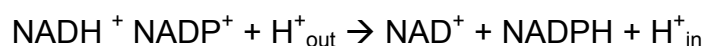
Fig. 20 Growth of *G. oxydans* 621H on 80 g l⁻¹ mannitol under oxygen excess (DO = 15%) and under oxygen limitation (2% O₂). Cells were grown oxygen saturated (DO = 15%) until an OD₆₀₀ of 3, then O₂-limitation was set with 2% O₂, arrows: time point of cell harvest for RNA isolation

Oxygen limitation elicited mainly downregulation of genes involved in the pentose phosphate pathway and in amino acid metabolism. Twenty-eight genes involved in chemotaxis or flagella synthesis were upregulated and 45 genes involved in electron transport and in the assembly of ATP synthase showed a differential regulation.

Table 8 Number of up- and downregulated genes (≥ 1.8 -fold change) in gene groups as defined by Prust *et al.* 2005 under the condition O₂ limitation/O₂ excess. Cells grown with mannitol under oxygen excess (15% DO) for 6 h and then shifted to O₂ limitation (2% O₂ dosage)

Gene group/function	Number of genes regulated	
	up	down
Amino acid metabolism	2	23
Biosynthesis of cofactors	11	10
Fatty acid biosynthesis + degradation	1	9
Cell envelope	5	11
Cell motility	28	0
Cell division	1	4
Detoxification	2	3
Signal transduction	5	1
Phosphate & sulphate	0	1
Nucleotide metabolism	3	8
DNA metabolism	8	8
RNA metabolism	0	6
Transcription	1	3
Citrate cycle	1	3
Glycolysis and gluconeogenesis	2	2
Pentose phosphate pathway	0	6
Sugar/alcohol degradation	2	3
Electron transport + ATP synthase	25	20
Protein fate	10	9
Protein biosynthesis	2	52
Transport	8	28
Phosphotransferase system	3	0

Genes encoding the cytochrome *bc*₁ complex were upregulated under oxygen limitation (**Table 9**), which was in good agreement with the demonstrated use of this complex under oxygen limitation. Genes encoding for the PntAB-transhydrogenase belonged to the most upregulated in *G. oxydans* under the tested conditions. PntAB transhydrogenases spend membrane potential for the supply of NADPH (Jackson 2003):



An enhanced transcription is then a hint for an increased need for NADPH for biomass production. Nevertheless, oxygen-limited cells showed decreased growth in contrast to cells grown under oxygen excess. Prust 2005 suggested a reverse use of the transhydrogenase in *G. oxydans*, which is possibly true under oxygen limitation. The function of the reverse PntAB transhydrogenase reaction is probably proton

translocation to the periplasm at the expense of NADPH, in order to keep up the proton motive force.

In *G. oxydans*, there are three gene clusters encoding for subunits of the ATP synthase (Prust 2005). One (GOX1310-GOX1314) encodes for the F₁ part of the ATP synthase and was partially downregulated, another (GOX1110-GOX1113) encodes for the F₀ part, which was downregulated in total. The cluster GOX2167-GOX2175 encodes a second ATP synthase with F₀ and F₁ part. This ATP synthase was upregulated indicating that there might be a correlation to the upregulation of flagella biosynthesis/chemotaxis involved genes (Table 8, 9).

Table 9 Selected genes differently expressed (> 1.8-fold) in cells grown with mannitol cultivated under oxygen excess (15% DO) for 6 h and then shifted to O₂ limitation (2% O₂ dosage). Results derived from at least three independent biological experiments.

Locus tag	Annotation	<u>O₂ Limitation</u> O ₂ excess	<i>p</i> - Value
GOX0258	Putative cytochrome <i>c</i> -552	1.06	0.2693
GOX0265	Membrane-bound glucose dehydrogenase (PQQ)	0.50	0.0000
GOX0278	Cytochrome <i>d</i> ubiquinol oxidase subunit I	2.22	0.1090
GOX0279	Cytochrome <i>d</i> ubiquinol oxidase subunit II	1.94	0.0089
GOX0310	NAD(P) transhydrogenase subunit alpha	10.37	0.0004
GOX0311	NAD(P) transhydrogenase subunit alpha	14.70	0.0013
GOX0312	NAD(P) transhydrogenase subunit beta	12.04	0.0004
GOX0516	Uncharacterized PQQ-dependent dehydrogenase 4	0.49	0.0054
GOX0564	Cytochrome <i>c</i> precursor	2.02	0.0011
GOX0565	Ubiquinol-cytochrome <i>c</i> reductase iron-sulphur subunit	2.49	0.0036
GOX0566	Ubiquinol-cytochrome <i>c</i> reductase cytochrome <i>b</i> subunit	2.20	0.0123
GOX0567	Ubiquinol-cytochrome- <i>c</i> reductase	1.80	0.0017
GOX0585	Cytochrome <i>c</i> subunit of aldehyde dehydrogenase	2.02	0.0005
GOX0586	Membrane-bound aldehyde dehydrogenase, small subunit	2.01	0.0011
GOX0587	Membrane-bound aldehyde dehydrogenase, large subunit	1.91	0.0023
GOX0771	Ferric uptake regulation protein	0.49	0.0003
GOX0811	Transcriptional regulator Fur family	1.99	0.0005
GOX0814	PTS system, IIA component	4.10	0.0002
GOX0854	D-Sorbitol dehydrogenase subunit SIdA	0.10	0.0000
GOX0855	D-Sorbitol dehydrogenase subunit SIdB	0.10	0.0001
GOX0882	Alpha-ketoglutarate decarboxylase	1.96	0.0005
GOX0984	Coenzyme PQQ synthesis protein D	0.51	0.0000
GOX0987	Coenzyme PQQ synthesis protein A	0.44	0.0040
GOX1110	ATP synthase B' chain	0.48	0.0034

IV Results

GOX1111	ATP synthase B' chain	0.40	0.0058
GOX1112	ATP synthase C chain	0.51	0.0028
GOX1113	F ₀ F ₁ ATP synthase subunit A	0.57	0.0060
GOX1138	Catalase	0.52	0.0054
GOX1190	Glucose-1-phosphatase	2.07	0.0034
GOX1230	Gluconate 2-dehydrogenase, cytochrome c subunit	0.23	0.0003
GOX1231	Gluconate 2-dehydrogenase alpha chain	0.19	0.0001
GOX1232	Gluconate 2-dehydrogenase gamma chain	0.26	0.0002
GOX1310	ATP synthase delta chain	0.58	0.0056
GOX1311	F ₀ F ₁ ATP synthase subunit alpha	0.62	0.0055
GOX1312	F ₀ F ₁ ATP synthase subunit gamma	0.62	0.0058
GOX1314	ATP synthase epsilon chain	0.50	0.0032
GOX1675	NADH dehydrogenase type II	0.37	0.0000
GOX1911	Cytochrome o ubiquinol oxidase subunit II	2.82	0.0016
GOX1912	Cytochrome o ubiquinol oxidase subunit I	2.70	0.0101
GOX1913	Cytochrome o ubiquinol oxidase subunit III	3.56	0.0000
GOX1914	Cytochrome o ubiquinol oxidase subunit IV	3.81	0.0039
GOX2167	F ₀ F ₁ ATP synthase subunit beta	2.81	0.0042
GOX2168	ATP synthase epsilon chain	3.14	0.0034
GOX2169	ATP synthase subunit AtpI	2.79	0.0047
GOX2170	Transmembrane protein	3.13	0.0135
GOX2171	ATP synthase subunit a	3.30	0.0073
GOX2172	ATP synthase subunit c	2.99	0.0007
GOX2173	ATP synthase subunit b	2.64	0.0060
GOX2174	F ₀ F ₁ ATP synthase subunit alpha	2.38	0.0080
GOX2175	ATP synthase gamma chain	1.96	0.0084
GOX2187	Gluconate 5-dehydrogenase	0.44	0.0006

Genes belonging to respiratory chain components acting as acceptors of electrons of reduced ubiquinol showed mainly upregulation, whereas dehydrogenases reducing the ubiquinol pool were mainly downregulated (**Table 9**). This shows that *G. oxydans* reduced the electron transport activity in the respiratory chain when the cells were oxygen-limited. At the same time, upregulation of the end oxidases allowed for capturing of oxygen at sub-optimal concentrations. The NADH dehydrogenase gene exhibited an expression ratio of 0.37. Interestingly, this decrease was not paralleled by the NADH dehydrogenase activity (**Table 10**) perhaps due to regulation at the protein level. The *in vitro* activity of oxygen-limited cells was only slightly decreased. In *Zymomonas mobilis*, NADPH can be oxidised via the membrane-bound NADH dehydrogenase (Kalnenieks *et al.* 2008). Since the composition of respiratory chain components is very similar in *G. oxydans* and *Z. mobilis* (Bringer *et al.* 1984, Kersters *et al.* 2006, Sahm *et al.* 2006, Kalnenieks *et al.* 2006, 2007), the question arose if *G. oxydans* can oxidise NADPH via the membrane-bound NADH dehydrogenase, too. However, activity with NADPH as electron donor neither was measured

photometrically nor potentiometrically in *G. oxydans* so that NADPH cannot be used for the energy supply of the cells but serves for anabolic reactions only.

The gene encoding the ferric uptake regulator (Fur) was upregulated. In *E. coli*, Fur mediates the regulation of iron acquisition and storage systems, respiration, the TCA cycle, glycolysis, methionine biosynthesis, phage-DNA packaging, purine metabolism, and redox-stress resistance (McHugh *et al.* 2003) by binding of Fe²⁺ and subsequent repression of the target genes.

Table 10 Stoichiometry of the intracellular NADH-dependent oxygen reduction. Measurements were performed with isolated cell membranes of cells grown under oxygen excess or under oxygen limitation, photometrically for NADH oxidation and in a Clark electrode chamber for O₂ reduction.

Sample	NADH oxidation (nmol mg ⁻¹ protein)	Oxygen consumption (nmol mg ⁻¹ protein)
Oxygen excess	1851 ± 105	832 ± 40
Oxygen limitation	1706 ± 98	788 ± 37

Genes involved in the pentose phosphate pathway had decreased mRNA-levels under oxygen limitation, as well as the genes encoding for the cytoplasmatic glucose dehydrogenase, indicating a decreased sugar metabolism under oxygen limitation. The catalase gene showed a strong downregulation, which in turn is an indication for decreased H₂O₂ concentrations under oxygen limitation compared to oxygen excess (Yoshpe-Purer and Henis 1976). Interestingly, the mRNA level of the EII^A component of the PTS system increased under oxygen limitation although the PTS system is supposed to be not functional in *G. oxydans* (Prust *et al.* 2005). Upregulation indicates that there are regulatory functions like catabolite repression left in EII^A.

Matsushita *et al.* 1989 reported an increased use of the more inefficient ubiquinol *bd* oxidase in cells grown under acidic conditions. However, this was shown indirectly only. In this work, the idea was put forward that the cytochrome *bc*₁ complex is necessary when the ubiquinol *bd* oxidase is preferably used in order to maintain proton motive force. Therefore, it was required to unambiguously show the increase of the ubiquinol *bd* oxidase at the transcriptional level to verify the indirect results of Matsushita *et al.* 1989. For comparison of the levels of mRNA of cells grown at pH 4 to those of cells grown at pH 6, both cultures were harvested at OD₆₀₀ of 2.5 in the same growth phase (**Fig. 21**). Ninety-five genes showed altered mRNA-levels, 41 of these genes encoding for transposases or hypothetical proteins. **Table 11** shows a

grouping of some selected genes according to Prust *et al.* 2005. Most of the genes with an altered mRNA-level were involved in electron transport (upregulation) and energy supply or in cellular transport processes (downregulation).

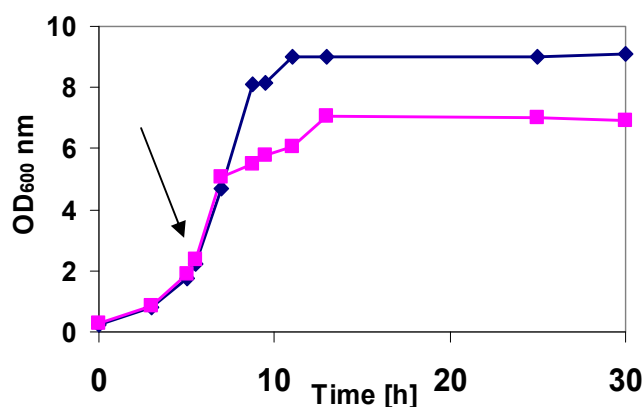


Fig. 21 Growth of *G. oxydans* 621H on 80 g l⁻¹ mannitol at pH 4 (-■-) and at pH 6 (-◆-), oxygen supply DO = 15%. Arrow: time-point of cell harvest for isolation of mRNA

Table 11 Number of up- and downregulated genes (≥1.8-fold change) in groups as defined by Prust *et al.* 2005 under the condition pH 4 vs. pH 6. Genes expressed in cells grown at pH 4 vs. pH 6

Gene group / function	Number of genes regulated	
	up	down
Amino acid metabolism	0	2
Biosynthesis of cofactors	0	1
Fatty acid biosynthesis/degradation	0	2
Detoxification	1	0
Nucleotide metabolism	0	4
DNA metabolism	2	1
Citrate cycle	0	2
Pentose phosphate pathway	1	0
Sugar/alcohol degradation	3	0
Electron transport + ATP synthase	10	1
Protein fate	1	1
Transport	1	10

The genes encoding the cytochrome *bc*₁ complex were not regulated in cells cultivated at pH 4. However, the gene encoding the ubiquinol *bd* oxidase was upregulated (**Table 12**) which is in agreement with the results of Matsushita *et al.* 1989. In contrary, the mRNA level of the cytochrome *c* subunit of the alcohol dehydrogenase did not increase, as postulated by Matsushita *et al.* 1989. Only the gene encoding for the 15 kDa subunit of the alcohol dehydrogenase was upregulated

at the mRNA level. Upregulation of the gene encoding catalase indicated that formation of H₂O₂ was enhanced during growth of cells at low pH.

mRNA-levels of many outer membrane receptor proteins were downregulated in pH 4 grown cells, so activity of uptake systems for e.g. sugars (GOX0524) was decreased. The most upregulated genes were those encoding for DNA-starvation/stationary phase protein Dps, which is involved in system against DNA-degradation, and bacterioferritin for iron storage. In conclusion, an acidic pH evokes systems against DNA-degradation and leads to storage of iron.

Table 12 Selected genes differently expressed (> 1.8-fold) in cells grown at pH 4 vs. genes expressed in cells grown at pH 6. Results derived from at least three independent biological experiments

Locus tag	Annotation	<u>pH 4</u> <u>pH 6</u>	<i>p</i> -value
GOX0207	Outer membrane receptor protein	0.22	0.0022
GOX0278	Cytochrome <i>d</i> ubiquinol oxidase subunit I	2.22	0.0109
GOX0279	Cytochrome <i>d</i> ubiquinol oxidase subunit II	1.59	0.0511
GOX0524	Outer membrane receptor protein	0.19	0.0086
GOX0707	DNA-starvation/stationary phase protein Dps	3.47	0.0421
GOX0756	Alcohol dehydrogenase 15 kDa subunit	1.83	0.0151
GOX0907	Outer membrane receptor protein	0.33	0.0020
GOX0945	Outer membrane receptor protein	0.39	0.0236
GOX1017	Outer membrane receptor protein	0.31	0.0048
GOX1138	Catalase	2.10	0.0016
GOX1173	Outer membrane heme receptor	0.40	0.0490
GOX1336	Isocitrate dehydrogenase	0.45	0.0227
GOX1441	Uncharacterized PQQ-dependent dehydrogenase 3	1.82	0.0190
GOX1748	Bacterioferritin	3.37	0.0020
GOX1857	Uncharacterised PQQ-containing dehydrogenase 1	0.40	0.0099
GOX1903	TonB-dependent receptor protein	0.42	0.0004

The cellular changes, which occur during the transition from phase I to phase II during growth on glucose in *G. oxydans*, are not fully understood yet. In order to throw light on the regulatory mechanisms leading to the phenotype of biphasic growth and oxidation during growth on glucose, genome-wide transcription analysis was performed in the wild type. For this DNA array experiment, cells were cultivated on glucose and cells were harvested during growth phase I and growth phase II. Since *G. oxydans* shows biphasic growth behaviour when cultivated on glucose (**Fig. 22**), the cells were harvested at different growth phases. Growth phase-

dependent changes in mRNA-levels increased the response to the regulation, which occurred during transition from phase I to phase II, explaining the strong response of downregulation of 332 genes whereas 276 genes showed upregulated mRNA levels. **Table 13** shows a functional grouping of some selected genes according to Prust *et al.* 2005. Many of these genes with altered mRNA-levels are involved in electron transport and energy supply, cellular transport processes or amino acid metabolism. Nearly all genes involved in gluconeogenesis, pentose phosphate pathway and Entner-Doudoroff pathway were upregulated (**Table 13, 14**), indicating for an enhanced sugar metabolism in phase II. The cytochrome *bc₁* complex genes were not regulated, although the deletion mutant devoid of the complex showed retarded growth in growth phase II.

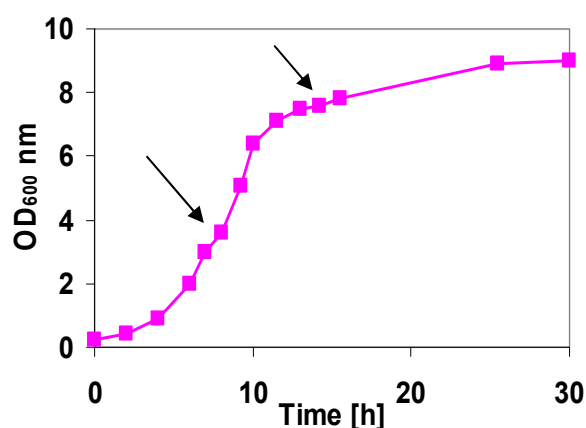


Fig. 22 Growth of *G. oxydans* 621H on 80 g l⁻¹ glucose at pH 6 and oxygen supply DO = 15%. Arrows: time-point of cell harvest for isolation of mRNA

Table 13 Number of up- and downregulated genes (≥ 1.8 -fold change) in gene groups as defined by Prust *et al.* 2005 under the condition growth phase II/growth phase I during growth on glucose. Cells grown with glucose, growth phase II (carbon source gluconate) compared to growth phase I (carbon source glucose)

Gene group / function	Number of genes regulated	
	up	down
Amino acid metabolism	7	24
Biosynthesis of cofactors	4	6
Fatty acid biosynthesis/degradation	1	12
Cell envelope	3	13
Cell motility	5	0
Cell division	3	7
Detoxification	3	1
Signal transduction	3	3
Phosphate & sulphate	0	3
Nucleotide metabolism	1	9

DNA metabolism	8	8
RNA metabolism	1	8
Transcription	0	3
Citrate cycle	1	3
Glycolysis and gluconeogenesis	5	0
Pentose phosphate pathway	6	0
Sugar/alcohol degradation	9	6
Electron transport + ATP synthase	18	16
Protein fate	4	5
Protein biosynthesis	4	58
Transport	20	31
Phosphotransferase system	2	0

The data obtained from the microarray analysis demonstrated an enhanced pentose phosphate pathway in the second growth phase. The activities of corresponding enzymes determined in cell-free extracts confirmed the results of the microarray analysis (**Table 14**) providing a second evidence for an enhanced, partly cyclic pentose phosphate pathway. Whereas the activity of glucose kinase remained constant in both growth phases, the activity of the gluconate kinase, the glucose 6-phosphate dehydrogenase and the 6-phosphogluconate dehydrogenase were 2- to 3.4-fold increased in the second growth phase. These results indicate that expression of the genes for gluconate kinase and the two dehydrogenases is activated or derepressed in the second growth phase. Since CO₂ production is high in the second growth phase (**Fig. 13b**, page 40), a third evidence for an enhanced and partly cyclic pentose phosphate pathway was provided.

Table 14 Specific enzyme activities of glucose kinase, gluconate kinase, glucose 6-phosphate dehydrogenase and 6-phosphogluconate dehydrogenase in the two growth phases

Enzyme	Activity [U/mg protein]		Factor III/I
	Growth-Phase I	Growth-Phase II	
Glucose kinase (GOX1182)	0.086 ± 0,0043	0.086 ± 0,0043	1.0
Gluconate kinase (GOX1709)	0.034 ± 0,0034	0.068 ± 0,0014	2.0
Glucose 6-phosphate DH (GOX0145)	0.280 ± 0,0056	0.940 ± 0,0094	3.4
6-Phosphogluconate DH (GOX1705)	0.180 ± 0,0018	0.420 ± 0,0084	2.3

Genes encoding the membrane-bound gluconate-2-dehydrogenase (GOX1230-1232) were upregulated in growth phase II in good agreement with a periplasmatic production of 2-ketogluconate in growth phase II. The enzyme responsible for cytoplasmatic oxidation of non-phosphorylated gluconate, gluconate 5-dehydrogenase (GOX2187), was upregulated in growth phase II. This may be a hint

that gluconate was taken up in phase II leading to an enhanced cytoplasmatic oxidation of the substrate (**Table 15**). Interestingly, the two dehydrogenases for sorbitol oxidation were contrarily regulated in the two growth phases on glucose. The PQQ-containing major polyol dehydrogenase was upregulated whereas the FAD-dependent enzyme, which is not functional in *G. oxydans* due to a frame shift (Prust *et al.* 2005), was downregulated. The upregulation of the major polyol dehydrogenase in growth phase II is in good agreement with an enhanced production of 5-ketogluconate in phase II since the major polyol dehydrogenase is the responsible enzyme for periplasmatic 5-ketogluconate production (Weenk *et al.* 1984).

In growth phase II genes encoding for the two ATP synthases, the transhydrogenase and the ubiquinol *bd* oxidase showed the same regulation pattern as in oxygen-limited cells leading to the assumption, that the transcription of these genes was subject to a common underlying condition in the two DNA microarray experiments. In both experimental setups, oxygen limitation and glucose metabolism, growth phase differences existed between the cells which were harvested for the corresponding mRNA-isolations. The identical regulation pattern of genes under the two conditions, indicated that their regulation was partly due to growth decrease causing stress (Wagner *et al.* 2009). The induction of genes encoding RNA polymerase factor sigma-32, a small heat shock protein (sHsp), and the chaperone DnaK was surprising in gluconate grown *G. oxydans*. As it is known that there are several unfavourable growth conditions that provoke heat shock response, e.g. heat, cold, salt, drought, osmotic and oxidative stresses (Jiang *et al.* 2009, Parsell *et al.* 1989; van Bogelen *et al.* 1996), the upregulation of genes encoding RNA polymerase factor sigma-32, sHsp, and DnaK is maybe an indication for a stress situation in growth phase II. In *G. oxydans* the gene encoding superoxide dismutase was upregulated 3.5-fold in gluconate grown cells, indicating oxidative stress under this condition. A direct explanation, why cells in growth phase II should be affected by oxygen stress is not clear. Nevertheless, the data described here indicate a stress situation, which is probably oxidative stress. Furthermore, the strong sigma-32 dependent induction of a small heat shock protein (sHSP) and of the chaperone DnaK (Hsp70) in *G. oxydans* was a consequence of the increased sigma-32 protein level. In *E. coli*, the sigma-32 regulon is essential for growth and cell division and highly responsive to growth phases (Wagner *et al.* 2009). Thus, the change from an

exponential growth in phase I to linear growth in phase II of *G. oxydans* may be a result of heat shock response, which in turn was caused by a stress situation.

The standard medium for cultivation of *G. oxydans* contained 0.5 g l⁻¹ glycerol. Genes involved in glycerol degradation and metabolism (GOX2087-GOX2090 and GOX2217) were upregulated showing that this polyol is metabolised within the second growth phase. The gene encoding the glycerol uptake facilitator protein was upregulated so that more glycerol was taken up in phase II. Glycerol metabolism was enhanced in growth phase II indicated by the increased mRNA-level of genes encoding for glycerol kinase, glycerol 3-phosphate dehydrogenase and triosephosphate isomerase leading finally to glyceraldehyde 3-phosphate. Glyceraldehyde 3-phosphate is then channeled into the PPP, explaining the 10-fold upregulation of the gene encoding triosephosphate isomerase. Furthermore, this sequential catabolism of glucose and glycerol points to catabolite repression in *G. oxydans*.

Table 15 Selected genes differently expressed (> 1.8-fold) in cells grown with glucose, growth phase II (carbon source gluconate) compared to growth phase I (carbon source glucose). Results derived from at least three independent biological experiments. Empty cell: *p*-value not calculable

Locus tag	Annotation	Gluconate/	
		glucose	<i>p</i> -value
GOX0145	Glucose-6-phosphate 1-dehydrogenase	2.75	0.0181
GOX0278	Cytochrome <i>d</i> ubiquinol oxidase subunit I	2.70	0.0010
GOX0279	Cytochrome <i>d</i> ubiquinol oxidase subunit II	1.75	0.0667
GOX0310	NAD(P) transhydrogenase subunit alpha	4.38	0.0003
GOX0311	NAD(P) transhydrogenase subunit alpha	6.02	0.0036
GOX0312	NAD(P) transhydrogenase subunit beta	5.06	0.0014
GOX0430	KDPG aldolase	0.94	0.3746
GOX0431	Phosphogluconate dehydratase	0.44	0.0063
GOX0506	RNA polymerase factor sigma-32	4.83	0.0063
GOX0855	D-Sorbitol dehydrogenase subunit SldB	1.92	0.0520
GOX0882	Alpha-ketoglutarate decarboxylase	1.83	0.0000
GOX1110	ATP synthase B' chain	0.37	0.0006
GOX1111	ATP synthase B' chain	0.41	0.0036
GOX1112	ATP synthase C chain	0.44	0.0001
GOX1113	F ₀ F ₁ ATP synthase subunit A	0.41	0.0015
GOX1230	Gluconate 2-dehydrogenase, cytochrome <i>c</i> subunit	2.75	0.0045
GOX1231	Gluconate 2-dehydrogenase alpha chain	2.33	0.0099
GOX1232	Gluconate 2-dehydrogenase gamma chain	2.17	0.0659
GOX1310	ATP synthase delta chain	0.35	0.0026
GOX1311	F ₀ F ₁ ATP synthase subunit alpha	0.44	0.0055
GOX1312	F ₀ F ₁ ATP synthase subunit gamma	0.43	0.0120

GOX1314	ATP synthase epsilon chain	0.51	0.0134
GOX1329	Small heat shock protein	18.31	0.0010
GOX1335	Aconitate hydratase	0.38	0.0071
GOX1336	Isocitrate dehydrogenase	0.29	0.0043
GOX1352	Ribulose-phosphate 3-epimerase	1.15	0.1776
GOX1375	Gluconolactonase	0.86	0.2487
GOX1381	Gluconolactonase	2.56	0.0026
GOX1643	Fumarate hydratase	0.50	0.0107
GOX1703	Transketolase	2.71	0.0040
GOX1704	Bifunctional transaldolase/phosphoglucose isomerase	2.85	0.0231
GOX1705	6-phosphogluconate dehydrogenase-like protein	2.72	0.0473
GOX1706	Putative hydrolase of the HAD superfamily	1.66	0.0149
GOX1707	6-Phosphogluconolactonase	1.86	0.0173
GOX1708	Ribose 5-phosphate isomerase	1.56	0.0400
GOX1709	Gluconokinase	1.62	0.0256
GOX2015	NAD(P)-dependent glucose 1-dehydrogenase	0.81	0.1283
GOX2018	Aldehyde dehydrogenase	1.18	0.2207
GOX2084	Ribokinase	0.88	0.0339
GOX2087	Glycerol-3-phosphate regulon repressor	1.84	0.0818
GOX2088	Glycerol-3-phosphate dehydrogenase	4.50	0.0040
GOX2089	Glycerol uptake facilitator protein	3.93	0.0140
GOX2090	Glycerol kinase	4.58	0.0099
GOX2096	Sorbitol dehydrogenase large subunit	0.44	0.0599
GOX2097	Sorbitol dehydrogenase small subunit	0.49	0.0492
GOX2167	F ₀ F ₁ ATP synthase subunit beta	2.09	0.0412
GOX2168	ATP synthase epsilon chain	3.27	
GOX2169	ATP synthase subunit AtpI	2.09	0.0104
GOX2170	Transmembrane protein	1.60	
GOX2171	ATP synthase subunit a	2.39	0.0139
GOX2172	ATP synthase subunit c	1.83	0.0284
GOX2173	ATP synthase subunit b	1.75	0.0389
GOX2174	F ₀ F ₁ ATP synthase subunit alpha	1.63	0.0611
GOX2175	ATP synthase gamma chain	1.41	
GOX2187	Gluconate 5-dehydrogenase	4.54	0.0008
GOX2217	Triosephosphate isomerase	10.78	0.0023

3. ¹³C-Metabolome analysis and flux analysis (MFA)

The metabolic changes from the first to the second growth and oxidation phase during growth on glucose were still not fully characterised. ¹³C-Metabolome analysis and metabolic flux analysis (MFA) were applied to solve the question of the quantity and oxidation state of the substrate entering the cell for catabolism. At the same time, metabolic flux analysis would allow an identification of the principal pathway of glucose catabolism since the annotation of all genes belonging to enzymes of the pentose phosphate pathway and the Entner-Doudoroff pathway in *G. oxydans* did not allow for a resolution of the relative contributions of the two pathways to overall catabolism. Since no defined medium for *G. oxydans* supporting growth to high cell

density was available, we used a complex medium for allocation of cell mass. Then, establishment of the ^{13}C -metabolome was by analysis of the metabolic intermediates rather than by amino acids analysis (Wiechert 2001, Zamboni *et al.* 2009).

Cells were harvested during the first and the second growth phase on labeled glucose (4.0% “natural” glucose, 7.7% 1- ^{13}C -glucose, and 88.3% U- ^{13}C) (for reference of cell growth on glucose pH 6, see **Fig. 12a**, page 39). Two independent cultures grown with ^{13}C -labeled glucose showed identical growth behavior and substrate oxidation rates as the reference culture cultivated with natural glucose. Biomass production in the second growth phase was only one fourth ($0.38 \text{ g l}^{-1} \text{ CDW}$) of that of the first growth phase ($1.5 \text{ g l}^{-1} \text{ CDW}$), although the concentration of accumulated gluconate (which then was used for energy supply and biomass formation in the second growth phase) was more than two thirds of the initial 80 g l^{-1} glucose concentration. Therefore, in phase II a theoretical biomass formation of two thirds of the biomass formation in phase I was possible. This was not the case, allowing the conclusion that oxidation of glucose is more efficient with respect to biomass production.

A reference culture with natural glucose showed the de facto CO_2 production, since short cell infrared detectors as used in the DasGip fermentation system quantify $^{13}\text{CO}_2$ not correctly (**Fig. 23**) (Hirano *et al.* 1979). In contrast to the identical total oxygen consumption in phases I and II, the total CO_2 production in phase II was 5.7-fold higher than in phase I. The increased CO_2 production in the second growth phase was not proportional to cell growth (which decreased in growth phase II when CO_2 production increased), indicating that metabolic activities were varying over time, i.e. the cells were in a state of metabolic non-stationarity (**Fig. 23**). Since metabolic stationarity is a prerequisite for metabolic flux analysis (Wiechert and Nöh 2005), the sample taken in the second growth was included in the LC-MS analysis, but excluded from flux analysis.

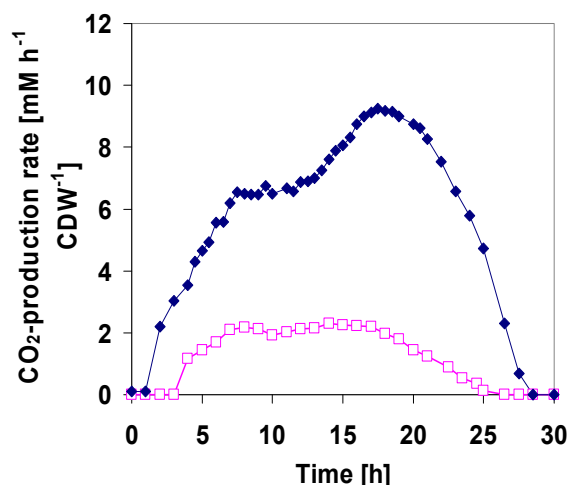


Fig. 23 Specific carbon dioxide production rates of *G. oxydans* 621H cultivated with 80 g l⁻¹ glucose in a bioreactor at pH 6 and optimal oxygen supply DO: 15%. Specific carbon dioxide production rate of the ¹³C-labeled culture (-□-) and of the non-labeled culture (-◆-); ¹³CO₂ is not fully detected by short cell infrared measurements

For metabolic flux analysis, it is important to quantify the carbon of all metabolic products during the growth of the cells (Wiechert and Nöh 2005). The premise of a closed carbon balance for MFA was met for growth phase I and also for the whole time of growth including phase II. The following calculations are based on data obtained after 30 h growth: By oxidation, 89% of the 440 mM initial glucose (=2640 mM C initially) was converted to gluconate and ketogluconates, which accumulated as products in the medium (**Table 16**). According to the estimation that carbon makes up 50% of cell dry weight (Stouthamer and Bettenhausen 1973), only about 3% (77 mM) of the carbon originally present as initial glucose (2640 mM) was used to form biomass (1.86 g l⁻¹ CDW). 10% of the initial carbon was converted to carbon dioxide (263 mM). So after 30 h of growth, 102% of the initial carbon was found as gluconate, ketogluconates, CO₂ and biomass, resulting in a closed carbon balance. After growth phase I, the carbon balance was closed, too, so that both premises for MFA (metabolic stationarity and closed carbon balance) were given for growth phase I.

Table 16 Carbon balance after growth of *G. oxydans* 621H for 10 h (phase I) and 30 h (phases I + II) with 80 g l⁻¹ glucose under pH and oxygen control C: carbon

<i>G. oxydans</i> 621H	mM C of glucose (t = 0 h)	mM C of products formed	mM CO ₂ formed	mM C assimilated in CDW	Carbon balance %
Phase I (t = 10 h)	2640	2420	39	64	96
Phases I+II (t =30h)	2640	2340	263	77	102

LC-MS analysis was the basis for MFA and gave some additional information on the growth phase II, where no MFA was possible due to metabolic instationarity. LC-MS analysis showed that labeling information, stemming either directly from glucose or indirectly from the oxidation product gluconate, was mainly distributed in the intermediates of glycolysis/glyconeogenesis and of the EDP and PPP of *G. oxydans* (**Fig. 24**). For these metabolites, no significant changes in the labeling patterns between the two growth phases were observed. Intermediates of the TCA cycle showed almost no labeling enrichment during the first phase, while in the second phase some slight increase in the labeling fractions for all mass isotopomers were detected. The fact that labeled succinate was measured does not allow to conclude a functional succinyl-CoA synthetase enzyme because succinyl-CoA is known to be unstable and can decompose to succinate spontaneously (Gao *et al.* 2007).

Overall, labeling of the TCA cycle intermediates was less pronounced than that of intermediates of the other metabolic pathways. For example, a high proportion of phosphoenolpyruvate was labeled in all three carbon atoms, whereas most of the measured citric acid was not labeled or labeled in just one or two carbon atoms (**Fig. 24**). Hence, for both phases, a clear cut between the labeling enrichment in the intermediates of the upper and lower parts of central metabolism was found, indicating that in the lower parts of the central metabolism supplementary reactions e.g. by amino acid uptake from the yeast extract occurred.



Fig. 24 Mass isotopomer labeling measurements of intracellular metabolites (red: growth phase I, green: growth phase II) arranged by pathways: fractional abundance over mass. Error bars indicate measurement standard deviations derived from two independent biological replicates. For abbreviations of metabolite names see **Table 17** (Appendix). A switch from predominantly fully labeled mass isotopomers in glycolytic and PPP intermediates to almost naturally labeled TCA cycle compounds is evident. m0: no carbon atom was labeled; m6: six carbon atoms were labeled

Furthermore, more CO₂ was measured during the growth on glucose than would be formed by total oxidation of the glucose and/or gluconate which entered the cells. The carbon balance of initial substrate concentration and the concentration of the products gluconate and ketogluconate measured by HPLC-analysis, resulted in a difference of 3 g l⁻¹ (16.5 mM) of C-6 carbohydrates or 100 mM CO₂ (total oxidation of one C-6 carbohydrate leads to maximal 6 CO₂) after 30 h of growth, stemming from intracellular sugar oxidation under the assumption that the PPP was partly cyclic. The analysed amount of total carbon dioxide was 263 mM after 30 h so that 160 mM surplus carbon dioxide was produced. Following the calculation, that nearly half of the CO₂ produced was not originating from central sugar metabolism supported the result described above, that amino acids were taken up in side reactions. A carbon balance only refers to balancing the initial glucose entering the cells and the products formed during growth (addition of accumulating gluconate and ketogluconate, substrate integration for biomass production and CO₂). For this reason, the additional 160 mM CO₂ not stemming from the initial carbon source had to be subtracted in the carbon balance. Nevertheless, the carbon balance was not much affected by subtracting the surplus 160 mM CO₂. It was still closed with 97% after 30 h cell growth. However, the results clarified, that the high CO₂ production in growth phase II is not only due to a cyclic PPP as was assumed in the past.

Nearly all measurable amino acids were unlabeled, supporting the assumption of uptake of amino acids from the medium, as well as the measured surplus CO₂. Indeed, qualitative determination of amino acids within the two growth phases showed, that Asp, Gly, Thr, Val, Phe, Ile and leu were mainly consumed during the transition from growth phase I into phase II (8 h to 14.5 h). In total, Glu, Asn, Ser and Ala were also used during the whole growth time. Exhaustion of amino acids could be one reason for the decreased growth in the second growth phase. However, increase of the concentration of yeast extract from 5 g l⁻¹ to 15 g l⁻¹ did not result in increased growth during the second growth phase so that a limitation of amino acids was excluded as an explanation for the decreased cell growth in phase II. On the contrary, the time point of transition from the first to the second growth phase did not change and cell growth was not enhanced in growth phase II, showing that the growth in phase II is mainly dependent from the sugar concentration. The point of time of total glucose oxidation determines the point of time of the beginning of decreased growth.

Based on the ^{13}C metabolome analysis, a flux analysis was only possible for the first growth phase (**Fig. 25**). Intracellular fluxes were estimated using the extracellular flux measurements, like accumulation rates of gluconate and ketogluconates in the medium, and the ^{13}C metabolite labeling data of sample point I in growth phase I. Repeated flux estimation with randomly chosen initial values for all independent fluxes showed good and reproducible agreement of measurements and model predictions for all reactions of the EMP, PPP and EDP. The model showed that almost all glucose (96.87%) was directly oxidised by the membrane-bound glucose dehydrogenase to gluconate, which to some extent was further oxidised to ketogluconates by the major polyol dehydrogenase (g5dh) and gluconate-2-DH (g2dh) (together 13.81%). 83.04% of the gluconate accumulated in the medium instead of being further oxidised in growth phase I. Based on the model, a small amount (3.13%) of glucose was taken up by the cells. These 3.13% were converted to gluconate by the cytoplasmic glucose dehydrogenase (gdh3) and gluconolactonase (gdh4). Additionally, PPP was calculated in the model to be cyclic, so that glucose 6-phosphate was formed without a net flux from glucose to glucose 6-phosphate. In contrast, the model showed a flux from glucose 6-phosphate to glucose (1.23%), which was added to the flux from glucose to gluconate resulting in a total net flux of 4.36% from glucose to gluconate. The intracellular gluconate was phosphorylated by gluconate kinase (gcnk) so that the model calculated a net flux of 3.36% for that reaction. A part of the gluconate was further oxidised cytoplasmatically by the gluconate 5-dehydrogenase, so that a net flux of 1.02% was calculated. The 5-ketogluconate was then contributing to the ketogluconate in the medium due to an export of 5-ketogluconate from the cytoplasm to the medium via the periplasm (1.02%).

The cytoplasmatic glucose 6-phosphate was channeled into the PPP and the lower part of the glycolysis as was demonstrated by the model. Due to the calculated cyclic operation of the PPP, a net flux of 1.29% from glucose 6-phosphate to 6-phosphogluconate was added to the flux of 3.36% coming from the phosphorylation reaction of gluconate to 6-phosphogluconate and so a net flux of 4.38% from 6-phosphogluconate to ribulose 5-phosphate was calculated. A small net flux of 0.28% from 6-phosphogluconate to 2-keto-3-deoxygluconate 6-phosphate (KDPG) showed, that the Entner-Doudoroff pathway was nearly inactive during growth phase I.

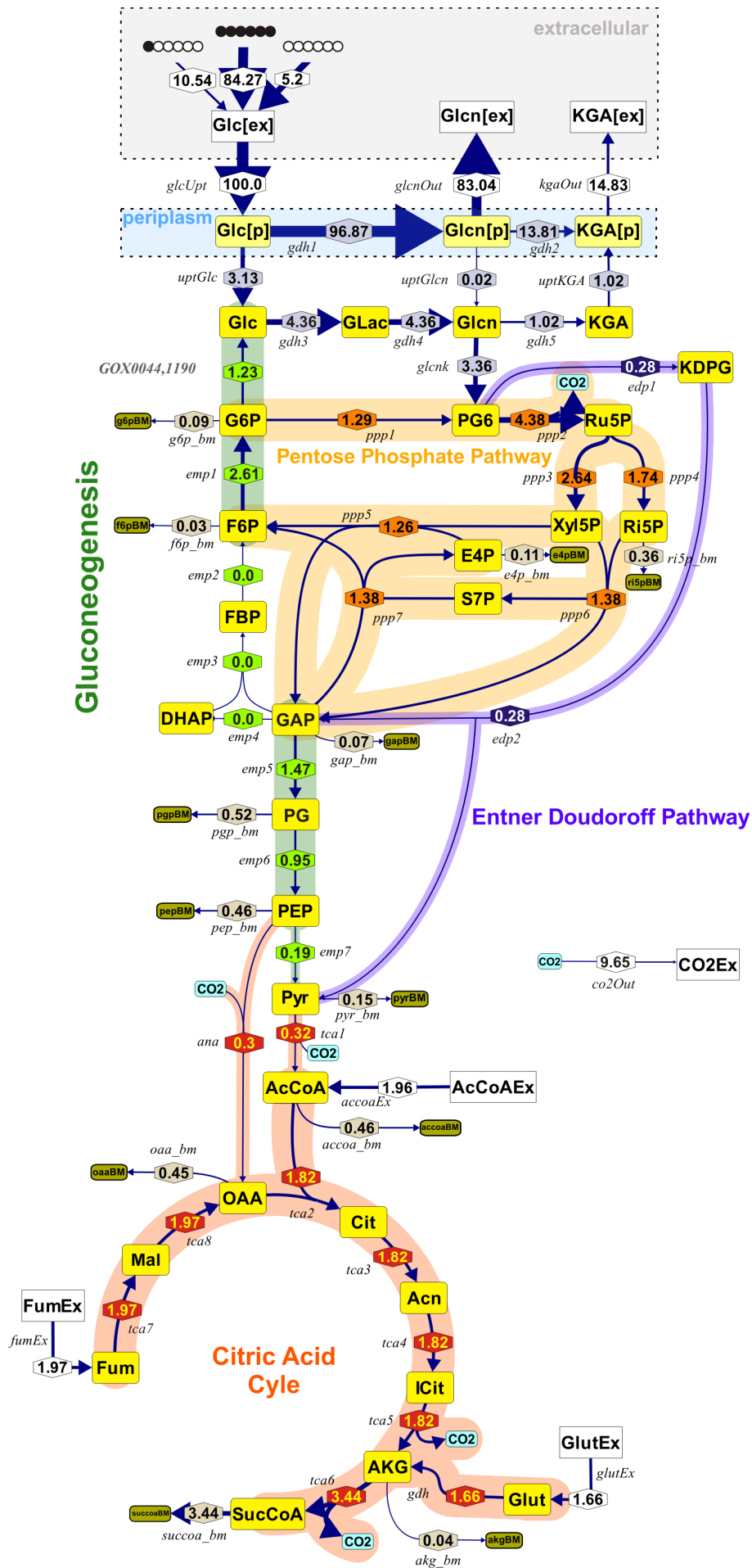


Fig. 25 *In vivo* flux distribution of *G. oxydans* 621H during growth with glucose (growth phase I). Main metabolic pathways that were in the focus of the ^{13}C -MFA study proceed in two compartments, periplasm and cytosol. All mass balanced metabolites are represented by rectangles (yellow: central metabolism, white: carbon sources, dark yellow: carbon sinks). Fluxes into biomass synthesis are in stone. Flux values (hexagons) are related to 100% glucose uptake (*glcUpt*) where a mixture of naturally labeled, $1\text{-}^{13}\text{C}$ and $\text{U-}^{13}\text{C}$ labeled glucose is exposed. The width of each flux edge is scaled proportional to its underlying value; flux arrows are pointing in net flux direction. For abbreviations of flux and metabolite names used in the model see **Table 17** (Appendix) (GOX0044: Phosphomannomutase; GOX1190: Glucose-1-phosphatase). The picture was generated with Omix - an editor for biochemical network visualization [<http://www.13cflux.net/omix>]. PG: 1,3 bisphosphoglycerate, 3-phosphoglycerate and 2-phosphoglycerate are lumped.

From the ribulose 5-phosphate, a net flux of 2.64% to xylulose 5-phosphate was calculated, whereas only 1.74% were converted to ribose 5-phosphate. That indicates that the ribulose 5-phosphate epimerase is more active than the ribulose 5-phosphate isomerase. The operations of the PPP and the EDP resulted in formation of fructose 6-phosphate, glyceraldehyde 3-phosphate and pyruvate. High fluxes for transaldolase (ppp7, 1.38%) and transketolase (ppp5, 1.26%) in the direction of fructose 6-phosphate formation and a high flux for glucose 6-phosphate isomerase (emp1, 2.61%) explain the formation of glucose 6-phosphate (**Fig. 25**) and show the cyclic operation of the PPP. According to the model, no flux was calculated for triosephosphate isomerase, fructose bisphosphatase and fructose-1,6-diphosphate aldolase. The model-predicted formation of unphosphorylated glucose from glucose 6-phosphate can be catalysed by phosphomannomutase (GOX0044) and glucose 1-phosphatase (GOX1190).

The model calculated a net flux of 1.47% from glyceraldehyde 3-phosphate to phosphoglycerate. Due to net fluxes into biomass, further fluxes to phosphoenolpyruvate (PEP) and subsequent pyruvate decreased. Since a net flux from KDGP of 0.28% to pyruvate via the 2-keto-3-deoxygluconate 6-phosphate aldolase (edp2) was added to the 0.19% carbon flux, which were channelled to pyruvate via the pyruvate kinase, a net flux of 0.32% from pyruvate to acetyl-CoA was possible. For the anaplerotic reaction from PEP to oxaloacetate, a net flux of 0.3% was estimated. Although less labeling information was present in intermediates of the citric acid cycle (TCA), a calculation of net fluxes in this part of the metabolism was possible assuming additional fluxes of acetyl-CoA, fumarate and glutamate predicted by the model. Those model based additional fluxes were in the range of about 2% each. Therefore, the model supported the idea of additional uptake reactions based on e.g.

balancing the CO₂ production with the uptake of glucose determined by HPLC analysis. The additional uptake reactions in the model served for a net flux of 1.82-3.44% in the TCA.

A model based estimation of 12 net fluxes into biomass was given. Those fluxes started from ribose 5-phosphate (0.36%), erythrose 4-phosphate (0.11%), glucose 6-phosphate (0.09%), fructose 6-phosphate (0.03%), glyceraldehyde 3-phosphate (0.07%), phosphoglycerates (0.52%), PEP (0.46%), pyruvate (0.15%), acetyl-CoA (0.46%), oxaloacetate (0.45%), succinyl-CoA (3.44%) and α -ketoglutaric acid (0.04%). Interestingly, an additional uptake flux of 1.96% of acetyl-CoA was predicted, at the same time, a flux of 0.46% acetyl-CoA into biomass was calculated indicating for a high requirement for acetyl-CoA for biomass production. A flux of 3.44% succinyl-CoA for biomass production was estimated since no succinyl-CoA accumulated in the medium, so that a flux into biomass was a good resolution for the “dead end” reaction in the TCA. Finally, a flux of about 10% was determined for CO₂ production. This model predicted value fitted best to the measured CO₂ production in the parallel fermentation system.

V Discussion

1. Analysis of physiological and metabolic functions of the cytochrome *bc*₁ complex in *G. oxydans*

G. oxydans with its numerous membrane-bound dehydrogenases offers various promising perspectives for industrial use of the organism (Campbell *et al.* 2000, Schedel 2000, Claret *et al.* 1994). Many of these dehydrogenases have been studied in the last decades (Matsushita *et al.* 1989, 1991), and in 2005 genome sequencing disclosed new dehydrogenases for prospective industrial use (Deppenmeier and Ehrenreich 2009). To almost the same extent both of the two terminal oxidases, ubiquinol *bd* and *bo*₃ have been the targets of intensive investigations for understanding their contribution to the energy supply of *G. oxydans* (Matsushita *et al.* 1989). Before genome sequencing the existence of a third pathway for electron transport via the cytochrome *bc*₁ complex remained undetected in *G. oxydans*. However, in the present work deletion of the genes encoding the cytochrome *bc*₁ complex was successful giving the opportunity to attain insight into its role for e.g. the energy supply of the cells via phenotyping of the mutant.

With mannitol as carbon source and under optimal growth conditions in a bioreactor system, the deletion mutant showed the same growth rate, substrate consumption, product formation and oxidation pattern like the wild type. Hence, the conditions, under which the cytochrome *bc*₁ complex is necessary in *G. oxydans*, had to be elucidated. A possible function of the complex is protection against oxidative stress, due to the presence of a periplasmatic cytochrome *c* peroxidase (CCP). This enzyme accepts electrons from reduced cytochrome *c* for reduction of H₂O₂ to water (Atack and Kelly 2007). H₂O₂ evolves when electrons are transferred to molecular oxygen under formation of superoxide ions, which then are converted by superoxide dismutase into hydrogen peroxide and oxygen (Fridovich 1978, 1995, Imlay and Fridovich 1991). Formation of superoxide ions is a normal side-reaction of the respiratory chain and occurs especially during cultivation under oxygen excess (Atack and Kelly 2007). The highly active oxidoreductases in the respiratory chain of *G. oxydans* most likely contribute indirectly to the production of H₂O₂ since they are responsible for the high flow of electrons through the respiratory chain. Under conditions of oxygen excess, the electrons are passed rapidly to the terminal acceptors and to oxygen. The side reaction leading to H₂O₂ is enhanced

simultaneously. This side reaction was found to proceed at the NADH dehydrogenase II (Messner and Imlay 1999). A second way for the production of H_2O_2 in *G. oxydans* is the old yellow enzyme (Adachi *et al.* 1979) which reduces O_2 to H_2O_2 under the oxidation of NADPH to $NADP^+$.

Bacterial cytochrome *c* peroxidases (CCP) contain two covalently bound *c*-heme types (Atack and Kelly 2007). The authors referred the CCP of *G. oxydans* to include three heme-binding sites. The function of the third heme was not clarified. RT-PCR during this work showed that transcription of the *ccp*-gene is enhanced in oxygen-limited, slowly growing cells, as well as in cells cultivated under oxygen excess. Atack and Kelly 2007 also referred an upregulation of the *ccp*-gene in oxygen-depleted cells. The authors call this regulation contradictory, since CCP is involved in detoxification of H_2O_2 , which is more likely present at high concentrations under oxygen excess. The authors suggested a general upregulation of enzymes transferring electrons to alternative electron end acceptors, such as e.g. H_2O_2 , fumarate or nitrate, under oxygen limitation. Since electrons are transferred not to molecular oxygen but to the alternative terminal acceptor H_2O_2 by the cytochrome *c* peroxidase, the upregulation of the gene encoding CCP under oxygen limitation makes sense. Assuming, that the cytochrome *bc*₁ complex is co-regulated with the CCP, since it reduces its electron acceptor, the deletion mutant devoid of the cytochrome *bc*₁ complex was investigated under oxygen limitation.

A second motivation for the investigation of the deletion mutant under oxygen limitation was given by the fact, that the non-proton pumping *bd* oxidase in oxygen-depleted *E. coli* is upregulated (Tseng *et al.* 1995). Since the same regulation takes place in *G. oxydans*, the cytochrome *bc*₁ complex might be involved in energy supply of the cells under conditions, when the concentration of the non-proton translocating *bd* type oxidase enhances. In *G. oxydans*, the ubiquinol *bd* oxidase was also upregulated under the condition of decreased pH-value during cultivation (Matsushita *et al.* 1989). In accordance, the mRNA-level of the ubiquinol *bd* oxidase enhanced under these two conditions as confirmed by microarray-analyses, whereas the transcription of genes encoding the cytochrome *bc*₁ complex was only enhanced under oxygen limitation. However, the deletion mutant, compared to the wild type, exhibited no differing phenotype when grown under oxygen depletion but it showed retarded growth and oxidation parameters at pH 4. The cytochrome *bc*₁ complex seems to be of importance under acidic growth conditions, possibly in order to

maintain the energy supply of the cells, which is decreased by an enhanced electron flow over the non-proton translocating ubiquinol *bd* oxidase (Matsushita *et al.* 1989). The deletion mutant only showed a phenotype in one (decreased pH) of the two conditions with increased ubiquinol *bd* oxidase. Under the condition of oxygen limitation the function of the cytochrome *bc*₁ complex may not manifest itself in growth differences.

The deletion mutant produced a reddish pigment under oxygen limitation. Difference spectra (reduced-oxidised) of the pigment showed two peaks in the range of the cytochrome *c* α -absorption peak at 550 nm (Nicholls and Ferguson 2002). The pigment was not associated with protein since it did not elute with the protein fraction in gel chromatography and the Bradford test was negative. The heme group itself may have absorption at longer wavelengths because the protein surroundings in cytochromes influence the absorption of the prosthetic group heme (Mauk *et al.* 2009). Cytochrome *c* possesses a covalently bound heme group, whereas in cytochrome *b* the heme is not covalently bound (Nicholls and Ferguson 2002). The cytochromes *b* of the cytochrome *bc*₁ complex have their α -absorption peaks at 560 and 566 nm. Therefore, the reddish pigment probably is the heme of the cytochromes *b* or *c* of the cytochrome *bc*₁ complex. The fact that hemes are hydrophobic and therefore difficult to dissolve (Lebrun *et al.* 1998) was reflected by the difficult removal of the pigment from the column. The presence of heme in the culture supernatant is an indication that the cytochrome *bc*₁ complex is functional under oxygen limitation. In the deletion mutant, the heme cannot bind to its apoenzyme and accumulates in the medium.

Interestingly, flagellin B was identified in the protein fraction of the culture supernatant of the oxygen-limited deletion mutant. In accordance, microarray analyses showed upregulation of many chemotaxis- and flagellum-specific genes in oxygen-limited cells, as well as of the gene encoding flagellin B. The assembly of flagella might be disturbed in the deletion mutant devoid of the cytochrome *bc*₁ complex since proton motive force drives the flagellum assembly (Minamo *et al.* 2008).

Short time kinetics were performed to analyse the oxidation capacity of selected oxidoreductases in the wild type and the deletion mutant devoid of the cytochrome *bc*₁ complex. The oxidation activities of the cell suspensions revealed unexpectedly lower enzyme activities in the deletion mutant compared to the wild type, when

glucose or ethanol were used as substrates. In contrast, during growth on glucose in phase I, when glucose was oxidised to gluconate, no growth differences were observed between the two strains. During growth, different factors influence biomass formation and oxidation activities, whereas the short time assays reflect the activity of only a single enzyme connected to the respiratory chain. Strongest growth effects of the deletion mutant were observed during growth on mannitol at pH 4 and gluconate at pH 6. Mannitol oxidation at the membranes of *G. oxydans* is catalysed by the major polyol dehydrogenase SLDH (Sugisawa and Hoshino 2002, Matsushita *et al.* 2003), whereas the oxidation of gluconate at pH 6 is catalysed by the membrane-bound gluconate-2-dehydrogenase (Shinagawa *et al.* 1984). The oxidation activity of the SLDH of the deletion mutant with mannitol as substrate showed a decrease of 44% at pH 4 and of 22% at pH 6, compared to the corresponding wild type activities. Here, the short time kinetics and the growth behaviour correlated since at pH 6 little differences in oxidation capacity and growth behaviour of the two strains was observed.

Two additional observations were made by comparing growth of the deletion mutant and the wild type as well as their oxidation capacities in the Clark electrode. I) when gluconate was used as substrate for oxidation at pH 6 via the gluconate-2-dehydrogenase, activity measurements with the Clark electrode showed a decrease of 34% of the mutant's activity compared to that of the wild type. Growth was also decreased compared to the wild type. II) At pH 6 with glucose and glucose dehydrogenase as corresponding enzyme, the mutant showed a decrease of 39% of oxidative activity but this strong decrease was not paralleled by differences in growth parameters of the deletion mutant and the wild type. Therefore, a decrease in the oxidation capacity of the deletion mutant did not necessarily result in a growth defect of the mutant. In conclusion, the decreased growth of gluconate grown mutant cells cannot only be attributed to a decreased activity of the gluconate-2-dehydrogenase.

The fact, that in the mutant the oxidation rates of ADH and mGDH showed the highest decrease in the deletion mutant pointed to an interaction between the cytochrome *bc*₁ complex and the ADH. The argumentation that interactions between components of the respiratory chain of *G. oxydans* must exist has also been discussed in the literature. Soemphol *et al.* 2008 reported an interaction between the ubiquinol *bd* oxidase with the FAD-dependent sorbitol dehydrogenase and a connection of the ubiquinol *bo*₃ oxidase with the PQQ-dependent sorbitol

dehydrogenase in *G. frateurii*. Matsushita *et al.* 1991 suggested that the cytochrome *c* subunit II of the ADH was an integral part of the respiratory chain of *G. oxydans* by not only accepting electrons originating from alcohol oxidation by its subunit I but also accepting and conducting electrons from and to other respiratory chain components as e.g. the glucose dehydrogenase and the ubiquinol *bd* oxidase (Matsushita *et al.* 1991, Shinagawa *et al.* 1990, Soemphol *et al.* 2008, Matsushita *et al.* 2004). The mGDH only exhibited ferricyanide reductase activity, when the cytochrome *c* subunit of the ADH was present (Matsushita *et al.* 2004, Shinagawa *et al.* 1990). Matsushita *et al.* 1989 reported that the ADH was interconnected with the ubiquinol *bd* oxidase. This connection was shown indirectly and the mechanism was not elucidated. Again, the cytochrome *c* subunit was important for the electron transfer between the ADH and the interaction partner (Matsushita *et al.* 1991, 2004). In addition, Matsushita *et al.* 1995 showed a proton motive force dependent activation of the ADH in resting cells. Combining these results, an involvement of the cytochrome *bc*₁ complex in the activation of the ADH was investigated. The decreased oxidation capacity of the ADH in the deletion mutant could be a hint for an interaction between the ADH and the cytochrome *bc*₁ complex, which contributes to the proton motive force. Indeed, the the cytochrome *bc*₁ complex plays a role in the activation, since results from the present work showed that the ADH of the deletion mutant was activated to a significantly lower extent, compared to the wild type situation. Matsushita *et al.* 1995 reported an activation of 310% for the wild type, in good agreement with the results described in this work (320%). However, for a more detailed picture of the function of the cytochrome *bc*₁ complex biochemical investigations are required. Therefore, first efforts have been made by co-purification experiments. The cytochrome *c* subunit of the ADH was tagged successfully resulting in a co-purified large subunit and the 15 kDa subunit of the enzyme. The protein eluates had a red colour displaying the high content of cytochrome *c* in the enzyme (Matsushita *et al.* 2008 reported four hemes *c* bound in subunit II). A supercomplex formation between the cytochrome *bc*₁ complex and the ADH, i.e. a co-purification of components of the cytochrome *bc*₁ complex, was not detectable. However, this result does not exclude a physical connection of the two complexes since the StrepTag II may have disturbed the interaction (Kim 2003).

The cytochrome *c* oxidase test with the chromogenic electron donor TMPD was performed in *G. oxydans* to trace a flux of electrons through the cytochrome *bc*₁

complex via soluble cytochrome *c* to a terminal acceptor. With cells of *G. oxydans* and of *C. glutamicum* TMPD did not change the colour. This can be interpreted that no electron flow from the cytochrome *bc*₁ complex via the soluble cytochrome *c* to a terminal oxidase occurred. However, this is not true in the case of *C. glutamicum* since the cytochrome *bc*₁ complex is functional in *C. glutamicum* and connected to the cytochrome *c* oxidase (Niebisch and Bott 2001). Interestingly, in *C. glutamicum* no soluble cytochrome *c*₅₅₂ is present. However, a second heme-binding motive CXXCH beside the standard heme-binding motive is present in the cytochrome *c* subunit of the cytochrome *bc*₁ complex in *C. glutamicum*. This additional prosthetic group substitutes the soluble cytochrome *c* and is involved in the transfer of electrons to the cytochrome *c* oxidase, which forms a supercomplex with the cytochrome *bc*₁ complex. Thus, the TMPD test result with *G. oxydans* is ambiguous: either no flux through the cytochrome *bc*₁ complex to a terminal oxidase, or existence of complex-bound cytochrome *c*₅₅₂.

To summarise, the decreased oxidation velocities of the deletion mutant point to an interaction between the ADH and the cytochrome *bc*₁ complex. Although the cytochrome *bc*₁ complex is involved in the activation of the ADH in pH 4 grown cells, a direct interaction was not demonstrated, but cannot be excluded. However, the decreased oxidation capacities of the deletion mutant can be interpreted in a second way. For evaluation of the results from short time kinetics, it was hypothesised in this work that the electrons underlie a reverse electron flow through the cytochrome *bc*₁ complex. Following this assumption, transfer of electrons via the cytochrome *bc*₁ complex would not be to an end acceptor, but to the ubiquinol pool in the membrane. In a standard situation with “normal” electron flow the electrons are passed through the cytochrome *bc*₁ complex as depicted in **Fig. 26**. Per ubiquinol oxidised, one electron is channelled to the soluble cytochrome *c* via the enzyme-bound [Fe-S]-cluster and the cytochrome *c* of the complex (Trumpower 1990a, b). The reduction of the [Fe-S]-cluster delivers the energy for the energetically non-favoured electron transfer from ubiquinol to the first cytochrome *b* of the complex, which has a lower redox-potential than that of ubiquinol. From the first cytochrome *b*, electrons flow to a second cytochrome *b*, which has a higher redox potential. Therefore, it is called cytochrome *b*_H and this electron flow is energetically favoured. Via the high potential cytochrome *b*, the electron is channelled back to the ubiquinol pool which has again a more positive redox-potential. This one electron transfer to the ubiquinone leads to

formation of a semiquinone (Trumpower 1990a, b). In a second oxidation round of another ubiquinone, the electron from the b_H is channeled to the semiquinone leading to a fully reduced ubiquinol. Therefore, half of the electrons stemming from the oxidation of the initial ubiquinol are transferred back to the ubiquinol-pool, this electron cycling is called “Q-cycle”. Due to the Q-cycle and different sites of ubiquinol oxidation and reduction, protons are translocated to the periplasm contributing to the proton motive force (Trumpower 1990a, b).

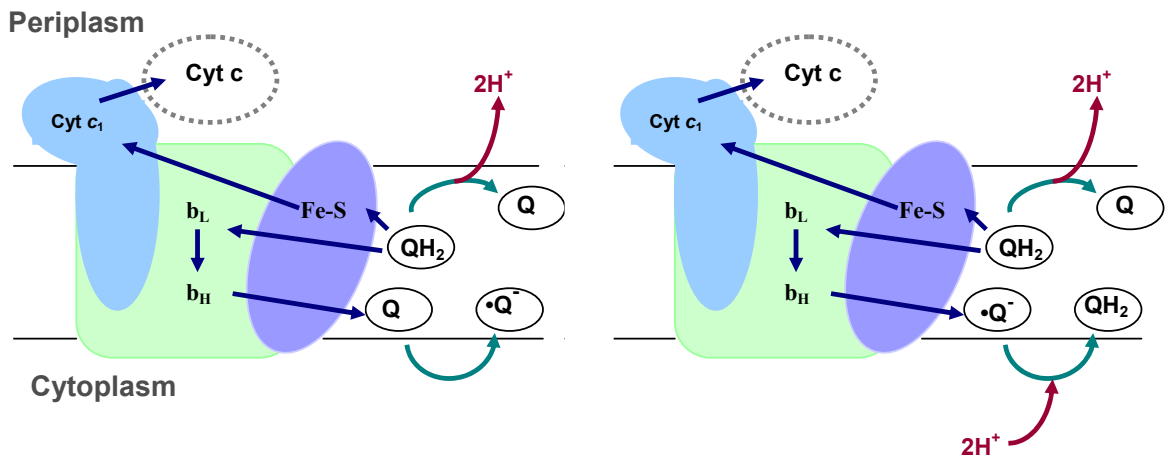


Fig. 26 Schematic electron flow through the prosthetic groups of the cytochrome bc_1 complex. Cyt: cytochrome; b_L : cytochrome b low potential; b_H : cytochrome b low potential; Fe-S: Iron-sulfur cluster; Q: oxidised ubiquinol; $\bullet Q^-$: semiquinone; QH_2 : reduced ubiquinol; left: first oxidation of the QH_2 , which results in a semiquinone after the first part of the “Q-cycle”; right: second oxidation of a QH_2 resulting in formation of a fully reduced ubiquinol after the second part of the “Q-cycle” and transfer of an electron to the semiquinone

A reverse electron flow was reported for e.g. *Paracoccus denitrificans* and *Rhodobacter capsulatus* (van der Oost *et al.* 1995, Osyczka *et al.* 2004). During the present work, a hypothesis was put forward that dehydrogenases with cytochrome c subunits transferred electrons to the cytochrome c subunit of the bc_1 complex, resulting in an energy-dependent reverse electron flow to a prosthetic group with a more negative redox-potential. The energy would be delivered by reverse proton translocation across the membrane into the cytoplasm, dissipating the proton motive force. Electrons finally would reach the ubiquinol-pool, where they were transferred to one of the two terminal oxidases. Since the deletion mutant showed low oxidation rates in the Clark electrode, indicating a disturbed oxidation of substrates in cells missing the cytochrome bc_1 complex, a reverse electron flow through the cytochrome bc_1 complex seemed possible. If such a phenomenon existed, the oxidation rates of the wild type had to be influenced by addition of an uncoupler dissipating the proton

gradient needed for the reverse electron flow. This was only the case with sorbitol as substrate. Thus, a reverse electron flow cannot be ruled out completely. A clear advantage of this reverse electron flow for the organism was not obvious. It would dissipate energy for the ability of oxidation of some additional substrates, which perhaps could not be oxidised otherwise.

2. Differential gene regulation at oxygen limitation and at low pH

In order to throw light on the regulation of the respiratory chain in conjunction with the overall metabolism, genome-wide DNA microarray analyses were carried out with *G. oxydans* 621H. An increasing content of the highly oxygen-affine ubiquinol *bd* oxidase was shown in oxygen-limited *E. coli* cells (Gennis and Stewart 1996). Therefore, a regulation of components of the respiratory chain under oxygen limitation seemed likely. Oxygen limitation of the cells affected the expression of nearly all components of the respiratory chain of *G. oxydans* resulting in an enhanced transcription or a decreased mRNA-level. In *G. oxydans*, the low oxygen-affine ubiquinol *bo*₃ oxidase genes were upregulated as well as two genes encoding the cytochrome *bc*₁ complex under oxygen limitation. In contrast, expression of genes encoding for ubiquinol reducing components of the respiratory chain was decreased. In accordance, transcription of PQQ-biosynthesis genes was decreased as well.

In the case of NADH dehydrogenase, the decline in transcription did not manifest itself in the *in vitro* measurable enzyme activity that remained stable, possibly due to posttranscriptional regulation. In this work it was shown that the NADH dehydrogenase of *G. oxydans* does not accept NADPH as electron donor, as it is the case for the NAD(P)H dehydrogenase in *Z. mobilis* (Kalnenieks *et al.* 2007). This organism possesses a similar respiratory chain as *G. oxydans* and occurs naturally in the same or in comparable habitats (Bringer *et al.* 1984, Kersters *et al.* 2006, Sahm *et al.* 2006, Kalnenieks *et al.* 2007); therefore, characteristics of enzymes of *Z. mobilis* were assumed to be similar to those of *G. oxydans*. In the case of the NADH dehydrogenase, this was certainly not true. However, in *G. oxydans* there is hardly any need to oxidise NADPH at the membranes, although there are three main reactions/reaction pathways for formation of NADPH: I) The membrane-bound nicotinamide nucleotide transhydrogenase (PntAB), II) the PPP dehydrogenases contributing to the balance between NADH and NADPH via their dual cofactor specificities and III) the cytoplasmatic NADP-dependent dehydrogenases which

oxidise glucose to gluconate and gluconate to 5-ketogluconate (Prust 2005, Merfort *et al.* 2006).

Genes *pntAB* encoding the membrane-bound nicotinamide nucleotide transhydrogenase were the most strongly upregulated genes in oxygen-limited cells of *G. oxydans*. As the NAD(P)H transhydrogenase couples hydride transfer between $\text{NADH} + \text{H}^+$ and NADP^+ to proton translocation across a membrane at the expense of the membrane potential Δp , in *G. oxydans* the enzyme might have two functions. The hydride transfer from NADH to NADP^+ results in an increased formation of NADPH used for biomass production. In *E. coli*, PntAB contributes to the balancing between the NADH and NADPH pools (Sauer *et al.* 2004). In *B. subtilis*, *Agrobacterium tumefaciens*, *Rhodobacter sphaeroides*, *Sinohizobium meliloti* and *Zymomonas mobilis*, but not in *E. coli*, the PPP dehydrogenases contribute to the balance between NADH and NADPH via their dual cofactor specificities (Fuhrer and Sauer 2009). This is also the case in *G. oxydans*. The NADPH required for biomass synthesis is provided by glucose 6-phosphate dehydrogenase and 6-phosphogluconate dehydrogenase, which accept both, NAD^+ and NADP^+ as electron acceptors (Adachi *et al.* 1982; Tonouchi *et al.* 2003). Thus, there is no direct need for formation of NADPH by the PntAB transhydrogenase in *G. oxydans*. Prust *et al.* 2005 suggested a second function of the PntAB transhydrogenase. Possibly, the transhydrogenase translocates cytoplasmic protons across the membrane, thereby contributing to the generation of Δp at the expense of NADPH . Thus, under oxygen-limited growth conditions the proton translocating pyridine nucleotide transhydrogenase possibly substituted the respiratory activity, which was probably decreased due to downregulated primary oxidoreductases. However, it was shown that over production of enzymes using NADP^+ as cofactors, like the cytoplasmic gluconate 5-dehydrogenase, resulted in a decreased growth due to accumulating NADPH (Klasen 1994). If the PntAB transhydrogenase is able to operate in the opposite function contributing to the proton motive force at an expense of NADPH , the accumulation of NADPH was not reasonable. Furthermore, the mRNA-levels of the two dehydrogenases of the PPP were strongly decreased under oxygen limitation in *G. oxydans*. Therefore, it is unlikely that enough NADPH was disposable for driving the reverse reaction of the PntAB transhydrogenase in the direction of proton translocation to the periplasm under expense of NADPH . The de facto function of the

PntAB transhydrogenase in oxygen-limited cells of *G. oxydans* should be investigated in future.

In *G. oxydans*, two distinct ATP synthases exist (Prust 2005). One is encoded in a single operon, the other in two different operons. Expression of the latter operons was decreased, whereas expression of the first was increased in oxygen-limited cells. Both ATP synthases most probably are active in *G. oxydans*, although one subunit of each of the ATP synthases was not correctly identified (Prust 2005). In gluconate-grown cells, the same regulation pattern of the two ATP synthases occurred leading to the assumption that growth phase effects could be responsible for the differently expressed ATP synthases. In both conditions, gene transcription for chemotaxis/flagellum assembly was enhanced. A correlation between chemotaxis and the upregulated ATP synthase is likely. In *Salmonella enterica*, Minamino *et al.* 2008b reviewed that the export of flagella proteins is driven by proton motive force. The ATPase FliI, which forms a monohexamer, similar to the basal body in F₀/F₁ ATP synthases, is more involved in releasing the proteins from the initial complex of FliH-FliI, which coordinates the protein to the export gate formed by flnAB. The upregulated ATP synthase in *G. oxydans* might contribute to the proton motive force by proton translocation into the periplasm operating in reverse direction. This would result in an enhanced energy supply for the energy-dependent chemotaxis/flagellum assembly (Minamino *et al.* 2008a, b).

The downregulation of the catalase encoding gene in oxygen-limited cells is consistent with the reduced formation of reactive oxygen species under the condition of low oxygen availability where less H₂O₂ is produced (Atack and Kelly 2007). Nevertheless, the gene encoding cytochrome *c* peroxidase was upregulated in those cells indicating another function beside detoxification of the cells. As discussed before, the enzyme possibly serves as terminal electron acceptor from the cytochrome *bc*₁ complex via the soluble cytochrome *c*.

ArcAB and FNR are known to be regulators induced by anaerobiosis in facultative anaerobes (Patschkowski *et al.* 2000) whose regulatory activities result in increased transcription of the genes encoding ubiquinol *bd* oxidase and decreased transcription of the genes encoding for NADH dehydrogenase II, isocitrate dehydrogenase and ubiquinol *bo*₃ oxidase. This regulation, with the exception of the gene encoding ubiquinol *bo*₃ oxidase, was observed in *G. oxydans*, too. However, no ArcAB or FNR homologues were annotated in *G. oxydans* up to now. FNR is closely related to the

catabolite repressor protein (CRP) (Spiro 1994); GOX0974 was annotated as CRP. However, using the BLAST program, GOX0974 shows more similarity to *E. coli* FNR (29 %) than to *E. coli* CRP (21 %). The FNR-binding motive TTGAT-4N-GTCAA (Mouncey and Kaplan 1998) is not fully present (TTGAT can be found), but there are the typical 4-5 cysteine residues in the coding region for binding of the $[4\text{Fe-4S}]^{2+}$ cluster. In its dimeric form with two $[4\text{Fe-4S}]^{2+}$ -clusters, FNR can bind to the DNA. In the presence of oxygen, the clusters are converted to $[2\text{Fe-2S}]^{2+}$ -clusters (Green *et al.* 2009). The regulator loses its dimeric structure and cannot bind to DNA. The function of FNR as an activator (e.g. of the nitrate reductase gene in *E. coli*) or as a repressor (e.g. of the *ndh* gene in *E. coli*) depends on the position of the binding motif in the promoter region (Guest *et al.* 1996) The *fnr* gene of *E. coli* is autoregulated (Spiro and Guest 1987). In *G. oxydans* a 0.7-fold downregulation of GOX0974 in oxygen-depleted cells was observed.

Thus, by profiling the transcriptome of oxygen-limited cells compared to cells cultivated under oxygen excess, a strong regulation of the PntAB was disclosed which lead to the notion of a reverse function of the transhydrogenase for maintaining the proton motive force under oxygen depletion. The respiratory activity was decreased shown by downregulation of primary oxidoreductases. Due to oxygen depletion, transcription of genes encoding terminal oxidases and genes involved in flagella assembly/chemotaxis was enhanced for capturing oxygen.

The regulatory response to acidic pH was less pronounced than that to oxygen limitation. There was no evidence from transcriptional analysis for an upregulation of the cytochrome *c* subunit of the ADH, as reported by Matsushita *et al.* 1989. Instead, transcription of the 15 kDa subunit of this enzyme was amplified. The 15 kDa subunit is probably a linker to the membrane and not involved in electron transport (Matsushita *et al.* 2008). The data resulting from our microarray analysis confirmed presence of amplified ubiquinol *bd* oxidase transcripts in cells cultivated at pH 4. The regulation of membrane-bound oxidases in the respiratory chain of *G. oxydans* differs from that of *E. coli*, where e.g. the gene encoding the *bd* oxidase is upregulated at pH 8.7 (Maurer *et al.* 2005).

3. Characterisation of growth of *G. oxydans* 621H on glucose with microarray-, ¹³C-metabolome- and flux-analysis

Genome-wide transcription analysis and ¹³C-metabolome analysis in cells of the two growth phases when cultivated with glucose focused on metabolic changes under these growth conditions. Since EMP and TCA cycle are incomplete (Prust *et al.* 2005), it was assumed that changes occurred in the relative activities of the PPP or the EDP. In this work, the quantitative carbon flux distribution in the central metabolism of *G. oxydans* was analysed by applying ¹³C-glucose feeding (Wiechert and Nöh 2005, Wiechert 2001, Zamboni *et al.* 2009). Parallel cultivation under controlled conditions allowed for collection of reproducible LC-MS data (biological and technical replicates) suitable for ¹³C-MFA.

G. oxydans grew exponentially in phase I and formed 80% of the biomass found at the end of the cultivation. During this phase, 440 mM glucose was oxidised at a high rate (70 mM h⁻¹) to gluconate via the membrane-bound glucose dehydrogenase (mGDH) and the transferred electrons were used to reduce 220 mM O₂ to water. This stoichiometry indicated that only negligible amounts of glucose were oxidised in the cell with concomitant formation of NADH that was subsequently oxidised by NADH dehydrogenase. Consistently, the flux model calculated that 97% of the glucose was oxidised in the periplasm by mGDH and only 3% entered the cytoplasm. Furthermore, the model predicted that cytoplasmic glucose was oxidised by the soluble GDH, rather than being phosphorylated by glucose kinase. In this work, an activity of 0.086 U mg⁻¹ cell-free protein of glucose kinase was determined, agreeing well with the glucose kinase activity of 0.060 U mg⁻¹ cell-free protein reported by Pronk *et al.* 1989. Activity measurements by the same authors of the cytoplasmic glucose dehydrogenase (cGDH) and the mGDH resulted in 0.15 and 4 U mg⁻¹ cell-free protein, i.e. cytoplasmic glucose dehydrogenation was 3.8% of the periplasmic activity. This result of *in vitro* determinations of enzyme activities is in agreement with our model prediction of the *in vivo* situation of carbon flux.

The attested cytoplasmic oxidation of unphosphorylated sugars is unusual, because in other bacteria sugars either are taken up by phosphoenolpyruvate-dependent phosphotransferase systems (PTS), or are immediately phosphorylated by a cytoplasmic sugar kinase. The PTS system is incomplete in *G. oxydans* because EII^B and EII^C are missing (Prust *et al.* 2005). The uptake mechanism for glucose is unclear yet. Most commonly, glycerol in bacteria is taken up by a facilitator protein (Stroud *et al.* 2003, Hénin *et al.* 2008). Since in *G. oxydans* only one gene

encoding for a facilitator was identified this permease most probably transports glycerol (Prust 2005). Genes encoding enzymes for glycerol uptake and degradation in *G. oxydans* are organised in an operon (GOX2087-GOX2090). Interestingly, glycerol, present at a low concentration of 0.5 g l^{-1} in the media is metabolised in the second growth phase of glucose-cultivated cells as indicated by the enhanced mRNA-levels of the glycerol operon in growth phase II. Glycerol 3-phosphate is then presumably channeled into the PPP, explaining the 10-fold upregulation of the gene encoding triosephosphate isomerase. This mode of glycerol catabolism strongly indicates that catabolite repression takes place in *G. oxydans*. Expression of the EII^A component of the PTS was enhanced in growth phase II, indicating, that the rudimentary PTS might still have a function in *G. oxydans*, e.g. of catabolite repression, since non-PTS sugars like glycerol have an influence to the phosphorylation state of EII^A (Eppler *et al.* 2002). The increased level of EII^A is maybe involved in an increased block of glycerol metabolism, if it is mostly dephosphorylated. Elevated mRNA-levels of the glycerol metabolism operon can perhaps abolish the effect of increased EII^A. The EII^A component of the PTS system and catabolite repression in *G. oxydans* require more detailed investigation.

Only a low growth rate and low biomass production were observed in the second growth phase, which probably was due to energy limitation of the cells, although 370 mM ketogluconates were formed from gluconate by membrane oxidation. For the reduction of 1 mM O₂, 2 mM gluconate had to be oxidised. Therefore, 185 mM O₂ must have been consumed by gluconate oxidation. De facto, 220 mM O₂ was reduced within this phase. Thus, the remaining 35 mM O₂ were reduced by electrons transferred to the respiratory chain via NADH oxidation. Under the conditions applied in this work, the main energy supply of the cells originated from substrate oxidation in the periplasm. However, in the second oxidation phase the oxidative activities of the ketogluconate-forming gluconate-2- and gluconate-5-dehydrogenases were 70–80% lower than the activity of the mGHD in the first oxidation phase, as determined in a Clark oxygen electrode. This might be the main reason for the energy limitation of the cells in growth phase II. Increasing the concentration of yeast extract from 5 g l^{-1} to 15 g l^{-1} did not affect the oxidation phases or the time point of transition from the first to the second one. The growth rate during the second oxidation phase was not increased, either. Therefore, nutrient limitation of e.g. amino acids can be excluded as reason for the decreased growth.

The genes responsible for chromosome partitioning GOX1062 and GOX1063 were downregulated in growth phase II, as well as many ribosomal proteins, indicating that diminished chromosome partitioning is probably another cause for the decreased growth rate in the growth phase II. Decreased mRNA-levels of the genes encoding for cell division proteins underline this assumption. Of course, it cannot be excluded that the decreased growth rate caused the downregulation of those genes. The induction of genes encoding RNA polymerase factor sigma-32, a small heat shock protein (sHsp), and DnaK was surprising in gluconate-grown cells (as well as in oxygen-limited cells). It is well known that heat shock response is provoked by several unfavourable growth conditions like heat, cold, salt, and drought, osmotic and oxidative stresses (Jiang *et al.* 2009, Parsell *et al.* 1989; van Bogelen *et al.* 1986), so that the heat shock response is not an answer to heat only. In *G. oxydans* the gene encoding superoxide dismutase was upregulated 3.5-fold in gluconate grown cells, indicating for increased concentrations of superoxide anion (Storz and Zheng 2000). This is possibly a hint, that oxidative stress occurred during the change from growth phase I into growth phase II of glucose-grown cells. The oxidative stress response is mediated by the regulators OxyR and SoxR, which sense H₂O₂ and superoxide anions (Storz and Zheng 2000). The responses of these regulators overlap with e.g. FNR (regulator of fumarate and nitrate reduction) or the sigma-38 regulon (the starvation/stationary phase sigma factor) (Storz and Zheng 2000). Due to this overlap of stress responses, it is not imperative that increased transcription of e.g. the superoxide dismutase was triggered by increased concentrations of superoxide anion.

The strong sigma-32 dependent induction of a small heat shock protein (sHSP) and of the chaperone DnaK (Hsp70) in *G. oxydans* was a consequence of the increased sigma-32 protein level. In *E. coli*, the sigma-32 regulon is essential for growth and cell division and highly responsive to growth phases (Wagner *et al.* 2009). Thus, the change from an exponential growth in phase I to linear growth in phase II of *G. oxydans* may be a result of heat shock response/oxidative stress response. However, it cannot be excluded that these findings are rather the consequence of the decreased growth rate than the reason for it. Due to the overlapping responses of heat hock, oxidative stress and stationary growth phase, it is difficult to find the initial factor, which induced the remaining regulatory answers.

The mRNA level of gluconate kinase was increased 1.6-fold in the second growth phase. Hence, gluconate is taken up into the cytoplasm and then phosphorylated by the substrate-induced gluconate kinase. In the second growth phase, the gluconate was oxidised to 2-ketogluconate as the main product via membrane-oxidation, which was mainly due to the constant pH value of 6 applied in the cultivations. At pH 6, the membrane-bound gluconate-2-dehydrogenase (gluconate-2-DH) has its pH optimum (Shinagawa *et al.* 1984). The expression levels of the genes encoding subunits of gluconate-2-DH were increased 2.1-2.7-fold. Formation of 5-ketogluconate production was low, owing to the fact that 5-ketogluconate formation from gluconate is optimally catalysed at pH 5 by the major polyol dehydrogenase encoded by the *sldAB* genes (Miyazaki *et al.* 2002; Gätgens *et al.* 2007). The preferred substrates of this enzyme are the polyols arabitol, sorbitol, and mannitol, however gluconate is oxidised to 5-ketogluconate at 4-40% the rate of arabitol oxidation (Sugisawa and Hoshino 2002, Matsushita *et al.* 2003, Elfari *et al.* 2005, Merfort *et al.* 2006 a, b).

During the second growth phase, when the periplasmatic oxidation of glucose to gluconate was almost completed, high amounts of carbon dioxide were produced. This was also reported by Olijve and Kok 1979. Balancing of the concentrations of substrate entering the cytoplasm (about 3%, calculated by product concentrations after growth subtracted from initial substrate concentration) with the carbon dioxide produced claimed an activated, partly cyclic PPP producing more than one mol carbon dioxide per mol gluconate. Complete glucose oxidation to carbon dioxide via a cyclic PPP theoretically can lead to the evolution of 6 CO₂ per mol of glucose. Prerequisites for a cyclic flow of carbon through this pathway are the absence of 6-phosphofruktokinase and presence of fructose-1,6-bisphosphatase, both premises being met by the organism (Prust 2005). By genome-wide transcription profiling of *G. oxydans* cells from growth phases I and II activation of the PPP indeed was shown: 15 genes encoding for enzymes of the PPP or EMP/gluconeogenesis were upregulated in growth phase II. Increased activity of selected PPP enzymes was also detected at the protein level due to enzyme activity measurements. In the cultivations described here, 10% of the glucose metabolised was converted to CO₂, in agreement with results from ¹⁴C-labeling experiments by Shinjoh *et al.* 1990, who reported that 7.1% of glucose were converted to CO₂. Furthermore, surplus CO₂ was not

explainable only with a complete cyclic PPP since more CO₂ was produced than the complete oxidation of the 3% substrate entering the cells would allow.

¹³C-Metabolome analysis showed a clear cut between the upper and the lower parts of glucose metabolism. Only low labeling information was found in the intermediates of the TCA cycle. In addition, the labeling patterns of the TCA cycle intermediates fitted to the metabolic model only when additional uptake reactions for unlabeled compounds of the yeast extract were included, at least some amino acids of the oxaloacetate family (lysine and aspartate). Exogenous acetyl-CoA entered the TCA cycle, presumably also derived from degradation of exogenous amino acids, e.g. leucine and lysine. Succinyl-CoA, the end product of the incomplete TCA cycle, is directed into biosyntheses. In *G. oxydans* heme synthesis starts with the formation of 5-aminolevulinic acid from succinyl-CoA and glycine, catalyzed by 5-aminolevulinic acid synthase (GOX1636) (Prust 2005). Furthermore, succinyl-CoA is required for lysine synthesis. Since *G. oxydans* does not secrete succinate it can be concluded that succinyl-CoA does not accumulate in the cells but is used in the synthesis of cellular components.

Thus, the ¹³C-metabolome analysis carried out in the present work has shown that in *G. oxydans* the intracellular carbon flux from glucose is directed into the PPP. In growth phase I only glucose is taken up by the cells, oxidised to gluconate before being phosphorylated to 6-phosphogluconate. Transition of cells from growth with glucose in phase I to growth with gluconate in phase II is accompanied by an increase of activity of gluconate kinase and the two PPP dehydrogenases, and decreased growth and oxygen consumption rates. Significant fluxes for the TCA cycle were estimated contributing more than half of the overall CO₂ produced.

VI References

- Abe S, Takayama K, Kinoshita S (1967) Taxonomical studies an glutamic acid producing bacteria. *J Gen Appl Microbiol* 13: 279-301
- Abramson J, Riistama S, Larsson G, Jasaitis A, Svensson M, Laakkonen L, Puustinen A, Iwata S, Wikström M (2000) The structure of the ubiquinol oxidase from *Escherichia coli* and its ubiquinone binding site. *Nat Struct Biol* 7: 910-917
nature structural biology 7:910-917
- Adachi O, Tayama K, Shinagawa E, Matsushita K, Ameyama M (1978) Purification and characterization of particulate alcohol dehydrogenase from *Gluconobacter suboxydans*. *Agric Biol Chem* 42: 2045-2056
- Adachi O, Matsushita K, Shinagawa E, Ameyama M (1979) Occurrence of old yellow enzyme in *Gluconobacter oxydans*, and the cyclic regeneration of NADP. *J Biochem* 86: 699-709
- Ameyama M, Shinagawa E, Matsushita K, and Osao Adachi O (1981) D-Glucose dehydrogenase of *Gluconobacter suboxydans*: solubilization, purification and characterization. *Agric Biol Chem* 45: 851-861
- Anraku Y, Gennis RB (1987) The aerobic respiratory chain of *Eschericehia coli*. *Trends Biochem Sci* 12: 262-266
- Attack JM and Kelly DJ (2007) Structure, mechanism and physiological roles of bacterial cytochrome c peroxidases. *Adv Microb Physiol* 52: 73-106
- Bartek T, Makus P, Klein B, Lang S, Oldiges M (2008) Influence of L-isoleucine and pantothenate auxotrophy for L-valine formation in *Corynebacterium glutamicum* resisted by metabolome analysis. *Bioprocess Biosyst Eng* 31: 217-225
- Battey AS, Schaffner DW (2001) Modelling bacterial spoilage in cold-filled ready to drink beverages by *Acinetobacter calcoaceticus* and *Gluconobacter oxydans*. *J Appl Microbiol* 91: 237-47
- Bekker M, de Vries S, Ter Beek A, Hellingwerf KJ, Teixeira de Mattos MJ (2009) Respiration of *Escherichia coli* can be fully uncoupled via the nonelectrogenic terminal cytochrome *bd-II* oxidase. *J Bacteriol* 191: 5510-5517
- Bott M (2001) A high-resolution reference map for cytoplasmic and membrane associated proteins of *Corynebacterium glutamicum*. *Electrophoresis* 22: 4404-4422
- Bratbak G, Dundas I (1984) Bacterial dry matter content and biomass estimations. *Appl Environ Microbiol* 48: 755-757
- Brazma A, Hingamp P, Quackenbush J, Sherlock G, Spellman P, Stoeckert C, Aach J, Ansorge W, Ball CA, Causton HC, Gaasterland T, Glenisson P, Holstege FC, Kim IF, Markowitz V, Matese JC, Parkinson H, Robinson A, Sarkans U, Schulze-Kremer S, Stewart J, Taylor R, Vilo J, Vingron M (2003) Minimum information

- about a microarray experiment (MIAME)-toward standards for microarray data. *Nucleic Acids Res* 31: 68-71
- Bremus C (2006) Bildung der Vitamin C-Vorstufe 2-Keto-L-Gulonsäure mit *Gluconobacter oxydans*. Dissertation at the Heinrich-Heine Universität Düsseldorf
- Bringer S, Finn RK, Sahm H (1984) Effect of oxygen on the metabolism of *Zymomonas mobilis*. *Arch Microbiol* 139: 376-381
- Campbell LK, Baker DE, Campbell RK (2000) Miglitol: assessment of its role in the treatment of patients with diabetes mellitus. *Ann Pharmacother* 34: 1291-1301
- Choi KH, Kumar A, Schweizer HP (2006) A 10 min method for preparation of highly electrocompetent *Pseudomonas aeruginosa* cells: Application for DNA fragment transfer between chromosomes and plasmid transformation. *J Microbiol Meth* 64: 391-397
- Claret C, Salmon JM, Romieu C, Bories A (1994) Physiology of *Gluconobacter oxydans* during dihydroxyacetone production from glycerol. *Appl Microbiol Biotechnol* 41: 359-65
- Cohen SN, Chang ACY, Hsu L (1972) Nonchromosomal antibiotic resistance in bacteria: Genetic transformation of *Escherichia coli* by R-factor DNA. *Proc Natl Acad Sci* 69: 2110-4
- Costa V, Moradas-Ferreira P (2001) Oxidative stress and signal transduction in *Saccharomyces cerevisiae*: insights into ageing, apoptosis and diseases. *Mol Aspects of Medicine* 22: 217-246
- De Ley J, Swings J (1981) The genera *Gluconobacter* and *Acetobacter*. In: *The Prokaryotes. A handbook on habitats, isolation, and identification of bacteria*. Hrsg.: Starr MP, Stolp H, Tröper, HG, Balows A, Schlegel, H. G. Springer Verlag, Berlin:771-778
- De Ley J, Gillis M, Swings J (1984) Genus *Gluconobacter*. In: *Bergey's Manual of Systematic Bacteriology*, vol 1. Krieg, NR, Holt, JG, eds. Williams and Wilkins, Baltimore: 267-278
- Deppenmeier U, Hoffmeister M, Prust C (2002) Biochemistry and biotechnological applications of *Gluconobacter* strains. *Appl Microbiol Biotechnol* 60: 233-42
- Deppenmeier U, Ehrenreich A (2008) Physiology of acetic acid bacteria in light of the genome sequence of *Gluconobacter oxydans*. *J Mol Microb Biotechnol* 16: 69-80
- Deppenmeier U, Ehrenreich A (2009) Physiology of acetic acid bacteria in light of the genome sequence of *Gluconobacter oxydans*. *J Mol Microbiol Biotechnol* 16: 69-80
- Dudoit S and Yang YJH (2003) Bioconductor R Packages for Exploratory Analysis and Normalization of cDNA Microarray Data. In: *The analysis of gene expression data*, Springer-Verlag London

- Elfari M, Ha SW, Bremus C, Merfort M, Khodaverdi V, Herrmann U, Sahm H, Görisch H (2005) A *Gluconobacter oxydans* mutant converting glucose almost quantitatively to 5-keto-D-gluconic acid. *Appl Microbiol Biotechnol* 66: 668-74
- Eppler T, Postma P, Schütz A, Völker U, Boos W (2002) Glycerol-3-phosphate-induced catabolite repression in *Escherichia coli*. *J Bacteriol* 184: 3044-3052
- Ferguson SJ, Stevens JM, Allen JWA, Robertson IB (2008) Cytochrome *c* assembly: A tale of ever increasing variation and mystery? *Biochim Biophys Acta* 1777: 980-984
- Fischer E, Zamboni N and Sauer U (2004) High-throughput metabolic flux analysis based on gas chromatography-mass spectrometry derived ¹³C constraints. *Anal Biochem* 325: 308-16
- Fraenkel DG and Levisohn SR (1967). Glucose and gluconate metabolism in *Escherichia coli* mutant lacking phosphoglucose isomerase. *J Bacteriol* 93: 1571-1578
- Fridovich I (1978) The biology of oxygen radicals. *Science* 201: 875–880
- Fridovich I (1995) Superoxide radical and superoxide dismutases. *Annu Rev Biochem* 64: 97-112
- Fritsche W (1999) Mikrobiologie. Spektrum, Akademischer Verlag, Heidelberg- Berlin.
- Fuhrer T and Sauer U (2009) Different biochemical mechanisms ensure network-wide balancing of reducing equivalents in microbial metabolism. *J Bacteriol* 191: 2112-2121
- Gallagher PR, Desjardins PR (2007) Quantitation of DNA and RNA with absorption and fluorescence spectroscopy. *Curr Protoc Hum Genet Appendix* 3D
- Gao L, Chiou W, Tang H, Chenga X, Campb HS, Burns DJ (2007) Simultaneous quantification of malonyl-CoA and several other short-chain acyl-CoAs in animal tissues by ion-pairing reversed-phase HPLC/MS. *Journal of Chromatogr.* 853: 303-313
- Gätgens C, Degner U, Bringer-Meyer S, Herrmann U (2007) Biotransformation of glycerol to dihydroxyacetone by recombinant *Gluconobacter oxydans* DSM2343. *Appl Microbiol Biotechnol* 76: 553-559
- Gennis RB, Stewart V (1996) Respiration. In: Neidhardt F C, et al., editors. *Escherichia coli and Salmonella: cellular and molecular biology*. 2nd ed. Vol. 1. Washington, D.C. ASM Press: 217-261
- Gilmour R, Goodhew CF, Pettigrew GW, Prazeres S, Moura JJG, Moura I (1994) The kinetics of the oxidation of cytochrome *c* by *Paracoccus* cytochrome *c* peroxidase. *Biochem J* 300: 907-914
- Goodhew CF, Wilson IBH, Hunter DJB, Pettigrew GW (1990) The cellular location and specificity of bacterial cytochrome *c* peroxidases. *Biochem J* 271: 707-712
- Gosselé F, Swings J, De Ley J (1980) Growth factor requirements of *Gluconobacter*. *Zbl Bakt* 4: 348-50

- Green J, Crack JC, Thomson AJ, LeBrun NE (2009) Bacterial sensors of oxygen. *Curr Op Microbiol* 12: 145-151
- Greenfield S, Claus GW (1972) Nonfunctional tricarboxylic acid cycle and the mechanism of glutamate biosynthesis in *Acetobacter suboxydans*. *J Bacteriol* 112: 1295-1301
- Guest JR, Green J, Irvine AS, Spiro S (1996) The FNR modulon and FNR-regulated gene expression. Regulation of gene expression in *Escherichia coli*, R.G. Landes Company, Austin, Texas 313-342
- Gupta A, Singh VK, Qazi GN, Kuma, A (2001) *Gluconobacter oxydans*: Its biotechnological applications. *J Mol Microbiol Biotechnol* 3: 445-56
- Hanahan D (1983) Studies on Transformation of *E. coli* with Plasmids. *J Mol Biol.* 166: 557-580
- Hancock RD (2009) Recent Patents on Vitamin C: Opportunities for Crop Improvement and Single-Step Biological Manufacture. *Recent Patents on Food, Nutrition & Agriculture* 1: 39-49
- Heefner DL, Claus GW (1976) Change in quantity of lipids and cell size during intracytoplasmic membrane formation in *Gluconobacter oxydans*. *J Bacteriol* 125: 1163-1171
- Hénin J, Tajkhorshid E, Schulten K, Chipot C (2008) Diffusion of glycerol through *Escherichia coli* aquaglyceroporin GlpF. *Biophys J* 94: 832-839
- Hirano S, Kanamatsu T, Takagi Y, Abei T (1997) A simple infrared spectroscopic method for the measurement of expired $^{13}\text{C}_2$. *Analyt Biochem* 96: 64-69
- Hölscher T, Weinert-Sepalage D, Görisch H (2007) Identification of membrane-bound quinoprotein inositol dehydrogenase in *Gluconobacter oxydans* ATCC 621H. *Microbiology* 153: 499-506
- Hölscher T, Schleyer U, Merfort M, Bringer-Meyer S, Görisch H, Sahm H (2009) D-glucose oxidation and PQQ-dependent dehydrogenases in *Gluconobacter oxydans*. *J Mol Microbiol Biotechnol* 16: 6-13
- Hoshino T, Sugisawa T, Shinjoh M, Tomiyama N, Miyazaki T (2003). Membrane-bound D-sorbitol dehydrogenase of *Gluconobacter suboxydans* IFO 3255 - enzymatic and genetic characterization. *Biochim Biophys Acta* 1647: 278-88
- Imlay JA, Linn S (1987) Mutagenesis and stress responses induced in *Escherichia coli* by hydrogen peroxide. *J Bacteriol* 169: 2967-2976
- Imlay JA, Fridovich I (1991) Assay of metabolic superoxide production in *Escherichia coli*. *J Biol Chem* 266: 1175-1178
- Jackson AL, Loeb LA (1999) Microsatellite instability induced by hydrogen peroxide in *Escherichia coli*. *Mutation Research* 447_2000: 187-198
- Jackson JB (2003) Proton translocation by transhydrogenase. *FEBS Letters* 545: 18-24
- Jiang C, Xu J, Zhang H, Zhang X, Shi J, Li M, Ming F (2009) A cytosolic class I small heat shock protein, RchSP17.8, of *Rosa chinensis* confers resistance to a

- variety of stresses to *Escherichia coli*, yeast and *Arabidopsis thaliana*. Plant, Cell and Environment:1-14
- Jongejan A, Machado SS, Jongejan JA (2000) The enantioselectivity of quinohaemoprotein alcohol dehydrogenases: mechanistic and structural aspects. J Molec Cat 8: 121-163
- Jünemann S (1997) Cytochrome *bd* terminal oxidase. Biochim Biophys Acta 1321: 107-127
- Kalnenieks U (2006) Physiology of *Zymomonas mobilis*: Some unanswered questions. Adv Microbial Physiol 51: 73-117
- Kalnenieks U, Rutkis R, Kravale Z, Strazdina I, Galinina N (2007). High aerobic growth with low respiratory rate: The *ndh* deficient *Zymomonas mobilis*. J Biotechnol 131S: 263-265
- Kalnenieks U, Galinina N, Strazdina I, Kravale Z, Pickford JL, Rutkis R, Poole RK (2008) NADH dehydrogenase deficiency results in low respiration rate and improved aerobic growth of *Zymomonas mobilis*. Microbiology 154: 989-994
- Katzen F, Becker A, Lelmini MV, Oddo CG, Ielpi L (1999) New mobilizable vectors suitable for gene replacement in Gram negative bacteria and their use in mapping of the 39 end of the *Xanthomonas campestris* pv. *campestris gum* operon. Appl Environ Microbiol 65: 278-282
- Kerstens K, De Ley J (1968) The occurrence of the Entner-Doudoroff pathway in bacteria. Antonie van Leeuwenhoek 34: 393-408
- Kerstens K, Lisdiyanti P, Komagata K, Swings J (2006) The family Acetobacteriaceae: The genera *Acetobacter*, *Acidomonas*, *Asaia*, *Gluconacetobacter*, *Gluconobacter*, and *Kozakia*, p. 163-200. In Dworkin M, Falkow S, Rosenberg E., Schleifer K-H, Stackebrandt E (eds), The Prokaryotes. Vol. 5, 3rd edition. Springer-Verlag GmbH, Heidelberg
- Klasen R, Bringer-Meyer S, Sahm H (1992) Incapability of *Gluconobacter oxydans* to produce Tartaric Acid. Biotechnol Bioeng 40: 183-86
- Kouvelis VN, Saunders E, Brettin TS, Bruce D, Detter C, Han C, Typas MA, Pappas KM (2009) Complete genome sequence of the ethanol producer *Zymomonas mobilis* NCIMB 11163. J Bacteriol 191: 7140–7141
- Kovacs N (1956) Identification of *Pseudomonas pyocyanea* by the oxidase reaction. Nature 29:703
- Kovach ME, Elzer PH, Hill DS, Robertson GT, Farris MA, Roop RM, Peterson KM (1995) Four new derivatives of the broad-host-range cloning vector pBBR1MCS, carrying different antibiotic-resistance cassettes. Gene 166: 175-176
- Krajewski V (2008) Modifikation des Glucosestoffwechsels in *Gluconobacter oxydans*. Dissertation Heinrich-Heine Universität Düsseldorf

- Kulhanek M (1989) Microbial dehydrogenations of monosaccharides. *Adv Appl Microbiol* 34: 141-81
- Laemmli UK (1970) Cleavage of structural proteins during the assembly of the head of bacteriophage T4. *Nature* 227: 680-685
- Lebrun F, Bazus A, Dhulster P, Guillochon D (1998) Solubility of heme in heme-iron enriched bovine hemoglobin hydrolysates. *J Agric Food Chem* 46: 5017-5025
- Lenz O, Schwartz E, Dervede J, Eitinger M, Friedrich B (1994) The *Alcaligenes eutrophus* H16 *hoxX* gene participates in hydrogenase regulation. *J Bacteriol* 176: 4385-4393
- Levering PR, Weenk G, Olijve W & Harder W (1988) Regulation of gluconate and ketogluconate production in *Gluconobacter oxydans* ATCC 621-H. *Arch Microbiol* 149: 534-539
- Lindroth P and Mopper K (1979) High performance liquid chromatographic determination of subpicomole amounts of amino acids by pre-column fluorescence derivatization with ophthaldialdehyde. *Anal Chem* 51: 1667-1674
- Luo B, Grönke K, Takors R, Wandrey C, Oldiges M (2007) Simultaneous determination of multiple intracellular metabolites in glycolysis, pentose phosphate pathway and tricarboxylic acid cycle by liquid chromatography-mass spectrometry. *J Chromatography A* 1147: 153-164
- Manoilov SE, Sedykh NV, Firsova VI, Vennikas OR, Chelyadina LD (1996) Effect of the catalase inhibitor 3-amino-1,2,4- triazole on oxidation-phosphorylation coupling and the state of the mitochondrial adenosine system in the liver of albino rats. *Biophys and Biochem* 6: 576-577
- Matsushita K, Ohno Y, Shinagawa E, Adachi O, Ameyama M (1980) Membrane-bound D-glucose dehydrogenase from *Pseudomonas* sp.: Solubilisation, purification and characterization. *Agric Biol Chem* 44:1505-1512
- Matsushita K, Shinagawa E, Adachi O, Ameyama M (1987) Purification, characterization and reconstitution of cytochrome o-type oxidase from *Gluconobacter suboxydans*. *Biochim Biophys Acta* 894: 304-312
- Matsushita K, Nagatani Y, Shinagawa E, Adachi O, Ameyama M (1989a). Effect of extracellular pH on the respiratory chain and energetics of *Gluconobacter suboxydans*. *Agric Biol Chem* 53: 2895-2902
- Matsushita K, Nagatani YI, Shinagawa E, Adachi O, Ameyama M (1991) Reconstitution of the ethanol oxidase respiratory chain in membranes of quinoprotein alcohol dehydrogenase-deficient *Gluconobacter suboxydans* subsp. α strains. *J Bacteriol* 173: 3440-3445
- Matsushita K, Toyoma H, Adachi O (1994) Respiratory chains and bioenergetics of acetic acid bacteria. *Adv Microb Physiol* 36: 247-301
- Matsushita K, Yakushi T, Toyama H, Shinagawa E and Adachi O (1995) Function of multiple heme c moieties in intramolecular electron transport and ubiquinone

- reduction in the quinohemoprotein alcohol dehydrogenase-cytochrome *c* complex of *Gluconobacter suboxydans*. *J Biol Chem* 271: 4850-4857
- Matsushita K, Fujii Y, Ano Y, Toyama H, Shinjoh M, Tomiyama N, Miyazaki T, Sugisawa T, Hoshino T, Adachi O (2003) 5-Keto-D-gluconate production is catalysed by a quinoprotein glycerol dehydrogenase, major polyol dehydrogenase, in *Gluconobacter* species *Appl. Environ Microb* 69: 1959-1966
- Matsushita K, Kobayashi Y, Mitzugushi M, Toyama H, Adachi O, Sakamoto K, Miyoshi H (2008) A tightly bound quinone functions in the ubiquinone reaction sites of quinoprotein alcohol dehydrogenase of an acetic acid bacterium, *Gluconobacter suboxydans*. *Biosci Biotech Biochem* 72: 2723-2731
- Mauk MR, Rosell FI, Mauk AG (2009) Metal ion facilitated dissociation of heme from b-type heme proteins. *J Am Chem Soc* 131:16976-16983
- Maurer LM, Yohannes E, Bondurant SS, Radmacher M, Slonczewski JL (2005) pH regulates genes for flagellar motility, catabolism and oxidative stress in *Escherichia coli* K-12. *J Bacteriol* 187: 304-319
- McHugh JP, Rodriguez-Quinones F, Abdul-Tehrani, H, Svistunenko DA, Poole RK, Cooper CE, Andrews SC (2003) Global iron-dependent gene regulation in *Escherichia coli* a new mechanism for iron homeostasis *J Biol Chem* 278: 29478-29486
- Meiberg JBM, Spa HA (1983) Microbial production of gluconic acids and gluconates. *J Microbiol* 49: 89-90
- Merfort M, Herrmann U, Bringer-Meyer S, Sahm H (2006a) High yield 5-keto-D-gluconic acid formation is mediated by soluble and membrane-bound gluconate-5-dehydrogenases of *Gluconobacter oxydans*. *Appl Microbiol Biotechnol* 73: 443-451
- Merfort M, Herrmann U, Ha S-W, Elfari M, Bringer Meyer S, Görisch H, Sahm H (2006b) Modification of the membrane-bound glucose oxidation system in *Gluconobacter oxydans* significantly increases gluconate and 5-keto-D-gluconic acid accumulation. *Biotechnol J* 1: 556-563
- Merford M (2009) PhD-Thesis, Forschungszentrum Jülich GmbH, Germany
- Messner KR, Imlay JA (1999) The identification of primary sites of superoxide and hydrogen peroxide formation in the aerobic respiratory chain and sulfite reductase complex of *Escherichia coli*. *J Biol Chem* 274: 10119-10128
- Millers MJ and Gennis RB (1985) The cytochrome *d* complex is a coupling site in the aerobic respiratory chain of *Escherichia coli*. *J Bacteriol Chem* 260: 14003-14008
- Minamino T, Imadaab K, Namba K (2008a) Mechanisms of type III protein export for bacterial flagellar assembly. *Mol BioSyst* 4: 1105-1115
- Minamino T, Namba K (2008b) Distinct roles of the FliI ATPase and proton motive force in bacterial flagellar protein export. *Nature* 451: 485-489

- Miyazaki T, Tomiyama N, Shinjoh M, Hoshino T (2002) Molecular cloning and functional expression of D-sorbitol dehydrogenase from *Gluconobacter suboxydans* IF03255, which requires pyrroloquinoline quinone and hydrophobic protein SldB for activity development in *E. coli*. *Biosci Biotechnol Biochem* 66: 262-270
- Mogi T, Matsushita K, Murase Y, Kawahara K, Miyoshi H, Ui H, Shiomi K, Omura S, Kita K (2009). Identification of new inhibitors for alternative NADH dehydrogenase (NDH-II). *FEMS Microbiol Lett* 291: 157-161
- Moritz B, Striegel K, de Graaf AA, Sahm H (2000). Kinetic properties of the glucose 6-phosphate and 6-phosphogluconate dehydrogenases from *Corynebacterium glutamicum* and their application for predicting pentose phosphate pathway flux *in vivo*. *Eur J Biochem* 267: 3442-3452
- Mostafa HE, Heller KJ, Geis A (2002) Cloning of *Escherichia coli lacZ* and *lacY* genes and their expression in *Gluconobacter oxydans* and *Acetobacter liquefaciens*. *Appl Environ Microbiol* 68: 2619-2623
- Mouncey NJ, Kaplan S (1998) Oxygen regulation of the *ccoN* gene encoding a component of the *cbb3* oxidase in *Rhodobacter sphaeroides* 2.4.1T: involvement of the FnrL protein. *J Bacteriol* 180: 2228-2231
- Mullis KB and Faloona FA (1987) Specific synthesis of DNA *in vitro* via a polymerasecatalysed chain reaction. *Methods Enzymol* 155: 335-350
- Nicholls DG and Ferguson SJ (2002) *Bioenergetics*. Academic Press, Elsevier Science Ltd
- Niebisch A, Bott M (2001) Molecular analysis of the cytochrome *bc₁-aa₃* branch of the *Corynebacterium glutamicum* respiratory chain containing an unusual diheme cytochrome *c*. *Arch of Microbiol* 175: 282-294
- Nöh K, Wahl A, Wiechert W (2006) Computational tools for isotopically instationary ¹³C labeling experiments under metabolic steady state conditions. *Metabolic Engineering* 8: 554-577
- Oijve W (1978) PhD Thesis, University of Groningen, The Netherlands
- Olijve W., Kok JJ (1979) Analysis of growth of *Gluconobacter oxydans* in glucose containing media. *Arch Microbiol* 121: 283-90
- Osyczka A, Moser CC, Daldal F, Dutton PL (2004) Reversible redox energy coupling in electron transfer chains. *Nature* 427: 607-612
- Pappin DJ, Hojrup P, Bleasby AJ (1993) Identification of proteins by peptide-mass fingerprinting. *Curr Biol* 3: 327-32
- Parsell DA, RT Sauer (1989) Induction of a heat shock-like response by unfolded protein in *Escherichia coli*: dependence on protein level not protein degradation. *Genes Dev* 3: 1226-1232

- Patschkowski T, Bates DM, Kiley PJ (2000) Mechanisms for sensing and responding to oxygen deprivation. Bacterial stress responses. Storz G, Hengge-Aronis R, eds., ASM Press, Washington, D. C.
- Polen T, VF Wendisch (2004) Genomewide expression analysis in amino acid-producing bacteria using DNA microarrays. *Appl Biochem Biotechnol* 118: 215-232
- Polen T, Schluesener D, Poetsch A, Bott M, Wendisch VF (2007) Characterization of citrate utilization in *Corynebacterium glutamicum* by transcriptome and proteome analysis. *FEMS Microbiol Lett* 273: 109-119
- Pope NR, Cole JA (1982) Generation of a membrane potential by one of two independent pathways for nitrite reduction by *Escherichia coli*. *Journal of Gen Microbiol* 128:219-222
- Pronk JT, Levering PR, Olijve W, Van Dijken JP (1989) Role of NADP dependent and quinoprotein glucose dehydrogenase in gluconic acid production by *Gluconobacter oxydans*. *Enzyme Microb Technol* 11: 160-164
- Prust C (2004) Dissertation: Entschlüsselung des Genoms von *Gluconobacter oxydans* 621H – einem Bakterium von industriellem Interesse. Mathematisch-Naturwissenschaftliche Fakultäten der Georg-August-Universität zu Göttingen
- Prust C, Hoffmeister M, Liesegang H, Wiezer A, Fricke WF, Ehrenreich A, Gottschalk G, Deppenmeier U (2005). Complete genome sequence of the acetic acid bacterium *Gluconobacter oxydans*. *Nat Biotechnol* 23: 195-200
- Rabinow P (1996) Making PCR: A story of biotechnology. University of Chicago Press
- Raspor P, Goranovič D (2008) Biotechnological applications of acetic acid bacteria. *Crit Rev Biotechnol* 28: 101-124
- Sahm H, Bringer-Meyer S, Sprenger GA (2006) The Genus *Zymomonas*. In Dworkin M, Falkow S, Rosenberg E, Schleifer K-H, Stackebrandt E (eds.), *The Prokaryotes*. Vol. 5, 3rd edition. Springer-Verlag GmbH, Heidelberg: 201-221
- Sambrook J, Fritsch EF, Maniatis T (1989) *Molecular Cloning. A laboratory manual*. Cold Spring Harbor Laboratory, Cold Spring Harbor, New York
- Sambrook J, Russel DW (2000) *Molecular cloning: a laboratory manual*. Cold Spring Harbour Laboratory Press, Cold Spring Harbour, New York
- Sauer U, Canonaco F, Heri S, Perrenoud A, Fischer E (2004) The soluble and the membrane-bound transhydrogenases *UdhA* and *PntAB* have divergent functions in NADPH metabolism of *Escherichia coli*. *J Bacteriol* 279: 6613-6619
- Schäfer A, Tauch A, Jäger W, Kalinowski J, Thierbach G, Pühler A (1994) Small mobilizable multi-purpose cloning vectors derived from the *Escherichia coli* plasmids pK18 and pK19: selection of defined deletions in the chromosome of *Corynebacterium glutamicum*. *Gene* 145: 69-73

- Schaffer S, Weil B, Nguyen VD, Dongmann G, Günther K, Nickolaus M, Hermann T, Schedel M (2000) Regioselective oxidation of aminosorbitol with *Gluconobacter oxydans*, a key reaction in the industrial synthesis of 1-deoxynojirimycin. In: Biotechnology, Biotransformations I.: Kelly DR. Wiley-VCH, Weinheim, 296-308
- Schleyer U, Bringer-Meyer S, Sahm H (2008) An easy cloning and expression vector system for *Gluconobacter oxydans*. J Food Microbiol 125: 91-95
- Shimizu T, Yamasaki S, Tsukamoto T, Takeda Y (1999) Analysis of the genes responsible for the O-antigen synthesis in enterohaemorrhagic *Escherichia coli* 0157. Microb Pathog 26: 235-247
- Shinagawa E, Matsushita K, Adachi O, Ameyama M (1984) D-Gluconate dehydrogenase, 2-keto-D-gluconate yielding, from *Gluconobacter dioxyacetonicus*: purification and characterization. Agricult Biol Chem 48: 1517-1522
- Shinagawa E, Matsushita K, Adachi O, Ameyama M (1990) Evidence for electron transfer *via* ubiquinone between quinoproteins D-glucose dehydrogenase and alcohol dehydrogenase of *Gluconobacter suboxydans*. J Biochem 107: 863-867
- Sievers M, Gaberthül C, Boesch C, Ludwig W, Teuber M (1995). Phylogenetic position of *Gluconobacter* species as a coherent cluster separated from all *Acetbacter* species on the basis of 16S ribosomal RNA sequences. FEMS Microbiol Lett 126: 123-126
- Simon R, Priefer U, Piihler A (1983) A broad host range mobilization system for *in vivo* genetic engineering: transposon mutagenesis in Gram-negative bacteria. Biotechnology 1: 784-791
- Skerra A, Schmidt TGM (2000) Use of the Strep-Tag and Streptavidin for detection and purification of recombinant proteins. In Methods in Enzymology. Academic Press, San Diego 326: 271-304
- Smith PK, Krohn RI, Hermanson GT, Mallia AK, Gartner FH, Provenzano MD, Fujimoto EK, Goeke NM, Olson BJ, Klenk DC (1985) Measurement of protein using bicinchoninic acid. Anal Biochem 150: 76-85
- Smyth GK (2005) limma: linear models for microarray data. In: Bioinformatics an computational biology solutions using R and bioconductor. Springer-Verlag NY
- Soemphol W, Adachi O, Matsushita K, Toyama H (2008) Distinct physiological roles of two membrane-bound dehydrogenases responsible for D-sorbitol oxidation in *Gluconobacter frateurii*. Biosci Biotechnol Biochem 72: 842–850
- Sootsuwan K, Lertwattanasakul N, Thanonkeo P, Matsushita K, Yamada, M (2008) Analysis of the respiratory chain in ethanologenic *Zymomonas mobilis* with a cyanide-resistant *bd*-type ubiquinol oxidase as the only terminal oxidase and its possible physiological roles. J Mol Microbiol Biotechnol 14: 163–175
- Spiro S, Guest JR (1987) Regulation and over-expression of the *fnr* gene of *Escherichia coli*. J Gen Microbiol 133: 3279-3288

- Spiro S (1994) The FNR family of transcriptional regulators. *Antonie van Leeuwenhoek*, Springer Netherlands, Volume 66
- Stroud RM, Miercke LJW, O'Connell J, Khademi S, Lee JK, Remis J, Harries W, Robles Y, Akhavan D (2003) Glycerol facilitator GlpF and the associated aquaporin family of channels. *Curr Op Struct Biol* 13: 424-431
- Sugisawa T, Hoshino T (2002) Purification and properties of membrane-bound D-sorbitol dehydrogenase from *Gluconobacter suboxydans* IFO 3255. *Biosci Biotechnol Biochem* 66: 57-64
- Swings J (1992) The genera *Acetobacter* and *Gluconobacter*. In: Barlows A, Trüper HG, Dwarkin M, Harder W, Schleifert KH *The Prokaryotes*. Springer Verlag, New York, 2268-2286
- Szyperski T, Glaser RW, Hochuli M, Fiaux J, Sauer U, Bailey JE, Wüthrich K (1999) Bioreaction network topology and metabolic flux ratio analysis by biosynthetic fractional ¹³C labeling and two-dimensional NMR spectroscopy. *Metab Eng* 1: 189-197
- Tanaka M, Murakami S, Shinke R, Aoki K (1999) Reclassification of the strains with low G+C contents of DNA belonging to the genus *Gluconobacter* Asai 1935. *Biosci Biotechnol Biochem* 63: 989-992
- Thöny-Meyer L, Fischer F, Künzler P, Ritz D, Hennecke H (1995) *Escherichia coli* Genes Required for Cytochrome c Maturation. *J Bacteriol* 177: 4321-4326
- Tonouchi N, Sugiyama M, Yokozeki K (2003) Coenzyme specificity of enzymes in the oxidative pentose phosphate pathway of *Gluconobacter oxydans*. *Biosci Biotechnol Biochem* 67: 2648-2651
- Toyama H, Mathews FS, Adachi O, Matsushita K (2004) Quinohemoprotein alcohol dehydrogenases: structure, function, and physiology. *Arch Biochem Biophys* 428: 10-21
- Toyama H, Furuya N, Saichana I, Ano Y, Adachi O, Matsushita K (2007) Membrane-bound, 2-keto-D-gluconate-Yielding D-gluconate dehydrogenase from "*Gluconobacter dioxyaceticus*" IFO 3271: Molecular properties and gene disruption. *Appl Environ Microbiol* 73: 6551-6556
- Trevors JT, Stradoub ME (1990) Electroporation of pKK1 silver-resistance plasmid from *Pseudomonas stutzeri* AG259 into *Pseudomonas putida* CYM318. *Curr Microbiol* 21: 103-7
- Trumpower B (1990a) Cytochrome *bc*₁ complexes of microorganism. *Microbiol Reviews* 54: 101-129
- Trumpower B (1990b) The proton motive Q-cycle. *J Biol Chem* 265: 11409-11412
- Tseng CP, Albrecht J, Gunsalus RP (1995) Effect of microaerophilic cell growth conditions on expression of the aerobic (*cyoABCDE* and *cydAB*) and anaerobic

- (*narGHJI*, *frdABCD*, and *dmsABC*) respiratory pathway genes in *Escherichia coli*. J Bacteriol 178: 1094-1098
- Van Bogelen RA, Kelley PM, Neidhardt FC (1987) Differential induction of heat shock, SOS, and oxidation stress regulons and accumulation of nucleotides in *Escherichia coli*. J Bacteriol 169: 26-32
- van der Oost J, Schepper M H, Stouthamer A, Westerhoff H, van Spanning RJM, de Gier JWL (1995) Reversed cytochrome *c* electron transfer through the *bc₁*-complex enables an oxidase mutant (Aaa3/cbb3) of *Paracoccus denitrificans* to grow on methylamine. FEBS Lett 371: 267-270
- Verkhovskaya ML, Garcia-Horsman A, Puustinen A, Rigaud JL, Morgan JE, Verkhovsky MI, Wikstrom M (1997) Glutamic acid 286 in subunit I of cytochrome *bo₃* is involved in proton translocation. Biochem 94: 10128-10131
- Wagner MA, Zahrl D, Rieser G, Koraimann G (2009) Growth phase- and cell division-dependent activation and inactivation of the sigma 32 regulon in *Escherichia coli*. J Bacteriol 191: 1695-1702
- Weenk G, Olijve W, Harder W (1984) Ketogluconate formation by *Gluconobacter* species. Appl. Microbiol. Biotechnol. 20: 400-405
- Wiechert W (2001) ¹³C Metabolic flux analysis. Metabolic Engineering 3: 195-206
- Wiechert W, Möllney M, Petersen S, de Graaf AA (2001) A universal framework for ¹³C metabolic flux analysis. Metabolic Engineering 3: 265-283
- Wiechert W and Nöh K (2005) From stationary to instationary metabolic flux analysis. Adv Biochem Engin/Biotechnol 92: 145-172
- Yamada Y, Yukphan P (2008) Genera and species in acetic acid bacteria. Int J Food Microbiol 125: 15-24
- Yanisch-Perron C, Vieira J, Messing J (1985) Improved M13 phage cloning vectors and host strains: nucleotide sequences of the M13mp18 and pUC19 vectors. Gene 33: 103-119
- Yoshpe-Purer Y. and Hensi Y (1976) Factors affecting catalase level and sensitivity to hydrogen peroxide in *Escherichia coli*. Appl Environm Microbiol 32: 465-469
- Zahn JA, Arciero DM, Hooper AB, Coats JR, DiSpirito AA (1997) Cytochrome *c* peroxidase from *Methylococcus capsulatus Bath* Arch Microbiol 168: 362-372
- Zamboni N, Fendt SM, Rühl M, Sauer U (2009) ¹³C-based metabolic flux analysis. Nature Protocols 4: 878-892
- Zeilstra-Ryallis JH, Gabbert K, Mouncey NJ, Kaplan S, Kranz RG (1997) Analysis of the *fnrL* gene and its function in *Rhodobacter capsulatus*. J Bacteriol 179: 7264-7273

VII Appendix

Table 17 List of main central metabolic reactions in the *G. oxydans* network model

Acronym	Generic name	Long Name	GeneID
	glcUpt	diffusion	
	glcnOut	diffusion	
	2kgaOut, 5kgaOut		
	kgaOut (lumped)	diffusion	
	co2Out	diffusion	
<i>mGDH</i>	gdh1	Glucose dehydrogenase (PQQ)	GOX0265
		Gluconolactonase (membrane-bound)	GOX1381
	g2DH, g5DH (lumped)	Gluconate dehydrogenases (periplasm)	GOX1230 -GOX1232 GOX2094, GOX2095, GOX2097
	uptGlc	unknown transporter	
<i>gntP</i>	uptGlc upt5KGA	Gluconate permease	GOX2188
	uptKGA (lumped)	unknown transporter	
<i>cGDH</i>	gdh3	Glucose dehydrogenase (NADP, cytoplasm)	GOX2015
<i>pg</i>	gdh4	Gluconolactonase (cytoplasm)	GOX1375
<i>gno</i>	gdh5	Gluconate-5-dehydrogenase (cytoplasm)	GOX2187
<i>hk</i>	glck	Glucose kinase	GOX2419
<i>gntk</i>	glcnk	Gluconokinase	GOX1709
<i>pgi</i>	emp1	Glucose 6-phosphate isomerase	GOX1704
<i>fbp</i>	emp2	Fructose biphosphatase	GOX1516
<i>fba</i>	emp3	Fructose-1,6-diphosphate aldolase	GOX1540
<i>tpi</i>	emp4	Triosephosphate isomerase	GOX2284
<i>gap</i>	emp5	Glyceraldehyde 3-phosphate dehydrogenase	GOX0508
<i>pgk</i>	emp6	Phosphoglycerate kinase	GOX0507
<i>pyk</i>	emp7	Pyruvate kinase	GOX2250
<i>zwf</i>	ppp1	Glucose 6-phosphate dehydrogenase	GOX0145
<i>gnd</i>	ppp2	6-Phosphogluconate dehydrogenase	GOX1705
<i>rpe</i>	ppp3	Ribulose 5-phosphate epimerase	GOX1352
<i>rpi</i>	ppp4	Ribulose 5-phosphate isomerase	GOX1708
<i>tka1</i>	ppp5	Transketolase	GOX1703
<i>tka2</i>	ppp6	Transketolase	GOX1703
		Bifunctional transaldolase/ glucose-6-phosphate isomerase	
<i>tal</i>	ppp7		GOX1704
<i>edd</i>	edp1	6-Phosphogluconate dehydratase	GOX0431
		2-Keto-3-deoxygluconate 6-phosphate aldolase	
<i>eda</i>	edp2		GOX0430
<i>pdhC</i>	tca1	Pyruvate dehydrogenase complex	GOX2289, GOX2290, GOX2292
<i>gltA</i>	tca2	Citrate synthase	GOX1999
<i>acn</i>	tca3	Aconitase	GOX1335
<i>acn</i>	tca4	Aconitase	GOX1335
<i>lcd</i>	tca5	Isocitrate dehydrogenase (NADP)	GOX1336
<i>ogdhC</i>	tca6	alpha Ketoglutarate dehydrogenase complex	GOX0882, GOX1073, GOX2292
<i>fum</i>	tca7	Fumarate hydratase	GOX1643
<i>mgo</i>	tca8	Malate:quinone oxidoreductase	GOX2070
<i>ppc</i>	ana	Phosphoenolpyruvate carboxylase	GOX0102

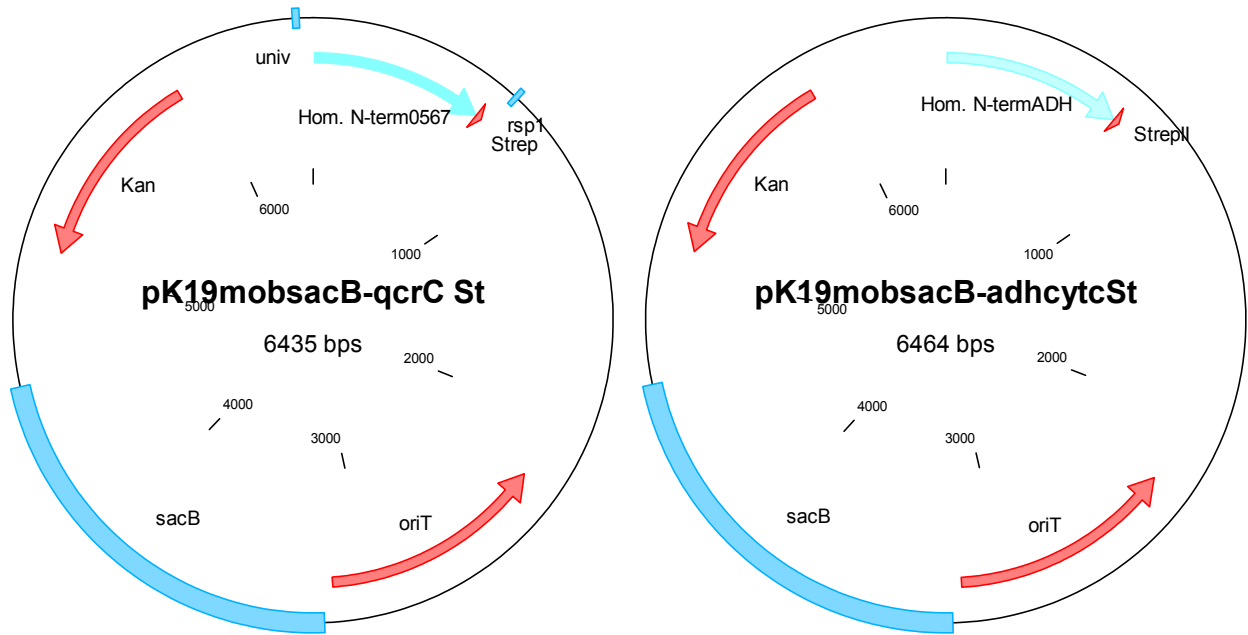


Fig. 27 Vectors for chromosomal integration of StrepTag

Kan: gene for kanamycin resistance; oriT: Origin of transfer; *sacB*: gene for the levansucrase; univ and *rsp1*: primer region for sequencing; hom.N-term0567: Homologous region for recombination in *qcrC*; hom.N-termADH: Homologous region for recombination in cytochrome *c* subunit of the ADH

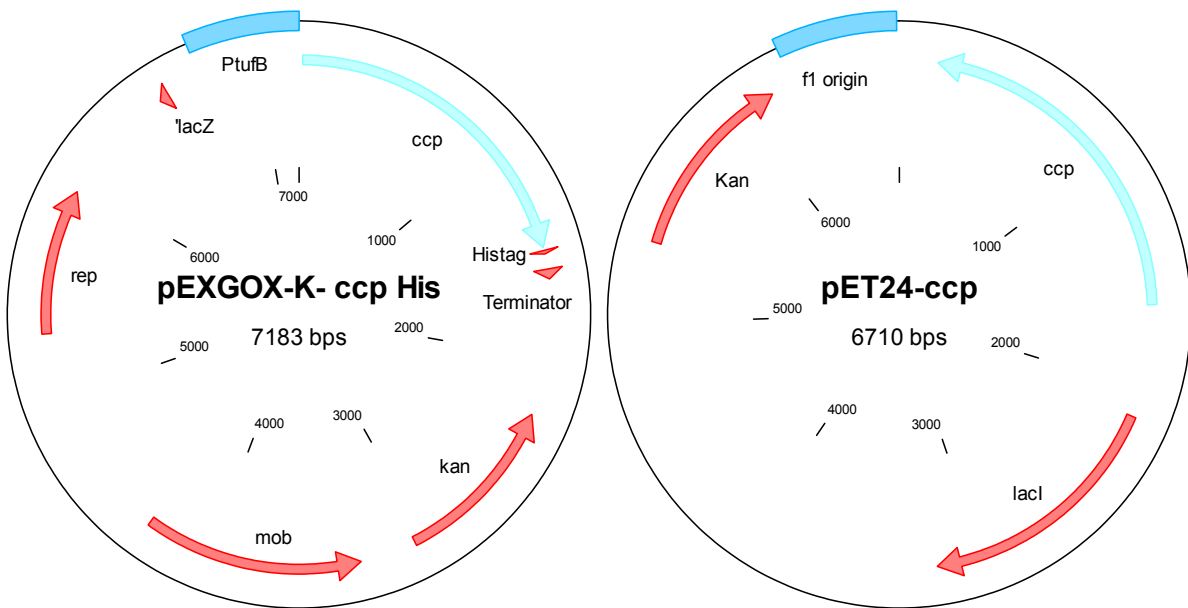


Fig. 28 Vectors for overexpression of the *ccp*-gene of *G. oxydans*

Left: Homologous overexpression in *G. oxydans*, right: overexpression in *E. coli*
 Kan: gene for kanamycin resistance; rep: replication origin; *lacZ*: rest of the *lacZ*-gene; *mob*: genes responsible for mobilisation; HisTag: HisTag sequence of pET24; Terminator: terminator sequence of pET24; *ccp*: *ccp*-gene of *G. oxydans*; *lacI*: Gene for lactose repressor; f1 origin: origin of replication

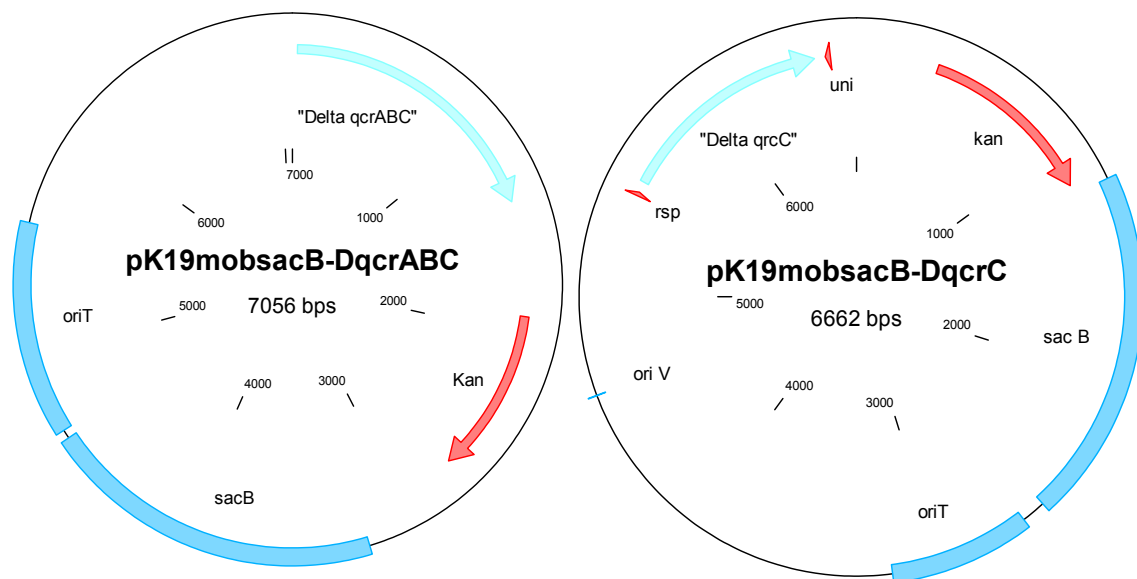


Fig. 29 Vectors for the marker-free deletion of *qcrABC* and *qcrC* of *G. oxydans*

Kan: gene for kanamycin-resistance; oriT: Origin of transfer; sacB: gene for the levansucrase; uni and *rsp1*: primer region for sequencing; "Delta *qcrABC*": regions flanking *qcrABC* for double homologous recombination in *G. oxydans* for marker-free deletion of *qcrABC*; "Delta *qcrC*": regions flanking *qcrC* for double homologous recombination in *G. oxydans* for marker-free deletion of *qcrC*

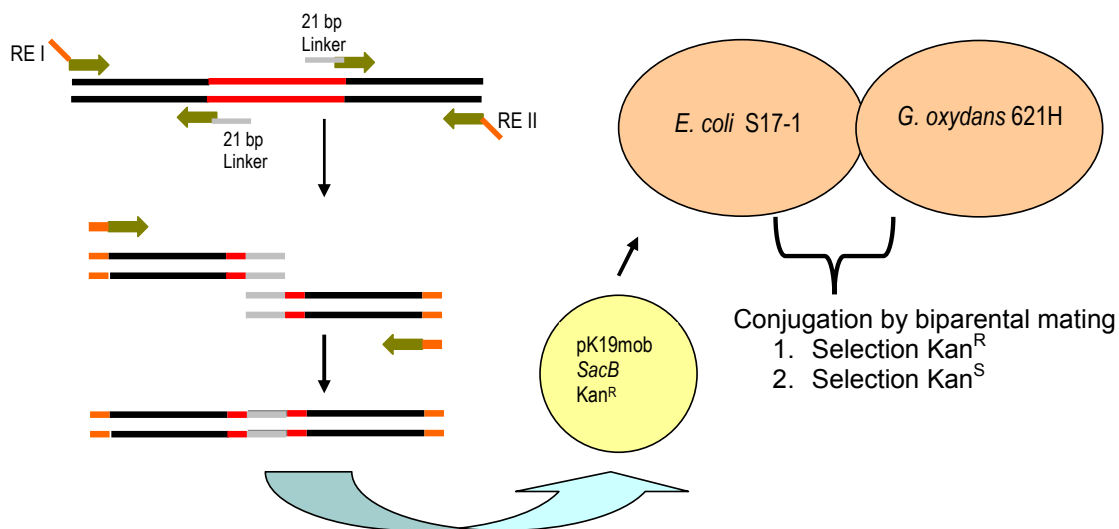


Fig. 30 Construction of deletion mutants by "Crossover-PCR" and biparental mating

Red region: Gene/operon to delete; black regions: flanking regions; green thick arrows: primer for amplification of the flanking regions; 21 bp linker: primer overhangs for "crossover-PCR"; REI+II: primer overhangs with sequence of the desired restriction enzyme for cloning into pK19mobsacB

Table 18 List of all genes with altered mRNA-levels of cells grown under oxygen limitation vs. oxygen excess, at pH 4 vs. pH 6 and during growth on gluconate vs. glucose, differently expressed (> 1.8-fold up- or downregulated, p-value ≤ 0.05)

Locus tag	Ratio O ₂ - limitation/ O ₂ - excess	p- value	Annotation
GOX0013	0.15	0.0001	Hypothetical protein GOX0013
GOX0017	0.52	0.0012	DNA polymerase III delta prime subunit DnaC
GOX0024	0.40	0.0022	Undecaprenyl pyrophosphate phosphatase
GOX0029	0.55	0.0033	Hypothetical protein GOX0029
GOX0031	2.16	0.0019	Hypothetical protein GOX0031
GOX0032	0.54	0.0024	Bacterial Peptide Chain Release Factor 1
GOX0035	0.42	0.0037	Hypothetical protein GOX0035
GOX0036	0.41	0.0024	Enoyl[acyl-carrier-protein] reductase
GOX0037	0.50	0.0008	Aspartate kinase
GOX0039	0.42	0.0032	Putative hemagglutinin-related protein
GOX0042	0.54	0.0010	Competence protein F
GOX0053	3.71	0.0003	Hypothetical protein GOX0053
GOX0057	1.89	0.0057	Sensory box/GGDEF family protein
GOX0070	1.97	0.0015	Hypothetical membrane-spanning protein
GOX0074	0.29	0.0015	Elongation factor Ts
GOX0075	0.27	0.0001	30S ribosomal protein S2
GOX0088	0.40	0.0007	Trigger factor
GOX0090	5.14	0.0009	Putative sugar kinase
GOX0103	0.23	0.0001	Carboxypeptidase-related protein
GOX0105	0.31	0.0001	Protein Translation Elongation Factor G
GOX0106	0.28	0.0003	50S ribosomal protein L28
GOX0116	0.24	0.0029	Fatty acid/phospholipid synthesis protein
GOX0117	0.37	0.0006	50S ribosomal protein L32
GOX0126	2.08	0.0017	Flagellar motor protein MotA
GOX0127	1.96	0.0052	Chemotaxis MotB protein
GOX0132	0.27	0.0000	Transcriptional regulator, LysR family
GOX0135	2.80	0.0037	Transcriptional regulator
GOX0137	2.86	0.0002	Hypothetical membrane-spanning protein
GOX0139	0.51	0.0056	50S ribosomal protein L21
GOX0140	0.44	0.0006	50S ribosomal protein L27
GOX0143	0.45	0.0036	Hypothetical protein GOX0143
GOX0145	0.45	0.0000	Glucose-6-phosphate 1-dehydrogenase
GOX0151	1.90	0.0141	Hypothetical protein GOX0151
GOX0160	0.51	0.0030	UDP-N-acetylenolpyruvylglucosamine reductase
GOX0162	0.51	0.0001	Cell division protein FtsQ
GOX0181	0.51	0.0095	Oligopeptide transporter
GOX0190	0.47	0.0000	Aspartate aminotransferase A
GOX0191	0.35	0.0004	3-Isopropylmalate dehydrogenase
GOX0192	0.32	0.0002	3-Isopropylmalate dehydratase, small su

GOX0193	0.24	0.0004	Isopropylmalate isomerase large subunit
GOX0194	0.28	0.0003	50S ribosomal protein L19
GOX0195	0.27	0.0002	tRNA (Guanine-N(1)-)-methyltransferase
GOX0196	0.36	0.0004	30S ribosomal protein S16
GOX0197	0.34	0.0009	Signal recognition particle protein
GOX0198	2.17	0.0006	Hypothetical protein GOX0198
GOX0200	0.10	0.0001	ATP-dependent RNA helicase
GOX0204	2.45	0.0011	Hypothetical protein GOX0204
GOX0207	0.18	0.0004	TonB-dependent outer membrane receptor
GOX0210	0.55	0.0004	Putative carboxylase
GOX0213	0.46	0.0001	Biotin carboxylase
GOX0216	0.51	0.0031	N-methylhydantoinase A
GOX0218	0.52	0.0005	D-3-phosphoglycerate dehydrogenase
GOX0254	0.44	0.0016	Putative Fe-S-cluster redox enzyme
GOX0261	0.52	0.0082	Phenylalanyl-tRNA synthetase subunit beta
GOX0262	0.45	0.0017	Phenylalanyl-tRNA synthetase alpha chain
GOX0263	0.34	0.0002	50S ribosomal protein L20
GOX0264	0.47	0.0010	LSU ribosomal protein L35P
GOX0265	0.50	0.0000	Membrane-bound glucose dehydrogenase (PQQ)
GOX0278	3.64	0.0001	Cytochrome d ubiquinol oxidase subunit I
GOX0279	1.94	0.0095	Cytochrome d ubiquinol oxidase subunit II
GOX0286	0.54	0.0036	Hypothetical protein GOX0286
GOX0304	0.35	0.0008	50S ribosomal protein L9
GOX0305	0.38	0.0002	30S ribosomal protein S18
GOX0306	0.34	0.0014	SSU ribosomal protein S6P
GOX0310	10.37	0.0004	NAD(P) transhydrogenase subunit alpha
GOX0311	14.70	0.0014	NAD(P) transhydrogenase subunit alpha
GOX0312	12.04	0.0004	NAD(P) transhydrogenase subunit beta
GOX0313	13.58	0.0007	NAD-dependent alcohol dehydrogenase
GOX0314	14.63	0.0023	Probable alcohol dehydrogenase-like oxidoreductase protein
GOX0321	0.30	0.0001	Carbamoyl phosphate synthase small su
GOX0322	0.32	0.0000	Carbamoyl phosphate synthase large subunit
GOX0326	0.35	0.0002	Hypothetical protein GOX0326
GOX0332	1.95	0.0000	Carboxy-terminal protease
GOX0333	2.24	0.0016	Hypothetical protein GOX0333
GOX0334	2.21	0.0001	Probable (di) nucleoside polyphosphate hydrolase
GOX0343	1.94	0.0005	Hypothetical protein GOX0343
GOX0345	0.41	0.0002	Ribonuclease HII
GOX0351	0.54	0.0020	Putative outer membrane drug efflux protein
GOX0352	0.36	0.0009	Hypothetical protein GOX0352
GOX0354	0.12	0.0009	Putative sugar/polyol transporter
GOX0355	0.36	0.0030	LSU ribosomal protein L17P
GOX0356	0.37	0.0028	DNA-directed RNA polymerase subunit α
GOX0357	0.37	0.0063	30S ribosomal protein S11
GOX0358	0.53	0.0004	30S ribosomal protein S13
GOX0359	0.39	0.0018	Adenylate kinase
GOX0360	0.39	0.0056	Preprotein translocase subunit SecY
GOX0361	0.45	0.0228	LSU ribosomal protein L15P

VII Appendix

GOX0362	0.37	0.0048	LSU ribosomal protein L30P
GOX0363	0.29	0.0016	30S ribosomal protein S5
GOX0364	0.25	0.0041	50S ribosomal protein L18
GOX0365	0.27	0.0005	50S ribosomal protein L6
GOX0366	0.27	0.0055	30S ribosomal protein S8
GOX0367	0.42	0.0045	30S ribosomal protein S14
GOX0368	0.16	0.0008	50S ribosomal protein L5
GOX0369	0.29	0.0010	LSU ribosomal protein L24P
GOX0370	0.31	0.0019	LSU ribosomal protein L14P
GOX0371	0.40	0.0000	SSU ribosomal protein S17P
GOX0372	0.35	0.0007	LSU ribosomal protein L29P
GOX0373	0.26	0.0004	50S ribosomal protein L16
GOX0374	0.25	0.0034	30S ribosomal protein S3
GOX0375	0.26	0.0031	50S ribosomal protein L22
GOX0376	0.24	0.0011	SSU ribosomal protein S19P
GOX0377	0.25	0.0001	50S ribosomal protein L2
GOX0378	0.30	0.0002	LSU ribosomal protein L23P
GOX0379	0.28	0.0002	50S ribosomal protein L4
GOX0380	0.30	0.0000	50S ribosomal protein L3
GOX0381	0.26	0.0029	30S ribosomal protein S10
GOX0382	0.30	0.0023	Elongation factor Tu
GOX0383	0.16	0.0025	30S ribosomal protein S7
GOX0384	0.22	0.0000	30S ribosomal protein S12
GOX0385	0.40	0.0031	DNA-directed RNA polymerase subunit β'
GOX0386	0.43	0.0069	DNA-directed RNA polymerase subunit β
GOX0387	0.21	0.0003	50S ribosomal protein L7/L12
GOX0388	0.20	0.0005	LSU ribosomal protein L10P
GOX0389	0.31	0.0039	50S ribosomal protein L1
GOX0390	0.43	0.0014	50S ribosomal protein L11
GOX0391	0.53	0.0004	Putative outer membrane channel protein
GOX0392	0.46	0.0007	Putative transport transmembrane protein
GOX0393	0.43	0.0005	Putative transport transmembrane protein
GOX0396	0.40	0.0047	DNA recombination protein RmuC-like protein
GOX0397	0.46	0.0002	Hypothetical protein GOX0397
GOX0404	0.13	0.0002	Hypothetical protein GOX0404
GOX0405	0.09	0.0002	TonB-dependent outer membrane receptor
GOX0407	1.94	0.0008	Hypothetical protein GOX0407
GOX0413	0.48	0.0057	Acetyl-coenzyme A synthetase
GOX0415	0.30	0.0003	Putative transport protein
GOX0416	0.33	0.0001	Protein-tyrosine phosphatase
GOX0421	2.18	0.0025	Flagellar motor switch protein
GOX0422	2.17	0.0193	Hypothetical protein GOX0422
GOX0425	3.04	0.0004	Basal-body rod modification protein FlgD
GOX0426	3.42	0.0023	Hypothetical protein GOX0426
GOX0435	0.49	0.0004	Acetyl-CoA carboxylase biotin carboxylase subunit
GOX0440	0.31	0.0009	Ornithine decarboxylase
GOX0442	2.21	0.0194	Hypothetical protein GOX0442
GOX0443	2.27	0.0003	Molybdopterin (MPT) converting factor, subunit 2
GOX0444	2.28	0.0025	Bifunctional molybdenum cofactor biosynthesis

GOX0445	3.07	0.0001	Molybdenum cofactor biosynthesis protein C
GOX0447	1.89	0.0006	Molybdopterin biosynthesis MoeA protein
GOX0451	0.22	0.0002	30S ribosomal protein S9
GOX0452	0.31	0.0104	50S ribosomal protein L13
GOX0474	0.48	0.0185	Hypothetical protein GOX0474
GOX0475	2.16	0.0012	Hypothetical protein GOX0475
GOX0497	0.41	0.0003	Hypothetical protein GOX0497
GOX0506	4.04	0.0000	RNA polymerase factor sigma-32
GOX0512	0.32	0.0013	Amino acid transport protein
GOX0513	0.39	0.0011	Glutamate uptake regulatory protein
GOX0515	0.18	0.0001	Hypothetical protein GOX0515
GOX0516	0.49	0.0051	Uncharacterized PQQ-dependent dehydrogenase 4
GOX0522	0.33	0.0021	Transcriptional regulator LysR family
GOX0524	0.13	0.0004	TonB-dependent outer membrane receptor
GOX0527	0.55	0.0002	Alkylphosphonate uptake protein PhnA
GOX0548	1.90	0.0002	Hypothetical protein GOX0548
GOX0549	2.51	0.0014	Hypothetical protein GOX0549
GOX0560	1.93	0.0147	Diguanylate cyclase
GOX0562	0.32	0.0017	Putative siderophore receptor protein
GOX0564	2.02	0.0012	Cytochrome c precursor
GOX0565	2.49	0.0038	Ubiquinol-cytochrome c reductase iron-sulfur su
GOX0566	2.20	0.0129	Ubiquinol-cytochrome c reductase cytochrome b su
GOX0568	0.33	0.0001	Hypothetical protein GOX0568
GOX0570	2.37	0.0000	Hypothetical protein GOX0570
GOX0571	2.62	0.0041	Hypothetical protein GOX0571
GOX0572	3.61	0.0017	Putative oxidoreductase
GOX0573	4.81	0.0017	Metallo-beta-lactamase superfamily protein
GOX0576	2.80	0.0027	Hypothetical protein GOX0576
GOX0585	2.02	0.0006	Cytochrome c subunit aldehyde dehydrogenase
GOX0586	2.01	0.0012	Membrane-bound aldehyde dehydrogenase, small subunit
GOX0587	1.91	0.0025	Membrane-bound aldehyde dehydrogenase, large subunit
GOX0593	1.90	0.0080	Glycosyltransferase
GOX0596	0.41	0.0001	30S ribosomal protein S1
GOX0599	0.39	0.0006	Hypothetical protein GOX0599
GOX0600	0.40	0.0063	Hypothetical protein GOX0600
GOX0607	2.51	0.0000	D-alanyl-D-alanine carboxypeptidase
GOX0609	2.85	0.0001	ATP-dependent Clp protease ATP-binding subunit ClpA
GOX0610	0.47	0.0019	Hypothetical protein GOX0610
GOX0618	2.46	0.0150	Hemolysin-related protein
GOX0619	2.56	0.0007	Hypothetical protein GOX0619
GOX0620	2.54	0.0001	Chemotactic signal-response protein CheL
GOX0621	1.87	0.0006	Flagellar basal body P-ring protein
GOX0635	2.01	0.0278	Hypothetical protein GOX0635
GOX0636	0.54	0.0076	GTP-binding protein
GOX0647	18.22	0.0400	Hypothetical protein GOX0647
GOX0651	1.95	0.0001	Hypothetical protein GOX0651

VII Appendix

GOX0673	5.86	0.0049	Ferrous iron transport protein A (FeoA)
GOX0674	3.24	0.0140	Ferrous iron transport protein B (FeoB)
GOX0683	2.13	0.0069	Sensor histidine kinase
GOX0689	0.41	0.0009	Probable outer membrane efflux lipoprotein
GOX0690	0.40	0.0008	Acriflavin resistance protein B
GOX0691	0.39	0.0002	Acriflavin resistance protein A
GOX0694	2.53	0.0005	Hypothetical protein GOX0694
GOX0695	2.56	0.0016	Hypothetical protein GOX0695
GOX0696	1.93	0.0013	Flagellar motor switch protein FlIM
GOX0697	2.40	0.0020	Flagellar FlIL protein
GOX0699	0.16	0.0000	L-asparagine permease
GOX0708	2.18	0.0147	Hypothetical protein GOX0708
GOX0745	0.29	0.0023	Hypothetical protein GOX0745
GOX0746	2.03	0.0006	FAD-dependent monooxygenase
GOX0747	2.05	0.0097	Serine O-acetyltransferase CysE
GOX0748	0.35	0.0000	Aldose 1-epimerase
GOX0755	2.36	0.0015	Hypothetical protein in adhS 5' region
GOX0758	0.19	0.0020	Porin
GOX0762	2.10	0.0004	Thioredoxin
GOX0765	1.85	0.0011	Methyl-accepting chemotaxis protein
GOX0766	1.95	0.0008	Methyl-accepting chemotaxis protein
GOX0767	0.49	0.0037	Hypothetical protein GOX0767
GOX0769	0.56	0.0006	Apolipoprotein N-acyltransferase
GOX0771	0.49	0.0003	Ferric uptake regulation protein
GOX0772	0.16	0.0001	Transcriptional regulator
GOX0774	0.49	0.0370	Ribosomal-protein-alanine acetyltransferase
GOX0775	0.46	0.0048	Hypothetical protein GOX0775
GOX0778	0.42	0.0065	Two component sensor histidine kinase
GOX0787	3.44	0.0020	Flagellin B
GOX0788	4.23	0.0014	Flagellin assembly protein
GOX0797	0.46	0.0005	Hypothetical protein GOX0797
GOX0801	0.55	0.0017	tRNA pseudouridine synthase A
GOX0805	0.45	0.0006	Hypothetical protein GOX0805
GOX0806	0.34	0.0039	Hypothetical protein GOX0806
GOX0807	0.33	0.0061	Hypothetical protein GOX0807
GOX0811	1.99	0.0006	Transcriptional regulator Fur family
GOX0812	1.83	0.0010	Phosphoenolpyruvate-protein phosphotransferase
GOX0813	2.20	0.0055	Phosphocarrier protein HPr
GOX0814	4.10	0.0002	PTS system, IIA component
GOX0815	6.53	0.0002	Hypothetical protein GOX0815
GOX0819	0.54	0.0002	Two component response regulator ChvI
GOX0820	1.96	0.0031	GrpE protein (HSP-70 cofactor)
GOX0823	0.48	0.0003	Threonyl-tRNA synthetase
GOX0826	0.50	0.0058	Hypothetical protein GOX0826
GOX0827	0.46	0.0001	Hypothetical protein GOX0827
GOX0828	0.49	0.0001	Hypothetical protein GOX0828
GOX0834	0.50	0.0024	Putative oxidoreductase
GOX0835	0.30	0.0016	Adenine phosphoribosyltransferase
GOX0845	0.44	0.0015	Hypothetical protein GOX0845

GOX0846	0.36	0.0011	Hypothetical protein GOX0846
GOX0849	0.44	0.0021	NADPH-dependent L-sorbose reductase
GOX0853	0.52	0.0001	Lipopolysaccharide biosynthesis protein
GOX0854	0.10	0.0000	D-Sorbitol dehydrogenase subunit SldA
GOX0855	0.10	0.0001	D-Sorbitol dehydrogenase subunit SldB
GOX0857	1.81	0.0016	Chaperone protein DnaK
GOX0859	0.31	0.0004	Shikimate 5-dehydrogenase
GOX0861	2.15	0.0156	Flavohepmaprotein
GOX0866	0.18	0.0012	S-adenosylmethionine synthetase
GOX0867	0.21	0.0001	SAM-dependent methyltransferase
GOX0868	0.28	0.0001	Electron transfer flavoprotein-ubiquinone oxidoreductase
GOX0869	0.53	0.0060	Electron transfer flavoprotein beta-subunit
GOX0870	0.55	0.0091	Electron transfer flavoprotein alpha-subunit
GOX0874	2.21	0.0003	Ferrochelatase
GOX0875	2.42	0.0001	AtsE protein
GOX0880	3.00	0.0154	Hypothetical protein GOX0880
GOX0882	1.96	0.0005	Alpha-ketoglutarate decarboxylase
GOX0886	3.46	0.0011	Hypothetical protein GOX0886
GOX0890	9.60	0.0028	Hypothetical protein GOX0890
GOX0901	0.43	0.0002	Xanthine/uracil permease
GOX0902	0.45	0.0000	Hypothetical protein GOX0902
GOX0903	0.46	0.0001	Hypothetical protein GOX0903
GOX0904	0.52	0.0019	Hypothetical protein GOX0904
GOX0905	0.37	0.0007	Putative oxidoreductase
GOX0907	0.23	0.0001	TonB-dependent outer membrane receptor
GOX0909	0.45	0.0010	Thiol:disulfide interchange protein DsbD
GOX0915	2.94	0.0091	Hypothetical protein GOX0915
GOX0922	0.51	0.0024	Hypothetical protein GOX0922
GOX0925	0.50	0.0003	Sugar-proton symporter
GOX0930	0.53	0.0022	Psp operon transcriptional activator PspF
GOX0934	1.85	0.0080	Hypothetical protein GOX0934
GOX0943	0.30	0.0000	Hypothetical protein GOX0943
GOX0944	0.42	0.0005	Hypothetical protein GOX0944
GOX0945	0.11	0.0002	TonB-dependent outer membrane receptor
GOX0946	2.29	0.0029	Putative oxidoreductase
GOX0952	2.79	0.0002	Flagellar basal P-ring biosynthesis protein FigA
GOX0953	3.54	0.0001	Flagellar basal body rod protein FigG
GOX0954	4.26	0.0014	Flagellar basal-body rod protein FigF
GOX0960	2.32	0.0000	Sensory box/GGDEF family protein
GOX0969	0.32	0.0000	Hypothetical protein GOX0969
GOX0970	0.49	0.0001	Outer membrane channel lipoprotein
GOX0971	0.49	0.0007	Cation efflux system protein CzcA
GOX0972	0.44	0.0012	Cation efflux system protein CzcB
GOX0973	3.39	0.0001	Outer membrane channel lipoprotein
GOX0976	0.51	0.0008	Deoxyribodipyrimidine photolyase
GOX0978	0.33	0.0020	Bifunctional riboflavin biosynthesis protein RibD
GOX0979	0.43	0.0015	Riboflavin synthase subunit alpha
GOX0980	0.35	0.0023	3,4-Dihydroxy-2-butanone 4-phosphate

VII Appendix

			synthase/GTP cyclohydrolase II
GOX0981	0.44	0.0008	6,7-Dimethyl-8-ribityllumazine synthase
GOX0984	0.51	0.0000	Coenzyme PQQ synthesis protein D
GOX0986	0.37	0.0000	Pyrrroloquinoline synthone biosynthesis protein PqqB
GOX0987	0.44	0.0038	Coenzyme PQQ synthesis protein A
GOX0990	0.56	0.0007	ATP phosphoribosyltransferase catalytic subunit
GOX0996	2.34	0.0017	Transposase (class II)
GOX1000	1.96	0.0328	Hypothetical protein GOX1000
GOX1003	0.44	0.0014	Septum formation associated protein (Maf-like protein)
GOX1010	0.54	0.0002	Levanase precursor
GOX1015	0.42	0.0013	TonB-dependent receptor of ferrichrome transport system
GOX1017	0.11	0.0001	TonB-dependent outer membrane receptor
GOX1022	0.41	0.0060	Transcriptional regulator
GOX1024	2.63	0.0000	Heat shock protein 90
GOX1025	3.69	0.0043	Flagellar hook-associated protein FlgL
GOX1026	2.76	0.0049	Flagellar hook-associated protein 1 FlgK
GOX1027	2.83	0.0022	Flagellar hook protein FlgE
GOX1029	0.47	0.0041	Hypothetical protein GOX1029
GOX1038	1.87	0.0027	Septum formation associated protein (Maf-like protein)
GOX1041	1.81	0.0005	Hypothetical protein GOX1041
GOX1070	0.46	0.0075	Transcription termination factor Rho
GOX1087	0.34	0.0003	Acetolactate synthase large subunit
GOX1088	0.35	0.0001	Acetolactate synthase 3 regulatory subunit
GOX1089	0.37	0.0006	Ketol-acid reductoisomerase
GOX1090	0.27	0.0006	S-adenosylmethionine decarboxylase proenzyme
GOX1091	0.11	0.0003	Spermidine synthase
GOX1092	0.51	0.0000	Transcriptional regulator MarR family
GOX1099	1.86	0.0003	Hypothetical protein GOX1099
GOX1107	3.16	0.0009	O-antigen biosynthesis protein RfbC
GOX1108	0.49	0.0007	Hypothetical protein GOX1108
GOX1110	0.48	0.0032	ATP synthase B' chain
GOX1111	0.40	0.0055	ATP synthase B' chain
GOX1112	0.51	0.0027	ATP synthase C chain
GOX1114	0.31	0.0001	Vitamin B12-dependent ribonucleotide reductase
GOX1131	2.17	0.0001	Pyrrroline-5-carboxylate reductase
GOX1132	3.01	0.0015	Hypothetical protein GOX1132
GOX1137	0.44	0.0014	Probable lipopolysaccharide modification acyltransferase
GOX1138	0.52	0.0051	Catalase
GOX1141	0.31	0.0002	LSU ribosomal protein L25P
GOX1142	0.31	0.0008	Peptidyl-tRNA hydrolase
GOX1151	0.54	0.0016	Hypothetical protein GOX1151
GOX1173	0.39	0.0014	Outer membrane heme receptor
GOX1174	0.49	0.0079	Purine-cytosine permease
GOX1176	0.50	0.0001	Hypothetical protein GOX1176
GOX1179	0.44	0.0003	Putative sugar uptake ABC transporter permease

GOX1190	2.07	0.0036	Glucose-1-phosphatase
GOX1192	0.49	0.0070	Probable transcriptional regulator
GOX1197	0.22	0.0006	Hypothetical protein GOX1197
GOX1198	0.25	0.0003	Sulfite reductase (Ferredoxin)
GOX1199	0.35	0.0014	Putative oxidoreductase
GOX1230	0.23	0.0003	Gluconate 2-dehydrogenase, cytochrome c subunit
GOX1231	0.19	0.0001	Gluconate 2-dehydrogenase alpha chain
GOX1232	0.26	0.0002	Gluconate 2-dehydrogenase gamma chain
GOX1235	0.55	0.0098	Heat shock protein HSP33
GOX1236	0.33	0.0009	Ornithine carbamoyltransferase
GOX1237	0.35	0.0010	Acetylmornithine aminotransferase
GOX1238	1.87	0.0029	D-aminopeptidase
GOX1239	2.32	0.0032	Hypothetical protein GOX1239
GOX1244	0.44	0.0004	Putative enolase-phosphatase
GOX1245	0.45	0.0034	Riboflavin kinase
GOX1246	2.33	0.0817	TonB-dependent receptor protein
GOX1247	1.92	0.0022	Hypothetical protein GOX1247
GOX1248	2.28	0.0014	Hypothetical protein GOX1248
GOX1269	0.29	0.0002	Hypothetical protein GOX1269
GOX1273	2.26	0.0016	Hypothetical protein GOX1273
GOX1280	1.82	0.0050	Hypothetical protein GOX1280
GOX1282	0.48	0.0004	Ribonuclease PH
GOX1286	0.16	0.0004	Hypothetical protein GOX1286
GOX1287	0.12	0.0004	Biopolymer transport ExbB protein
GOX1288	0.16	0.0000	Biopolymer transport ExbD protein
GOX1289	0.18	0.0004	Biopolymer transport ExbD protein
GOX1290	0.39	0.0000	Hypothetical protein GOX1290
GOX1291	1.82	0.0054	Flagellar basal body L-ring protein
GOX1302	2.16	0.0028	Paraquat-inducible protein A
GOX1303	1.96	0.0004	Paraquat-inducible protein B
GOX1313	0.51	0.0111	F0F1 ATP synthase subunit beta
GOX1314	0.50	0.0030	ATP synthase epsilon chain
GOX1322	2.25	0.0135	Transposase (class I)
GOX1329	5.29	0.0003	Small heat shock protein
GOX1335	0.13	0.0002	Aconitate hydratase
GOX1336	0.17	0.0002	Isocitrate dehydrogenase
GOX1351	0.29	0.0002	Putative isomerase
GOX1352	0.54	0.0013	Ribulose-phosphate 3-epimerase
GOX1355	2.27	0.0102	Hypothetical protein GOX1355
GOX1359	2.59	0.0024	Excinuclease ABC subunit A
GOX1360	1.82	0.0038	Hypothetical protein GOX1360
GOX1365	0.33	0.0000	ABC transporter permease protein
GOX1366	0.33	0.0000	ABC transporter ATP-binding protein
GOX1370	0.52	0.0060	Ferredoxin, 2Fe-2S
GOX1381	0.39	0.0003	Gluconolactonase
GOX1392	0.49	0.0000	Hypothetical protein GOX1392
GOX1414	2.18	0.0052	Chaperone protein DnaJ
GOX1416	0.15	0.0003	Porin B precursor
GOX1417	0.52	0.0002	Ferrichrome receptor FcuA

VII Appendix

GOX1418	0.19	0.0000	Carbohydrate-selective porin
GOX1424	2.26	0.0045	Hypothetical protein GOX1424
GOX1432	0.46	0.0014	NADP-D-sorbitol dehydrogenase
GOX1433	1.99	0.0005	Putative DnaJ-like protein
GOX1434	0.56	0.0107	Hypothetical protein GOX1434
GOX1436	0.44	0.0004	Adenosine deaminase
GOX1440	0.49	0.0023	S-adenosylmethionine:tRNA ribosyltransferase-isomerase
GOX1442	8.96	0.0007	Hypothetical protein GOX1442
GOX1449	1.82	0.0022	Hypothetical protein GOX1449
GOX1455	0.27	0.0004	ATP-dependent RNA helicase
GOX1462	2.69	0.0051	Putative oxidoreductase
GOX1463	3.42	0.0011	ATP-dependent Clp protease, ATP-binding subunit ClpB
GOX1483	0.50	0.0002	Capsule polysaccharide export protein
GOX1486	0.53	0.0065	Capsule polysaccharide export ATP-binding protein
GOX1489	0.55	0.0009	Putative glycosyltransferase
GOX1490	0.50	0.0001	Putative glycosyltransferase
GOX1500	4.07	0.0003	Hypothetical protein GOX1500
GOX1501	3.88	0.0000	Hypothetical protein GOX1501
GOX1509	1.85	0.0042	Hypothetical protein GOX1509
GOX1516	0.38	0.0040	Fructose 1,6-bisphosphatase II
GOX1521	2.07	0.0012	Hypothetical protein GOX1521
GOX1525	2.18	0.0030	Flagellar biosynthetic protein FliQ
GOX1526	2.55	0.0006	Flagellar hook-basal body protein FliE
GOX1527	2.65	0.0031	Flagellar basal body rod protein FlgC
GOX1528	3.41	0.0062	Flagellar basal-body rod protein FlgB
GOX1541	0.53	0.0034	Hypothetical protein GOX1541
GOX1542	0.40	0.0002	Putative aluminum resistance protein
GOX1543	0.43	0.0011	Hypothetical protein GOX1543
GOX1549	2.06	0.0006	Methyl-accepting chemotaxis protein
GOX1550	2.32	0.0003	Chemotaxis protein CheX
GOX1551	2.16	0.0001	Chemotaxis protein CheY
GOX1552	1.98	0.0004	Chemotaxis protein CheA
GOX1560	1.89	0.0013	Hypothetical protein GOX1560
GOX1563	0.21	0.0044	Hypothetical protein GOX1563
GOX1567	0.48	0.0008	DedA family protein
GOX1569	0.40	0.0003	Tricorn protease homolog
GOX1572	0.43	0.0004	Amino acid ABC transporter ATP-binding protein
GOX1573	0.53	0.0047	Amino acid ABC transporter binding protein and permease protein
GOX1576	2.70	0.0023	Transposase (class II)
GOX1577	2.82	0.0000	ATP-dependent Clp protease ATP-binding subunit ClpA
GOX1578	2.92	0.0015	Hypothetical protein GOX1578
GOX1579	0.39	0.0015	Hypothetical protein associated with nus operon
GOX1582	0.51	0.0008	Translation initiation factor IF-2
GOX1587	0.53	0.0071	Putative 2-nitropropane dioxygenase
GOX1593	0.52	0.0002	Nucleoside hydrolase

GOX1613	3.78	0.0019	Sensory box/GDEF family protein
GOX1617	2.32	0.0004	Hypothetical protein GOX1617
GOX1628	2.00	0.0023	Protease
GOX1636	4.60	0.0016	5-aminolevulinatase synthase
GOX1639	0.51	0.0004	Hypothetical protein GOX1639
GOX1641	0.52	0.0001	Bacteriophytochrome protein
GOX1642	0.20	0.0000	Carboxypeptidase-related protein
GOX1645	0.51	0.0004	Hypothetical protein GOX1645
GOX1646	0.55	0.0042	Hypothetical protein GOX1646
GOX1654	2.39	0.0004	Hypothetical protein GOX1654
GOX1662	0.39	0.0067	Hypothetical protein GOX1662
GOX1664	2.22	0.0022	Recombination factor protein RarA
GOX1671	0.29	0.0041	O-succinylhomoserine sulfhydrylase
GOX1675	0.37	0.0000	NADH dehydrogenase type II
GOX1688	3.06	0.0000	Peptidoglycan-associated lipoprotein
GOX1689	1.99	0.0011	Hypothetical protein GOX1689
GOX1697	2.44	0.0059	Hypothetical protein GOX1697
GOX1698	2.00	0.0089	Aminopeptidase
GOX1699	0.27	0.0004	Hypothetical protein GOX1699
GOX1703	0.47	0.0089	Transketolase
GOX1704	0.44	0.0163	Bifunctional transaldolase/phosphoglucose isomerase
GOX1705	0.44	0.0228	6-phosphogluconate dehydrogenase-like protein
GOX1719	1.85	0.0024	Adenine deaminase
GOX1734	0.55	0.0007	Hypothetical protein GOX1734
GOX1736	0.47	0.0032	Hypothetical protein GOX1736
GOX1742	2.37	0.0094	Hypothetical protein GOX1742
GOX1745	2.13	0.0026	Hypothetical protein GOX1745
GOX1747	0.55	0.0007	Aaspartyl-tRNA synthetase
GOX1752	2.27	0.0001	Deoxyguanosinetriphosphate triphosphohydrolase
GOX1768	2.22	0.0038	Alkylated DNA repair protein AlkB
GOX1773	3.29	0.0019	Putative LacX protein
GOX1774	4.03	0.0002	Putative ATP-sensitive potassium channel protein
GOX1775	1.99	0.0012	SpoJ rRNA methylase family protein
GOX1779	6.93	0.0000	Putative LysM domain protein
GOX1780	0.27	0.0005	30S ribosomal protein S4
GOX1781	0.18	0.0009	Bacterial Peptide Chain Release Factor 3
GOX1796	0.45	0.0049	TonB-dependent outer membrane receptor
GOX1814	0.50	0.0023	Undecaprenyl pyrophosphate synthetase
GOX1815	0.45	0.0111	Phosphatidate cytidyltransferase
GOX1827	0.51	0.0012	Putative inner membrane protein translocase component YidC
GOX1828	0.44	0.0001	GTPase EngB
GOX1829	0.49	0.0021	Acetylglutamate kinase
GOX1832	0.43	0.0013	Succinyl-diaminopimelate desuccinylase
GOX1834	0.50	0.0001	tRNA pseudouridine synthase A
GOX1841	3.32	0.0002	Hypothetical protein GOX1841
GOX1851	0.19	0.0002	Putative oxidoreductase
GOX1852	0.23	0.0004	Glutamate synthase
GOX1857	0.12	0.0001	Uncharacterized PQQ-containing DH1

VII Appendix

GOX1858	2.02	0.0007	Hypothetical protein GOX1858
GOX1861	0.53	0.0037	glutathione synthetase
GOX1863	3.42	0.0003	Hypothetical protein GOX1863
GOX1864	2.97	0.0016	Protoheme IX farnesyltransferase
GOX1870	2.32	0.0320	Hypothetical protein GOX1870
GOX1873	0.41	0.0007	DNA mismatch repair protein
GOX1875	2.05	0.0012	Hypothetical protein GOX1875
GOX1883	2.13	0.0011	Porphobilinogen deaminase
GOX1890	1.90	0.0021	Hypothetical protein GOX1890
GOX1895	4.12	0.0015	Hypothetical protein GOX1895
GOX1896	6.43	0.0017	Coproporphyrinogen III oxidase
GOX1898	2.08	0.0012	Hypothetical protein GOX1898
GOX1900	2.09	0.0163	Putative carboxymethylenebutenolidase
GOX1903	0.12	0.0001	TonB-dependent receptor protein
GOX1911	2.82	0.0016	Cytochrome <i>o</i> ubiquinol oxidase subunit II
GOX1912	2.70	0.0105	Cytochrome <i>o</i> ubiquinol oxidase subunit I
GOX1913	3.56	0.0000	Cytochrome <i>o</i> ubiquinol oxidase subunit III
GOX1914	3.81	0.0040	Cytochrome <i>o</i> ubiquinol oxidase subunit IV
GOX1917	2.12	0.0152	ATP-dependent DNA helicase
GOX1923	2.06	0.0016	Hypothetical protein GOX1923
GOX1928	2.94	0.0000	Hypothetical protein GOX1928
GOX1942	2.25	0.0008	Hypothetical protein GOX1942
GOX1951	2.42	0.0036	Hypothetical protein GOX1951
GOX1953	7.10	0.0004	5-Methylcytosine-specific restriction enzyme
GOX1957	0.40	0.0000	Putative thiol:disulfide interchange protein II
GOX1971	0.26	0.0009	Galactose-proton symporter
GOX1972	0.27	0.0009	Putative transport protein
GOX1980	1.82	0.0033	Putative corrin/porphyrin methyltransferase
GOX1982	0.25	0.0001	Hypothetical protein GOX1982
GOX1988	5.54	0.0006	Pyridoxamine 5'-phosphate oxidase
GOX1992	2.73	0.0000	Osmotically inducible protein C
GOX1994	0.51	0.0079	Ribonucleotide-diphosphate reductase subunit beta
GOX1995	2.52	0.0016	Hypothetical protein GOX1995
GOX1999	0.50	0.0008	Citrate synthase
GOX2010	0.40	0.0454	1-Acyl-sn-glycerol-3-phosphate acyltransferase
GOX2015	0.44	0.0031	NAD(P)-dependent glucose 1-dehydrogenase
GOX2028	0.17	0.0001	Hypothetical protein GOX2028
GOX2030	0.16	0.0045	Chaperone protein DnaK
GOX2039	0.41	0.0024	Acyl-carrier-protein S-malonyltransferase
GOX2041	0.47	0.0008	Acyl carrier protein
GOX2042	0.55	0.0161	3-Oxoacyl-(acyl carrier protein) synthase II
GOX2051	2.52	0.0024	Hypothetical protein GOX2051
GOX2052	2.83	0.0064	Hypothetical protein GOX2052
GOX2053	2.34	0.0339	Hypothetical protein GOX2053
GOX2062	0.51	0.0036	Hypothetical protein GOX2062
GOX2063	2.38	0.0002	Hypothetical protein GOX2063
GOX2066	8.58	0.0013	Glutaminase
GOX2069	2.94	0.0014	Transcriptional regulator
GOX2071	0.52	0.0027	D-Lactate dehydrogenase

GOX2073	0.39	0.0031	Formyltetrahydrofolate deformylase
GOX2074	0.41	0.0000	5-Methyltetrahydrofolate-S-homocysteine methyltransferase
GOX2109	1.80	0.0015	Hypothetical protein GOX2109
GOX2134	0.40	0.0001	Peptidyl-dipeptidase DCP
GOX2135	0.47	0.0000	Hypothetical protein GOX2135
GOX2136	0.47	0.0010	Aminopeptidase
GOX2142	0.45	0.0000	Hypothetical protein GOX2142
GOX2143	0.38	0.0012	ABC transporter ATP-binding protein
GOX2147	0.50	0.0061	Endonuclease
GOX2151	0.42	0.0021	Hypothetical protein GOX2151
GOX2152	2.58	0.0007	Hypothetical protein GOX2152
GOX2153	2.63	0.0020	Hypothetical protein GOX2153
GOX2163	3.04	0.0001	Cold shock protein
GOX2165	2.11	0.0090	Transposase (class II)
GOX2167	2.81	0.0044	F ₀ F ₁ ATP synthase subunit beta
GOX2168	3.14	0.0035	ATP synthase epsilon chain
GOX2169	2.79	0.0049	ATP synthase subunit Atpl
GOX2170	3.13	0.0139	Transmembrane protein
GOX2171	3.30	0.0076	ATP synthase subunit a
GOX2172	2.99	0.0007	ATP synthase subunit c
GOX2173	2.64	0.0062	ATP synthase subunit b
GOX2174	2.38	0.0084	F ₀ F ₁ ATP synthase subunit alpha
GOX2175	1.96	0.0089	ATP synthase gamma chain
GOX2187	0.44	0.0006	Gluconate 5-dehydrogenase
GOX2199	5.62	0.0000	Probable myosin-crossreactive antigen
GOX2200	5.37	0.0000	Probable myosin-crossreactive antigen
GOX2205	2.02	0.0083	Hypothetical protein GOX2205
GOX2206	2.00	0.0042	5-methyltetrahydropteroyltriglutamate--homocysteine methyltransferase
GOX2207	2.20	0.0119	Methylenetetrahydrofolate reductase
GOX2209	2.05	0.0218	Truncated transposase (class I)
GOX2225	2.10	0.0001	Thiamine biosynthesis protein ThiC
GOX2228	1.90	0.0000	Thiamine-phosphate pyrophosphorylase
GOX2237	1.98	0.0005	Protein translocase subunit SecB
GOX2243	1.88	0.0015	Hypothetical protein GOX2243
GOX2246	3.52	0.0001	Hypothetical protein GOX2246
GOX2248	1.82	0.0009	Hypothetical protein GOX2248
GOX2252	2.60	0.0001	Hypothetical protein GOX2252
GOX2253	2.46	0.0001	Putative oxidoreductase
GOX2255	1.84	0.0002	Hypothetical protein GOX2255
GOX2256	0.52	0.0040	Putative aminotransferase
GOX2258	0.45	0.0004	Putative phytoene synthase
GOX2260	0.42	0.0005	Squalene-hopene cyclase
GOX2272	2.51	0.0002	Membrane-bound dipeptidase
GOX2274	2.83	0.0001	CDP-diacylglycerol-glycerol-3-phosphate 3-phosphatidyltransferase
GOX2278	2.53	0.0001	Hypothetical protein GOX2278
GOX2293	0.51	0.0055	Lipoyl synthase

VII Appendix

GOX2299	0.49	0.0027	Adenylosuccinate lyase
GOX2308	3.08	0.0000	Delta-aminolevulinic acid dehydratase
GOX2310	0.54	0.0068	Serine hydroxymethyl transferase
GOX2311	2.03	0.0014	Hypothetical protein GOX2311
GOX2313	1.97	0.0027	Lipopolysaccharide core biosynthesis mannosyltransferase
GOX2326	3.03	0.0003	Hypothetical protein GOX2326
GOX2366	2.04	0.0148	Hypothetical protein GOX2366
GOX2373	3.72	0.0018	Ring-hydroxylating dioxygenase
GOX2376	0.44	0.0033	Putative aldehyde dehydrogenase
GOX2379	3.62	0.0003	Hypothetical protein GOX2379
GOX2386	1.88	0.0012	Hypothetical protein GOX2386
GOX2392	1.86	0.0054	DNA repair protein RadC
GOX2397	2.32	0.0004	Small heat shock protein
GOX2398	0.55	0.0064	50S ribosomal protein L31
GOX2401	0.48	0.0002	Protein-export membrane protein
GOX2402	0.39	0.0025	Preprotein translocase subunit SecD
GOX2406	2.53	0.0034	Putative RNA polymerase sigma-E factor protein 1
GOX2408	0.53	0.0082	Putative sensory transduction histidine kinase
GOX2409	2.26	0.0000	Transport ATP-binding protein CydD
GOX2410	2.48	0.0030	Transport ATP-binding protein CydD
GOX2413	3.24	0.0003	Hypothetical protein GOX2413
GOX2443	1.95	0.0008	Hypothetical protein GOX2443
GOX2455	2.55	0.0036	Putative phage-related protein
GOX2457	2.75	0.0006	Phage DNA Packaging Protein
GOX2461	2.19	0.0070	Hypothetical protein GOX2461
GOX2470	2.54	0.0048	Hypothetical protein GOX2470
GOX2471	2.32	0.0100	Putative transcriptional regulator
GOX2487	3.80	0.0008	Outer membrane protein TolC
GOX2488	2.35	0.0002	Hypothetical protein GOX2488
GOX2491	0.35	0.0002	Dihydroxy-acid dehydratase
GOX2494	1.87	0.0046	Hypothetical protein GOX2494
GOX2500	2.13	0.0011	Formamidopyrimidine-DNA glycosylase

Locus tag	Ratio pH4/pH6	p-value	Annotation
GOX0013	1.96	0.0052	Hypothetical protein GOX0013
GOX0204	0.39	0.0349	Hypothetical protein GOX0204
GOX0207	0.22	0.0023	TonB-dependent outer membrane receptor
GOX0208	0.43	0.0473	Putative glucarate/galactarate transporter
GOX0209	0.42	0.0036	Hypothetical protein GOX0209
GOX0210	0.44	0.0049	Putative carboxylase
GOX0211	0.40	0.0033	Hypothetical protein GOX0211
GOX0212	0.44	0.0062	Biotin carboxyl carrier protein of acetyl-CoA carboxylase
GOX0213	0.47	0.0016	Biotin carboxylase
GOX0216	0.48	0.0007	N-methylhydantoinase A
GOX0244	2.19	0.0458	Hypothetical membrane-spanning protein
GOX0278	2.22	0.0111	Cytochrome d ubiquinol oxidase subunit I
GOX0291	2.34	0.0009	Putative ferredoxin subunit of ring-hydroxylating dioxygenase

GOX2520	4.15	0.0010	Hypothetical protein GOX2520
GOX2536	1.85	0.0072	Hypothetical protein GOX2536
GOX2546	0.42	0.0039	Replication protein A
GOX2547	0.52	0.0008	Replication protein B
GOX2560	0.49	0.0029	RND-type multidrug efflux pump, membrane permease
GOX2561	0.50	0.0012	RND-type multidrug efflux pump, outer membrane protein
GOX2571	1.83	0.0042	Hypothetical protein GOX2571
GOX2578	0.46	0.0019	Putative isochorismatase
GOX2579	0.51	0.0011	Transcriptional regulator
GOX2580	0.42	0.0003	Hypothetical protein GOX2580
GOX2603	0.42	0.0007	Replicator initiator RepC
GOX2616	0.35	0.0041	DotI
GOX2646	3.15	0.0021	DNA integration/recombination/inversion protein
GOX2647	2.15	0.0000	Hydroxyacylglutathione hydrolase
GOX2649	1.84	0.0028	LysR family transcriptional regulator
GOX2650	1.82	0.0103	Putative C4-dicarboxylate transport protein
GOX2659	2.38	0.0009	Transposase
GOX2660	1.91	0.0027	Transposase
GOX2662	1.95	0.0024	Hypothetical protein GOX2662
GOX2668	1.93	0.0032	MucR family transcriptional regulator
GOX2675	2.47	0.0003	Transposase
GOX2684	3.17	0.0001	NAD(P)H-dependent 2-cyclohexen-1-one reductase
GOX2685	2.77	0.0021	Transposase
GOX2698	1.85	0.0007	Hypothetical protein GOX2698
GOX2699	2.17	0.0000	Hypothetical protein GOX2699
GOX2701	0.51	0.0062	DNA integration/recombination/inversion protein
GOX2719	10.98	0.0001	Transposase
GOX2720	12.34	0.0002	Hypothetical protein GOX2720
GOX2725	1.94	0.0079	Hypothetical protein GOX2725
GOX2733	2.00	0.0074	Hypothetical protein GOX2733

GOX0352	2.20	0.0262	Hypothetical protein GOX0352
GOX0433	2.50	0.0045	Hypothetical protein GOX0433
GOX0470	2.24	0.0339	Putative peroxidase
GOX0497	2.31	0.0005	Hypothetical protein GOX0497
GOX0524	0.19	0.0087	TonB-dependent outer membrane receptor
GOX0553	2.75	0.0065	Hypothetical protein GOX0553
GOX0576	2.11	0.0250	Hypothetical protein GOX0576
GOX0647	12.91	0.0015	Hypothetical protein GOX0647
GOX0652	0.34	0.0276	Xanthine dehydrogenase Xdh C protein
GOX0653	0.34	0.0009	Xanthine dehydrogenase XdhB protein
GOX0679	3.20	0.0443	Conserved protein of the SAM superfamily
GOX0707	3.47	0.0421	DNA starvation/stationary phase protection protein Dps
GOX0726	2.76	0.0088	Hypothetical protein GOX0726
GOX0756	1.83	0.0155	Alcohol dehydrogenase 15 kDa subunit
GOX0768	0.49	0.0214	Transcriptional regulator

VII Appendix

GOX0902	0.47	0.0282	Hypothetical protein GOX0902
GOX0903	0.33	0.0018	Hypothetical protein GOX0903
GOX0904	0.44	0.0021	Hypothetical protein GOX0904
GOX0907	0.34	0.0020	TonB-dependent outer membrane receptor
GOX0943	3.13	0.0094	Hypothetical protein GOX0943
GOX0944	2.48	0.0199	Hypothetical protein GOX0944
GOX0945	0.35	0.0236	TonB-dependent outer membrane receptor
GOX1017	0.31	0.0049	TonB-dependent outer membrane receptor
GOX1068	2.40	0.0610	Alcohol dehydrogenase large subunit
GOX1082	1.91	0.0387	Hypothetical protein GOX1082
GOX1138	2.10	0.0017	Catalase
GOX1173	0.40	0.0490	Outer membrane heme receptor
GOX1209	0.36	0.0182	Hypothetical protein GOX1209
GOX1210	0.25	0.0460	Hypothetical protein GOX1210
GOX1225	0.47	0.0081	Putative phage tail protein
GOX1276	2.02	0.0161	Organophosphate acid anhydrase
GOX1335	0.49	0.0020	Aconitate hydratase
GOX1336	0.45	0.0223	Isocitrate dehydrogenase
GOX1351	2.10	0.0293	Putative isomerase
GOX1374	3.02	0.0036	DNA topoisomerase I
GOX1462	2.10	0.0054	Putative oxidoreductase
GOX1494	1.86	0.0074	Putative oxidoreductase
GOX1495	1.93	0.0059	Oxidoreductase, iron-sulphur binding subunit
GOX1538	2.02	0.0290	Short chain dehydrogenase
GOX1615	2.54	0.0150	Putative oxidoreductase
GOX1660	0.35	0.0391	Hypothetical protein GOX1660
GOX1712	2.15	0.0049	Aldehyde dehydrogenase
GOX1713	2.08	0.0014	Protease I
GOX1748	3.37	0.0020	Bacterioferritin
GOX1749	0.37	0.0140	Hypothetical protein GOX1749
GOX1784	0.33	0.0015	Hypothetical protein GOX1784
GOX1785	0.37	0.0009	Carbonic anhydrase
GOX1841	3.36	0.0255	Hypothetical protein GOX1841
GOX1851	0.39	0.0004	Putative oxidoreductase
GOX1852	0.35	0.0040	Glutamate synthase
GOX1857	0.40	0.0097	Uncharacterized PQQ-containing dehydrogenase 1
GOX1903	0.42	0.0005	TonB-dependent receptor protein
GOX1951	2.27	0.0019	Hypothetical protein GOX1951
GOX1961	0.54	0.0338	DNA polymerase III, epsilon chain
GOX1982	0.36	0.0039	Hypothetical protein GOX1982
GOX1992	2.01	0.0072	Osmotically inducible protein C
GOX2017	0.31	0.0117	Hypothetical protein GOX2017
GOX2079	2.13	0.0015	Hypothetical protein GOX2079
GOX2083	2.15	0.0236	Hypothetical protein GOX2083
GOX2092	0.22	0.0006	Bacterial ring hydroxylating dioxygenase alpha-subunit
GOX2096	2.21	0.0016	Sorbitol dehydrogenase large subunit
GOX2097	2.22	0.0128	Sorbitol dehydrogenase small subunit
GOX2256	0.41	0.0087	Putative aminotransferase
GOX2676	2.45	0.0247	Putative alcohol/aldehyde dehydrogenase

Locus tag	Ratio Glucanate / Glucose	p-value	Annotation
GOX0016	0.55	0.0140	Methionyl-tRNA synthetase
GOX0017	0.44	0.0004	DNA polymerase III delta prime subunit DnaC
GOX0018	0.38	0.0029	Thymidylate kinase
GOX0024	0.46	0.0132	Undecaprenyl pyrophosphate phosphatase
GOX0025	0.45	0.0020	Amino acid permease
GOX0032	0.39	0.0027	Bacterial Peptide Chain Release Factor 1 (RF-1)
GOX0035	0.31	0.0239	Hypothetical protein GOX0035
GOX0037	0.53	0.0028	Aspartate kinase
GOX0042	0.55	0.0137	Competence protein F
GOX0053	2.32	0.0074	Hypothetical protein GOX0053
GOX0074	0.51	0.0164	Elongation factor Ts
GOX0075	0.47	0.0011	30S ribosomal protein S2
GOX0077	0.46	0.0012	Lipoprotein releasing system ATP-binding protein
GOX0079	0.53	0.0052	Prolyl-tRNA synthetase
GOX0088	0.49	0.0011	Trigger factor
GOX0090	2.39	0.0438	Putative sugar kinase
GOX0092	0.54	0.0121	ATP-dependent RNA helicase
GOX0093	0.42	0.0028	tRNA (Uracil-5-) -methyltransferase
GOX0103	0.30	0.0001	Carboxypeptidase-related protein
GOX0105	0.38	0.0002	Protein Translation Elongation Factor G (EF-G)
GOX0106	0.32	0.0036	50S ribosomal protein L28
GOX0107	0.49	0.0036	ABC transporter ATP-binding protein
GOX0109	0.35	0.0037	Putative thiamin pyrophosphokinase
GOX0111	0.48	0.0023	Putative permease
GOX0116	0.25	0.0137	Fatty acid/phospholipid synthesis protein
GOX0117	0.45	0.0001	50S ribosomal protein L32
GOX0128	0.52	0.0033	Hypothetical protein GOX0128
GOX0129	0.47	0.0125	Dolichol-phosphate mannosyltransferase
GOX0132	0.24	0.0001	Transcriptional regulator, LysR family
GOX0135	2.45	0.0347	Transcriptional regulator
GOX0143	0.45	0.0133	Hypothetical protein GOX0143
GOX0145	2.75	0.0197	Glucose-6-phosphate 1-dehydrogenase
GOX0146	2.42	0.0019	Hypothetical protein GOX0146
GOX0155	0.48	0.0080	Phospho-N-acetylmuramoyl-pentapeptide-transferase
GOX0156	0.50	0.0056	UDP-N-acetylmuramoylalanine-D-glutamate ligase
GOX0159	0.41	0.0027	UDP-N-acetylmuramate--L-alanine ligase
GOX0160	0.33	0.0019	UDP-N-acetylenolpyruvoylglucosamine reductase
GOX0161	0.52	0.0046	D-alanine-D-alanine ligase
GOX0162	0.37	0.0096	Cell division protein FtsQ
GOX0163	0.44	0.0025	Cell division protein FtsA
GOX0168	0.54	0.0241	NAD-dependent DNA ligase
GOX0174	0.47	0.0002	Xanthine-guanine phosphoribosyltransferase
GOX0181	0.41	0.0345	Oligopeptide transporter
GOX0189	0.32	0.0109	Aspartate aminotransferase A
GOX0190	0.33	0.0013	Aspartate aminotransferase A

VII Appendix

GOX0191	0.46	0.0051	3-Isopropylmalate dehydrogenase
GOX0192	0.43	0.0060	3-Isopropylmalate dehydratase, small subunit
GOX0193	0.36	0.0250	Isopropylmalate isomerase large subunit
GOX0194	0.42	0.0056	50S ribosomal protein L19
GOX0195	0.39	0.0063	tRNA (Guanine-N(1)-)-methyltransferase
GOX0196	0.41	0.0026	30S ribosomal protein S16
GOX0197	0.45	0.0033	Signal recognition particle protein
GOX0198	4.13	0.0038	Hypothetical protein GOX0198
GOX0200	0.48	0.0051	ATP-dependent RNA helicase
GOX0207	0.32	0.0300	TonB-dependent outer membrane receptor
GOX0218	0.51	0.0102	D-3-phosphoglycerate dehydrogenase
GOX0235	4.68	0.0008	Hypothetical protein GOX0235
GOX0254	0.44	0.0001	Putative Fe-S-cluster redox enzyme
GOX0255	0.48	0.0187	Argininosuccinate synthase
GOX0258	0.52	0.0062	Putative cytochrome c-552
GOX0263	0.43	0.0353	50S ribosomal protein L20
GOX0278	2.70	0.0012	Cytochrome <i>d</i> ubiquinol oxidase subunit I
GOX0286	0.51	0.0498	Hypothetical protein GOX0286
GOX0288	0.45	0.0602	Hypothetical protein GOX0288
GOX0289	0.52	0.0294	Hypothetical protein GOX0289
GOX0290	2.03	0.0086	Putative oxidoreductase
GOX0302	0.51	0.0014	Dimethyladenosine transferase
GOX0303	2.23	0.0054	Cyclopropane-fatty-acyl-phospholipid synthase
GOX0304	0.45	0.0043	50S ribosomal protein L9
GOX0305	0.55	0.0112	30S ribosomal protein S18
GOX0306	0.50	0.0102	SSU ribosomal protein S6P
GOX0310	4.38	0.0003	NAD(P) transhydrogenase subunit alpha
GOX0311	6.02	0.0037	NAD(P) transhydrogenase subunit alpha
GOX0312	5.06	0.0015	NAD(P) transhydrogenase subunit beta
GOX0313	5.53	0.0007	NAD-dependent alcohol dehydrogenase
GOX0314	4.84	0.0009	Probable alcohol dehydrogenase-like oxidoreductase protein
GOX0318	1.83	0.0163	Hypothetical protein GOX0318
GOX0319	2.22	0.0053	Putative oxidoreductase
GOX0321	0.56	0.0081	Carbamoyl phosphate synthase small subunit
GOX0326	2.91	0.0004	Hypothetical protein GOX0326
GOX0329	2.28	0.0033	Stress response protein CsbD
GOX0336	2.19	0.0132	Poly(A) polymerase/t-RNA nucleotidyltransferase
GOX0337	3.09	0.0003	Hypothetical protein GOX0337
GOX0339	0.47	0.0000	Hypothetical protein GOX0339
GOX0344	0.49	0.0097	Adenine DNA methyltransferase
GOX0345	0.35	0.0009	Ribonuclease HII
GOX0347	2.04	0.0078	Hypothetical protein GOX0347
GOX0350	0.53	0.0070	Acriflavin resistance protein F
GOX0354	0.24	0.0003	Putative sugar/polyol transporter
GOX0355	0.44	0.0016	LSU ribosomal protein L17P
GOX0356	0.40	0.0072	DNA-directed RNA polymerase subunit alpha
GOX0357	0.41	0.0218	30S ribosomal protein S11
GOX0358	0.41	0.0135	30S ribosomal protein S13
GOX0359	0.39	0.0048	Adenylate kinase
GOX0360	0.42	0.0203	Preprotein translocase subunit SecY
GOX0362	0.48	0.0219	LSU ribosomal protein L30P
GOX0363	0.39	0.0170	30S ribosomal protein S5
GOX0364	0.30	0.0179	50S ribosomal protein L18
GOX0365	0.33	0.0079	50S ribosomal protein L6
GOX0366	0.36	0.0578	30S ribosomal protein S8
GOX0367	0.45	0.0203	30S ribosomal protein S14
GOX0368	0.27	0.0091	50S ribosomal protein L5
GOX0369	0.34	0.0222	LSU ribosomal protein L24P
GOX0370	0.41	0.0340	LSU ribosomal protein L14P
GOX0371	0.51	0.0017	SSU ribosomal protein S17P
GOX0372	0.48	0.0065	LSU ribosomal protein L29P
GOX0373	0.36	0.0041	50S ribosomal protein L16
GOX0374	0.36	0.0128	30S ribosomal protein S3
GOX0375	0.39	0.0137	50S ribosomal protein L22
GOX0376	0.36	0.0080	SSU ribosomal protein S19P
GOX0378	0.39	0.0053	LSU ribosomal protein L23P
GOX0379	0.34	0.0096	50S ribosomal protein L4
GOX0380	0.39	0.0009	50S ribosomal protein L3
GOX0381	0.41	0.0376	30S ribosomal protein S10
GOX0382	0.44	0.0453	Elongation factor Tu
GOX0383	0.33	0.0107	30S ribosomal protein S7
GOX0384	0.29	0.0044	30S ribosomal protein S12
GOX0387	0.38	0.0093	50S ribosomal protein L7/L12
GOX0388	0.30	0.0014	LSU ribosomal protein L10P
GOX0392	0.53	0.0051	Putative transport transmembrane protein
GOX0393	0.43	0.0076	Putative transport transmembrane protein
GOX0394	0.46	0.0005	Two component sensor histidine kinase
GOX0395	0.44	0.0000	DNA binding response regulator
GOX0397	0.48	0.0135	Hypothetical protein GOX0397
GOX0399	0.51	0.0241	Glutathione S-transferase
GOX0400	0.49	0.0099	Septum formation inhibitor
GOX0401	0.53	0.0013	Cell division inhibitor MinD
GOX0402	0.53	0.0259	Cell division inhibitor MinE
GOX0403	0.52	0.0004	Hypothetical protein GOX0403
GOX0404	2.41	0.0180	Hypothetical protein GOX0404
GOX0405	0.36	0.0044	TonB-dependent outer membrane receptor
GOX0406	2.38	0.0024	Hypothetical protein GOX0406
GOX0412	0.40	0.0015	DNA polymerase III subunit delta
GOX0413	0.43	0.0144	Acetyl-coenzyme A synthetase
GOX0415	0.31	0.0015	Putative transport protein
GOX0428	0.47	0.0061	Bifunctional phosphoribosylaminoimidazolecarboxamide formyltransferase/IMP cyclohydrolase
GOX0429	0.49	0.0282	Hypothetical membrane-spanning protein
GOX0431	0.44	0.0057	Phosphogluconate dehydratase
GOX0433	2.16	0.0036	Hypothetical protein GOX0433
GOX0434	0.43	0.0029	Hypothetical protein GOX0434
GOX0435	0.36	0.0045	Acetyl-CoA carboxylase biotin carboxylase subunit
GOX0436	0.36	0.0063	Biotin carboxyl carrier protein of acetyl-CoA carboxylase

VII Appendix

GOX0437	0.40	0.0022	3-Dehydroquininate dehydratase
GOX0440	0.47	0.0040	Ornithine decarboxylase
GOX0442	4.72	0.0057	Hypothetical protein GOX0442
GOX0445	1.86	0.0283	Molybdenum cofactor biosynthesis protein C
GOX0451	0.32	0.0055	30S ribosomal protein S9
GOX0452	0.20	0.0281	50S ribosomal protein L13
GOX0458	1.83	0.0052	Putative oxidoreductase
GOX0470	2.03	0.0040	Putative peroxidase
GOX0475	3.40	0.0021	Hypothetical protein GOX0475
GOX0487	2.10	0.0014	DNA integration/recombination/inversion protein
GOX0497	4.53	0.0027	Hypothetical protein GOX0497
GOX0498	4.62	0.0017	Hypothetical protein GOX0498
GOX0499	2.45	0.0029	Putative NAD-dependent aldehyde dehydrogenase
GOX0503	2.06	0.0144	Hypothetical protein GOX0503
GOX0506	4.83	0.0067	RNA polymerase factor sigma-32
GOX0512	0.40	0.0153	Amino acid transport protein
GOX0514	2.06	0.0005	NifS-like protein
GOX0515	4.56	0.0007	Hypothetical protein GOX0515
GOX0524	0.29	0.0149	TonB-dependent outer membrane receptor
GOX0532	2.07	0.0052	ExbB protein
GOX0533	0.52	0.0032	Hypothetical protein GOX0533
GOX0548	2.22	0.0011	Hypothetical protein GOX0548
GOX0549	2.98	0.0009	Hypothetical protein GOX0549
GOX0559	1.93	0.0000	Putative hydroxylase
GOX0563	2.35	0.0008	Hypothetical protein GOX0563
GOX0568	4.02	0.0042	Hypothetical protein GOX0568
GOX0570	5.20	0.0010	Hypothetical protein GOX0570
GOX0576	3.04	0.0157	Hypothetical protein GOX0576
GOX0577	3.23	0.0020	Transcriptional regulator
GOX0596	0.48	0.0123	30S ribosomal protein S1
GOX0599	0.51	0.0028	Hypothetical protein GOX0599
GOX0600	0.55	0.0283	Hypothetical protein GOX0600
GOX0608	2.37	0.0081	ATP-dependent Clp protease adaptor protein ClpS
GOX0610	0.51	0.0118	Hypothetical protein GOX0610
GOX0615	0.52	0.0048	Ceramide glucosyltransferase
GOX0626	2.22	0.0028	Thioredoxin
GOX0636	0.48	0.0169	GTP-binding protein
GOX0642	0.52	0.0016	Putative oxidoreductase
GOX0644	2.10	0.0001	Putative 2,5-diketo-D-gluconic acid reductase
GOX0673	2.42	0.0013	Ferrous iron transport protein A (FeoA)
GOX0679	3.31	0.0000	Conserved protein of the SAM superfamily
GOX0689	0.44	0.0078	Probable outer membrane efflux lipoprotein
GOX0690	0.54	0.0223	Acriflavin resistance protein B (multidrug efflux system)
GOX0691	0.43	0.0068	Acriflavin resistance protein A (multidrug efflux system)
GOX0697	2.68	0.0040	Flagellar FlilL protein
GOX0699	0.16	0.0011	L-asparagine permease
GOX0701	0.53	0.0028	Phosphate regulon sensor protein PhoR
GOX0707	2.03	0.0013	DNA starvation/stationary phase protection protein Dps
GOX0708	2.16	0.0123	Hypothetical protein GOX0708

GOX0716	2.91	0.0046	Short chain dehydrogenase
GOX0726	4.57	0.0063	Hypothetical protein GOX0726
GOX0734	2.91	0.0017	Hypothetical protein GOX0734
GOX0740	2.09	0.0117	Putative protease
GOX0741	2.95	0.0001	Hypothetical protein GOX0741
GOX0743	0.42	0.0273	Ammonium transporter AmtB
GOX0745	0.54	0.0018	Hypothetical protein GOX0745
GOX0750	2.07	0.0020	Hypothetical protein GOX0750
GOX0752	0.53	0.0003	Putative acetyltransferase
GOX0758	2.74	0.0473	Porin
GOX0762	1.86	0.0026	Thioredoxin
GOX0771	0.51	0.0030	Ferric uptake regulation protein
GOX0772	0.43	0.0000	Transcriptional regulator
GOX0774	2.83	0.0006	Ribosomal-protein-alanine acetyltransferase
GOX0784	0.53	0.0089	Multidrug resistance protein A
GOX0788	1.99	0.0103	Flagellin assembly protein
GOX0796	0.55	0.0240	Hypothetical protein GOX0796
GOX0801	0.50	0.0019	tRNA pseudouridine synthase A
GOX0802	0.53	0.0028	Hypothetical protein GOX0802
GOX0808	0.45	0.0048	Galactose-proton symporter
GOX0809	0.31	0.0010	L-asparaginase II
GOX0813	2.07	0.0130	Phosphocarrier protein HPr
GOX0814	2.79	0.0027	PTS system, IIA component
GOX0815	3.12	0.0001	Hypothetical protein GOX0815
GOX0833	4.74	0.0001	Cold shock protein
GOX0835	0.48	0.0284	Adenine phosphoribosyltransferase
GOX0838	0.42	0.0446	Hypothetical protein GOX0838
GOX0841	2.00	0.0230	Hypothetical protein GOX0841
GOX0849	2.46	0.0024	NADPH-dependent L-sorbose reductase
GOX0855	1.92	0.0584	D-Sorbitol dehydrogenase subunit SldB
GOX0857	2.31	0.0060	Chaperone protein DnaK
GOX0859	2.51	0.0008	Shikimate 5-dehydrogenase
GOX0866	0.33	0.0162	S-adenosylmethionine synthetase
GOX0867	0.34	0.0006	SAM-dependent methyltransferase
GOX0868	0.52	0.0004	Electron transfer flavoprotein-ubiquinone oxidoreductase/ putative oxidoreductase
GOX0874	2.03	0.0220	Ferrocyclase
GOX0875	2.39	0.0088	AtsE protein
GOX0880	5.40	0.0000	Hypothetical protein GOX0880
GOX0882	1.83	0.0000	Alpha-ketoglutarate decarboxylase
GOX0886	1.97	0.0084	Hypothetical protein GOX0886
GOX0903	0.41	0.0053	Hypothetical protein GOX0903
GOX0904	0.55	0.0097	Hypothetical protein GOX0904
GOX0905	0.40	0.0132	Putative oxidoreductase
GOX0907	0.36	0.0062	TonB-dependent outer membrane receptor
GOX0922	6.26	0.0038	Hypothetical protein GOX0922
GOX0923	1.99	0.0403	Hypothetical protein GOX0923
GOX0925	3.05	0.0034	Sugar-proton symporter
GOX0945	0.19	0.0008	TonB-dependent outer membrane receptor

VII Appendix

GOX0946	2.25	0.0046	Putative oxidoreductase
GOX0953	1.81	0.0079	Flagellar basal body rod protein FlgG
GOX0965	3.08	0.0031	Probable phosphoglycerate mutase 2
GOX0966	4.89	0.0065	Hypothetical protein GOX0966
GOX0967	3.64	0.0057	Hypothetical protein GOX0967
GOX0970	0.36	0.0109	Outer membrane channel lipoprotein
GOX0971	0.28	0.0021	Cation efflux system protein CzcA
GOX0972	0.26	0.0088	Cation efflux system protein CzcB
GOX0973	0.56	0.0025	Outer membrane channel lipoprotein
GOX0974	2.68	0.0030	Transcriptional regulator AadR (cyclic AMP receptor protein)
GOX0975	1.85	0.0456	Hypothetical protein GOX0975
GOX0977	1.96	0.0011	Hypothetical protein GOX0977
GOX0979	2.09	0.0056	Riboflavin synthase subunit alpha
			Coenzyme PQQ synthesis protein A (Pyrroloquinoline quinonebiosynthesis protein A)
GOX0987	2.13	0.0251	
GOX1000	3.67	0.0155	Hypothetical protein GOX1000
GOX1002	0.52	0.0194	Bacterial Protein Translation Initiation Factor 1 (IF-1)
GOX1003	0.46	0.0265	Septum formation associated protein (Maf-like protein)
GOX1010	0.41	0.0043	Levanase precursor
GOX1017	0.30	0.0044	TonB-dependent outer membrane receptor
GOX1029	0.42	0.0007	Hypothetical protein GOX1029
GOX1038	2.82	0.0077	Septum formation associated protein (Maf-like protein)
GOX1041	2.06	0.0009	Hypothetical protein GOX1041
GOX1060	1.82	0.0368	DNA integration/recombination/inversion protein
GOX1062	0.46	0.0042	Chromosome partitioning protein ParB
GOX1063	0.43	0.0034	Chromosome partitioning protein ParA
GOX1069	0.49	0.0082	O6-Methylguanine-DNA methyltransferase
GOX1070	0.40	0.0092	Transcription termination factor Rho
GOX1091	0.51	0.0024	Spermidine synthase
GOX1095	0.31	0.0049	Aminomethyltransferase (Glycine cleavage system T protein)
GOX1096	0.29	0.0026	Glycine cleavage system H protein
GOX1097	0.29	0.0317	Glycine dehydrogenase
GOX1107	2.33	0.0062	O-antigen biosynthesis protein RfbC
GOX1109	0.45	0.0040	Dolichol-phosphate mannosyltransferase
GOX1110	0.37	0.0006	ATP synthase B' chain
GOX1111	0.41	0.0033	ATP synthase B' chain
GOX1112	0.44	0.0001	ATP synthase C chain
GOX1113	0.41	0.0014	F ₀ F ₁ ATP synthase subunit A
GOX1114	0.37	0.0099	Vitamin B12-dependent ribonucleotide reductase
GOX1122	2.47	0.0031	Putative NAD-dependent aldehyde dehydrogenase
GOX1132	2.78	0.0119	Hypothetical protein GOX1132
GOX1137	0.42	0.0064	Probable lipopolysaccharide modification acyltransferase
GOX1139	1.84	0.0138	Putative oxidoreductase
GOX1141	0.36	0.0067	LSU ribosomal protein L25P
GOX1142	0.29	0.0009	Peptidyl-tRNA hydrolase
GOX1148	0.47	0.0048	Nicotinic acid mononucleotide adenylyltransferase
GOX1150	0.55	0.0312	Hypothetical protein GOX1150
GOX1151	0.28	0.0033	Hypothetical protein GOX1151
GOX1155	0.44	0.0020	UDP-N-acetylglucosamine 4-epimerase

GOX1171	2.24	0.0032	Histidinol-phosphate aminotransferase
GOX1185	3.36	0.0025	Hypothetical protein GOX1185
GOX1186	6.28	0.0085	Hypothetical protein GOX1186
GOX1193	0.43	0.0176	Alanine racemase
GOX1197	0.33	0.0069	Hypothetical protein GOX1197
GOX1198	0.41	0.0058	Sulfite reductase (Ferredoxin)
GOX1200	0.54	0.0147	Magnesium and cobalt transport protein CorA
GOX1222	0.45	0.0437	Hypothetical protein GOX1222
GOX1226	0.43	0.0463	Hypothetical protein GOX1226
GOX1230	2.75	0.0050	Gluconate 2-dehydrogenase, cytochrome c subunit
GOX1231	2.33	0.0110	Gluconate 2-dehydrogenase alpha chain
GOX1232	2.17	0.0723	Gluconate 2-dehydrogenase gamma chain
GOX1237	0.43	0.0253	Acetylornithine aminotransferase
GOX1245	0.49	0.0367	Riboflavin kinase
GOX1246	0.50	0.0131	TonB-dependent receptor protein
GOX1248	1.90	0.0080	Hypothetical protein GOX1248
GOX1250	0.53	0.0125	Putative lipoprotein signal peptidase
GOX1253	3.25	0.0029	D-Lactate dehydrogenase
GOX1256	0.49	0.0023	Putative permease
GOX1269	3.37	0.0065	Hypothetical protein GOX1269
GOX1273	1.98	0.0064	Hypothetical protein GOX1273
GOX1282	0.40	0.0116	Ribonuclease PH
GOX1284	0.54	0.0077	Penicillin-binding protein 1 (Peptidoglycan synthetase)
GOX1286	0.16	0.0015	Hypothetical protein GOX1286
GOX1287	0.20	0.0127	Biopolymer transport ExbB protein
GOX1288	0.21	0.0022	Biopolymer transport ExbD protein
GOX1289	0.21	0.0077	Biopolymer transport ExbD protein
GOX1290	0.36	0.0014	Hypothetical protein GOX1290
GOX1299	5.28	0.0024	Transcriptional regulator
GOX1300	4.67	0.0002	D-3-phosphoglycerate dehydrogenase
GOX1305	0.39	0.0074	Transcription antitermination protein NusG
GOX1306	0.40	0.0010	Protein translocase subunit SecE
GOX1310	0.35	0.0024	ATP synthase delta chain
GOX1311	0.44	0.0049	F ₀ F ₁ ATP synthase subunit alpha
GOX1312	0.43	0.0109	F ₀ F ₁ ATP synthase subunit gamma
GOX1313	0.49	0.0367	F ₀ F ₁ ATP synthase subunit beta
GOX1314	0.51	0.0117	ATP synthase epsilon chain
GOX1328	2.61	0.0024	Hypothetical protein GOX1328
GOX1329	18.31	0.0010	Small heat shock protein
GOX1332	2.37	0.0028	Alkyl hydroperoxide reductase subunit C
GOX1333	1.84	0.0203	Alkyl hydroperoxide reductase subunit F
GOX1335	0.38	0.0065	Aconitate hydratase
GOX1336	0.29	0.0040	Isocitrate dehydrogenase
GOX1351	1.92	0.0244	Putative isomerase
GOX1356	3.98	0.0029	Oxidoreductase, iron-sulphur binding subunit
GOX1357	4.18	0.0085	Putative electron transport protein
GOX1358	3.49	0.0036	Hypothetical protein GOX1358
GOX1360	3.18	0.0042	Hypothetical protein GOX1360
GOX1366	0.41	0.0057	ABC transporter ATP-binding protein

VII Appendix

GOX1378	2.10	0.0371	Hypothetical protein GOX1378
GOX1381	2.56	0.0029	Gluconolactonase
GOX1383	4.68	0.0052	Hypothetical protein GOX1383
GOX1390	0.50	0.0184	Methyltransferase
GOX1392	0.32	0.0121	Hypothetical protein GOX1392
GOX1399	0.55	0.0024	3-Ketoacyl-(acyl-carrier-protein) reductase
GOX1414	2.26	0.0254	Chaperone protein DnaJ
GOX1416	0.30	0.0067	Porin B precursor
GOX1421	0.55	0.0218	Murein transglycosylase
GOX1422	0.51	0.0104	O-antigene export system permease protein
GOX1427	0.41	0.0006	FAD-dependent thymidylate synthase
GOX1436	0.38	0.0047	Adenosine deaminase
GOX1437	0.45	0.0001	Purine nucleoside permease
GOX1439	0.52	0.0058	Queuine tRNA-ribosyltransferase
GOX1440	0.42	0.1149	S-adenosylmethionine:tRNA ribosyltransferase-isomerase
GOX1442	10.74	0.0015	Hypothetical protein GOX1442
GOX1444	0.53	0.0033	N-acetyl-gamma-glutamyl-phosphate reductase
GOX1448	0.54	0.0045	Adenylosuccinate synthetase
GOX1455	0.45	0.0007	ATP-dependent RNA helicase
GOX1490	0.49	0.0226	Putative glycosyltransferase
GOX1493	3.65	0.0011	Hypothetical protein GOX1493
GOX1494	5.67	0.0016	Putative oxidoreductase
GOX1495	4.68	0.0018	Oxidoreductase, iron-sulphur binding subunit
GOX1499	3.45	0.0001	Hypothetical protein GOX1499
GOX1500	2.64	0.0011	Hypothetical protein GOX1500
GOX1501	2.43	0.0025	Hypothetical protein GOX1501
GOX1530	2.23	0.0036	Hypothetical protein GOX1530
GOX1540	3.18	0.0004	Fructose-1,6-bisphosphate aldolase
GOX1543	0.54	0.0079	Hypothetical protein GOX1543
GOX1569	0.47	0.0008	Tricorn protease homolog
GOX1572	0.34	0.0003	Amino acid ABC transporter ATP-binding protein
GOX1573	0.41	0.0046	Amino acid ABC transporter binding protein and permease protein
GOX1578	2.11	0.0000	Hypothetical protein GOX1578
GOX1579	0.39	0.0047	Hypothetical protein associated with nus operon
GOX1581	0.54	0.0252	Hypothetical protein GOX1581
GOX1582	0.44	0.0003	Translation initiation factor IF-2
GOX1586	0.49	0.0139	Polynucleotide phosphorylase/polyadenylase
GOX1587	0.36	0.0060	Putative 2-nitropropane dioxygenase
GOX1600	2.03	0.0000	Two component response regulator
GOX1602	1.84	0.0273	Hypothetical protein GOX1602
GOX1606	1.87	0.0029	Lipopolysaccharide N-acetylglucosaminyltransferase I
GOX1617	3.31	0.0032	Hypothetical protein GOX1617
GOX1626	0.47	0.0073	Cation efflux system protein
GOX1630	0.42	0.0046	Putative oxidoreductase
GOX1633	10.00	0.0041	Hypothetical protein GOX1633
GOX1634	2.45	0.0022	Pirin-like protein
GOX1639	0.40	0.0023	Hypothetical protein GOX1639
GOX1643	0.50	0.0095	Fumarate hydratase

GOX1647	0.49	0.0021	Cytochrome c-type biogenesis protein CycH
GOX1648	0.48	0.0016	Cytochrome c-type biogenesis protein CycL precursor
GOX1649	0.38	0.0152	Thiol:disulfide interchange protein DsbE precursor
GOX1651	0.54	0.0078	Cytochrome c-type biogenesis protein CcmE
GOX1664	2.19	0.0029	Recombination factor protein RarA
GOX1675	2.96	0.0021	NADH dehydrogenase type II
GOX1682	0.52	0.0094	Holliday junction DNA helicase B
GOX1685	0.50	0.0089	ExbD/TolR family protein
GOX1686	0.49	0.0092	Hypothetical protein GOX1686
GOX1693	2.58	0.0200	Cell cycle transcriptional regulator CtrA
GOX1695	1.80	0.0051	Hypothetical protein GOX1695
GOX1699	0.46	0.0001	Hypothetical protein GOX1699
GOX1703	2.71	0.0044	Transketolase
GOX1704	2.85	0.0250	Bifunctional transaldolase/phosphoglucose isomerase
GOX1707	1.86	0.0198	6-Phosphogluconolactonase
GOX1712	3.70	0.0008	Aldehyde dehydrogenase
GOX1713	4.85	0.0022	Protease I
GOX1716	0.47	0.0063	Hypothetical protein GOX1716
GOX1737	0.56	0.0001	Rod shape-determining protein MreB
GOX1742	1.86	0.0003	Hypothetical protein GOX1742
GOX1745	2.34	0.0201	Hypothetical protein GOX1745
GOX1747	0.47	0.0024	Aspartyl-tRNA synthetase
GOX1749	0.36	0.0027	Hypothetical protein GOX1749
GOX1751	2.49	0.0019	HesB family protein
GOX1752	1.98	0.0014	Deoxyguanosinetriphosphate triphosphohydrolase
GOX1766	1.93	0.0043	Non-heme chloroperoxidase
GOX1768	2.12	0.0069	Alkylated DNA repair protein AlkB
GOX1773	3.46	0.0018	Putative LacX protein
GOX1774	2.12	0.0020	Putative ATP-sensitive potassium channel protein
GOX1779	3.38	0.0035	Putative LysM domain protein
GOX1780	0.31	0.0000	30S ribosomal protein S4
GOX1781	0.25	0.0017	Bacterial Peptide Chain Release Factor 3 (RF-3)
GOX1791	0.45	0.0012	Acetyl-CoA carboxylase carboxyltransferase subunit alpha
GOX1796	0.53	0.0006	TonB-dependent outer membrane receptor
GOX1799	0.48	0.0007	Protein translocase subunit YajC
GOX1810	0.48	0.0050	Ribonuclease III
GOX1812	0.51	0.0072	Uridylate kinase
GOX1815	0.44	0.0460	Phosphatidate cytidyltransferase
GOX1827	0.45	0.0004	Putative inner membrane protein translocase component YidC
GOX1828	0.40	0.0019	GTPase EngB
GOX1829	0.52	0.0009	Acetylglutamate kinase
GOX1831	0.50	0.0182	2,3,4,5-Tetrahydropyridine-2-carboxylate N-succinyltransferase
GOX1832	0.38	0.0008	Succinyl-diaminopimelate desuccinylase
GOX1833	0.49	0.0010	Hypothetical protein GOX1833
GOX1834	0.53	0.0143	tRNA pseudouridine synthase A
GOX1837	2.82	0.0060	Small heat shock protein HspA
GOX1838	2.86	0.0060	Hypothetical protein GOX1838
GOX1840	3.79	0.0020	Hypothetical protein GOX1840
GOX1841	5.22	0.0043	Hypothetical protein GOX1841

VII Appendix

GOX1847	0.47	0.0153	Ribonuclease D
GOX1849	1.99	0.0000	Putative oxidoreductase
GOX1850	1.95	0.0013	Hypothetical protein GOX1850
GOX1857	11.96	0.0169	Uncharacterized PQQ-containing dehydrogenase 1
GOX1858	1.98	0.0104	Hypothetical protein GOX1858
GOX1867	0.49	0.0014	Putative processing protease protein
GOX1871	0.55	0.0169	Hypothetical protein GOX1871
GOX1873	0.42	0.0047	DNA mismatch repair protein
GOX1875	2.56	0.0003	Hypothetical protein GOX1875
GOX1879	3.58	0.0002	Superoxide dismutase
GOX1885	0.51	0.0077	Preprotein translocase subunit SecB
GOX1886	2.42	0.0043	Putative translocase transmembrane protein
GOX1890	2.94	0.0050	Hypothetical protein GOX1890
GOX1896	1.89	0.0183	Coproporphyrinogen III oxidase
GOX1903	0.17	0.0003	TonB-dependent receptor protein
GOX1905	0.55	0.0096	Lysyl-tRNA synthetase
GOX1910	3.23	0.0118	Hypothetical protein GOX1910
GOX1918	2.72	0.0123	Leucine aminopeptidase
GOX1937	0.44	0.0203	Exopolyphosphatase
GOX1938	0.54	0.0088	CDP-diacylglycerol pyrophosphatase
GOX1940	0.54	0.0054	Putative acid phosphatase
GOX1946	2.39	0.0003	Two component response regulator
GOX1952	2.49	0.0243	Hypothetical protein GOX1952
GOX1953	4.37	0.0008	5-Methylcytosine-specific restriction enzyme
GOX1957	0.45	0.0008	Putative thiol:disulfide interchange protein II
GOX1960	0.43	0.0036	Dephospho-CoA kinase
GOX1968	0.50	0.0133	Hypothetical protein GOX1968
GOX1971	2.27	0.0072	Galactose-proton symporter
GOX1972	2.30	0.0122	Putative transport protein
GOX1982	0.19	0.0011	Hypothetical protein GOX1982
GOX1992	1.95	0.0034	Osmotically inducible protein C
GOX1995	2.32	0.0066	Hypothetical protein GOX1995
GOX2028	12.24	0.0048	Hypothetical protein GOX2028
GOX2030	0.18	0.0009	Chaperone protein DnaK
GOX2034	0.56	0.0309	Metalloprotease
GOX2035	0.49	0.0110	Hypothetical protein GOX2035
GOX2036	5.26	0.0025	Putative oxidoreductase
GOX2050	1.86	0.0036	Hypothetical protein GOX2050
GOX2062	0.55	0.0089	Hypothetical protein GOX2062
GOX2063	2.22	0.0114	Hypothetical protein GOX2063
GOX2064	2.34	0.0161	Hypothetical protein GOX2064
GOX2066	3.53	0.0011	Glutaminase
GOX2073	0.37	0.0001	Formyltetrahydrofolate deformylase
GOX2074	0.48	0.0094	5-Methyltetrahydrofolate-S-homocysteine methyltransferase
GOX2078	1.89	0.0195	Hypothetical protein GOX2078
GOX2079	31.69	0.0003	Hypothetical protein GOX2079
GOX2083	2.42	0.0032	Hypothetical protein GOX2083
GOX2088	4.50	0.0040	Glycerol-3-phosphate dehydrogenase
GOX2089	3.93	0.0141	Glycerol uptake facilitator protein

GOX2090	4.58	0.0099	Glycerol kinase
GOX2096	0.44	0.0568	Sorbitol dehydrogenase large subunit
GOX2097	0.49	0.0440	Sorbitol dehydrogenase small subunit
GOX2108	1.84	0.0259	NADH-dependent iron-containing alcohol dehydrogenase
GOX2109	7.65	0.0007	Hypothetical protein GOX2109
GOX2112	0.54	0.0087	Outer membrane protein
GOX2114	2.14	0.0048	Transcriptional regulator
GOX2126	0.55	0.0043	ABC transporter ATP-binding protein
GOX2127	0.44	0.0008	ABC transporter permease protein
GOX2134	0.55	0.0027	Peptidyl-dipeptidase DCP
GOX2135	0.52	0.0051	Hypothetical protein GOX2135
GOX2143	0.48	0.0138	ABC transporter ATP-binding protein
GOX2151	0.55	0.0234	Hypothetical protein GOX2151
GOX2154	2.07	0.0170	Hypothetical protein GOX2154
GOX2163	2.97	0.0041	Cold shock protein
GOX2167	2.09	0.0459	F ₀ F ₁ ATP synthase subunit beta
GOX2169	2.09	0.0117	ATP synthase subunit AtpI
GOX2171	2.39	0.0149	ATP synthase subunit a
GOX2172	1.83	0.0326	ATP synthase subunit c
GOX2181	2.42	0.0245	Putative polyol dehydrogenase
GOX2182	2.42	0.0218	Probable mannitol/sorbitol ABC transporter permease protein
GOX2183	2.43	0.0330	Probable mannitol/sorbitol ABC transporter ATP-binding protein
GOX2184	2.26	0.0317	Probable mannitol/sorbitol ABC transporter permease protein
GOX2185	3.05	0.0300	Periplasmic mannitol/sorbitol binding protein
GOX2186	2.34	0.0336	Ribulokinase
GOX2187	4.54	0.0009	Gluconate 5-dehydrogenase
GOX2188	3.46	0.0008	Gluconate permease
GOX2199	4.69	0.0012	Probable myosin-crossreactive antigen
GOX2200	4.47	0.0003	Probable myosin-crossreactive antigen
GOX2203	2.37	0.0086	Hypothetical protein GOX2203
GOX2205	0.48	0.0046	Hypothetical protein GOX2205
GOX2206	0.47	0.0272	5-Methyltetrahydropteroyltryglutamate--homocysteine methyltransferase
GOX2211	1.95	0.0017	Hypothetical protein GOX2211
GOX2217	10.78	0.0023	Triosephosphate isomerase
GOX2218	4.96	0.0012	Ribose-5-phosphate isomerase B
GOX2219	4.08	0.0076	Ribose ABC transporter, periplasmic binding protein
GOX2220	1.95	0.0000	Ribose ABC transporter, ATP-binding protein
GOX2222	1.85	0.0060	Dihydroxyacetone kinase
GOX2223	2.16	0.0029	Transposase (class V)
GOX2231	3.82	0.0007	Putative sugar transporter
GOX2246	3.38	0.0008	Hypothetical protein GOX2246
GOX2250	1.88	0.0030	Pyruvate kinase
GOX2257	2.55	0.0033	Hypothetical protein GOX2257
GOX2258	0.42	0.0039	Putative phytoene synthase
GOX2260	0.51	0.0086	Squalene-hopene cyclase
GOX2279	2.31	0.0128	Enolase
GOX2288	1.87	0.0008	Indole-3-glycerol phosphate synthase
GOX2361	2.28	0.0049	Hypothetical protein GOX2361

VII Appendix

GOX2374	2.78	0.0010	Hypothetical protein GOX2374
GOX2376	2.26	0.0206	Putative aldehyde dehydrogenase
GOX2379	2.83	0.0026	Hypothetical protein GOX2379
GOX2388	0.53	0.0053	Putative acetyltransferase (Antibiotic resistance) protein
GOX2393	0.50	0.0067	Phosphoribosylaminoimidazole carboxylase ATPase subunit
GOX2397	4.84	0.0014	Small heat shock protein
GOX2401	0.52	0.0051	Protein-export membrane protein
GOX2402	0.35	0.0254	Preprotein translocase subunit SecD
GOX2405	2.40	0.0065	Two-component response regulator
GOX2406	1.99	0.0484	Putative RNA polymerase sigma-E factor (sigma-24) protein 1
GOX2407	1.92	0.0240	Putative RNA polymerase sigma-E factor (sigma-24) protein 2
GOX2420	2.63	0.0041	Hypothetical protein GOX2420
GOX2439	4.29	0.0012	Hypothetical protein GOX2439
GOX2462	1.96	0.0068	Transcriptional regulator
GOX2471	2.19	0.0116	Putative transcriptional regulator
GOX2493	2.73	0.0008	Peptide methionine sulfoxide reductase
GOX2501	0.45	0.0217	SSU ribosomal protein S20P
GOX2519	1.90	0.0082	Hypothetical protein GOX2519
GOX2520	2.24	0.0257	Hypothetical protein GOX2520
GOX2525	11.59	0.0001	Hypothetical protein GOX2525
GOX2529	6.50	0.0018	Hypothetical protein GOX2529
GOX2530	2.02	0.0048	Hypothetical protein GOX2530
GOX2553	8.55	0.0006	Hypothetical protein GOX2553
GOX2554	5.81	0.0017	Plasmid stability-like protein
GOX2561	0.38	0.0026	RND-type multidrug efflux pump, outer membrane protein
GOX2564	3.27	0.0009	Toxin ChpA
GOX2565	4.17	0.0009	PemI-like protein
GOX2571	2.48	0.0021	Hypothetical protein GOX2571
GOX2578	0.51	0.0317	Putative isochorismatase
GOX2579	0.49	0.0438	Transcriptional regulator
GOX2590	2.49	0.0338	Hypothetical protein GOX2590
GOX2603	0.29	0.0119	Replicator initiator RepC
GOX2608	2.74	0.0002	Hypothetical protein GOX2608
GOX2609	2.27	0.0041	Hypothetical protein GOX2609
GOX2615	0.38	0.0486	Hypothetical protein GOX2615
GOX2652	3.79	0.0000	Hypothetical protein GOX2652
GOX2658	1.86	0.0164	Putative terminal quinol oxidase, subunit DoxD
GOX2659	3.12	0.0029	Transposase
GOX2660	1.90	0.0135	Transposase
GOX2661	1.83	0.0074	Hypothetical protein GOX2661
GOX2662	2.36	0.0120	Hypothetical protein GOX2662
GOX2666	3.84	0.0014	Hypothetical protein GOX2666
GOX2676	2.38	0.0045	Putative alcohol/aldehyde dehydrogenase
GOX2681	5.45	0.0010	Hypothetical protein GOX2681
GOX2682	3.81	0.0003	Hypothetical protein GOX2682
GOX2684	2.14	0.0128	NAD(P)H-dependent 2-cyclohexen-1-one reductase
GOX2685	13.66	0.0009	Transposase
GOX2688	6.11	0.0003	Hypothetical protein GOX2688
GOX2694	2.31	0.0147	ParA-like protein

GOX2701	0.55	0.0226	DNA integration/recombination/inversion protein
GOX2711	2.21	0.0156	Conjugal transfer protein, TraD
GOX2712	3.46	0.0203	Hypothetical protein GOX2712
GOX2719	2.61	0.0002	Transposase
GOX2720	3.67	0.0012	Hypothetical protein GOX2720
GOX2725	1.87	0.0407	Hypothetical protein GOX2725
GOX2726	2.53	0.0233	Hypothetical protein GOX2726
GOX2732	1.84	0.0360	Replication protein
GOX2735	4.49	0.0011	PemK-like protein

Acknowledgement

The present work was carried out at the Institut für Biotechnologie 1, Forschungszentrum Jülich. My sincere thanks go to Prof. Dr. Hermann Sahm for the assignment of the theme, for his encouragement and his interest in the progress of this work. This work was pushed forward due to his scientific discussions and his fair comments.

I would like to thank Prof. Dr. Michael Bott for taking over the review of my thesis and his support for the completion of the work.

I am most grateful to Dr. Stephanie Bringer-Meyer for her supervision and her encouragement. She was always patient and enthusiastic in answering scientific problems and had many good advises for the progress of my work.

I would like to thank our industrial partner “DSM nutritional products” for the good cooperation and for the constant information exchange. My special thanks go to Dr. Petra Simic, Dr. Nigel Mouncey and Dr. Hans-Peter Hohmann.

Especially I would like to thank my teammates Vera Krajewski, Verena Engels, Tobias Georgi, Ursula Degner, Carsten Bäumchen, Florian Heuser, Marthe Chmielus, Stefanie Schweikert, Janine Richhardt, Helga Etterich, Solvej Siedler, Tino Polen and Frank Lausberg for their friendliness and good advises.

I thank all the members of the IBT 1 and IBT 2 for the friendly and familiar atmosphere and their cooperativeness. I am thankful for the support by the DasGip AG, especially for the readiness for support of Dr. Christoph Bremus and Christian Mörl.

Above all, I want to show my gratefulness and appreciation to my parents Brigitte Balfen and Achim Hanke, to my family and to my friends for their support, example and tolerance during my studies and life.

Declaration

This thesis is a presentation of my original research work. Wherever contributions of others are involved, every effort is made to indicate this clearly, with due reference to the literature, and acknowledgement of collaborative research and discussions.

Jülich, Dezember 2009

Tanja Hanke